ESCUELA TÉCNICA SUPERIOR DE INGENIERÍA

(ICAI)

COMPARISON OF CALCULATION METHODS FOR HVDC FAULT CURRENTS

Autor: Pablo Garcia Mate

Director: Andreas Saçiak

Madrid

Junio 2018

AUTHORIZATION FOR DIGITALIZATION, STORAGE AND DISSEMINATION IN THE NETWORK OF END-OF-DEGREE PROJECTS, MASTER PROJECTS, DISSERTATIONS OR BACHILLERATO REPORTS

1. Declaration of authorship and accreditation thereof.

The author Mr. /Ms. Pablo García Mate

HEREBY DECLARES that he/she owns the intellectual property rights regarding the piece of work: Comparison of calculation methods for HVDC fault currents
that this is an original piece of work, and that he/she holds the status of author, in the sense granted by the Intellectual Property Law.

2. Subject matter and purpose of this assignment.

With the aim of disseminating the aforementioned piece of work as widely as possible using the University's Institutional Repository the author hereby **GRANTS** Comillas Pontifical University, on a royalty-free and non-exclusive basis, for the maximum legal term and with universal scope, the digitization, archiving, reproduction, distribution and public communication rights, including the right to make it electronically available, as described in the Intellectual Property Law. Transformation rights are assigned solely for the purposes described in a) of the following section.

3. Transfer and access terms

Without prejudice to the ownership of the work, which remains with its author, the transfer of rights covered by this license enables:

a) Transform it in order to adapt it to any technology suitable for sharing it online, as well as including metadata to register the piece of work and include "watermarks" or any other security or protection system.

b) Reproduce it in any digital medium in order to be included on an electronic database, including the right to reproduce and store the work on servers for the purposes of guaranteeing its security, maintaining it and preserving its format.

c) Communicate it, by default, by means of an institutional open archive, which has open and cost-free online access.

d) Any other way of access (restricted, embargoed, closed) shall be explicitly requested and requires that good cause be demonstrated.

e) Assign these pieces of work a Creative Commons license by default.

f) Assign these pieces of work a HANDLE (*persistent* URL). by default.

4. Copyright.

The author, as the owner of a piece of work, has the right to:

a) Have his/her name clearly identified by the University as the author

b) Communicate and publish the work in the version assigned and in other subsequent versions using any medium.

c) Request that the work be withdrawn from the repository for just cause.

d) Receive reliable communication of any claims third parties may make in relation to the work and, in particular, any claims relating to its intellectual property rights.

5. Duties of the author.

The author agrees to:

a) Guarantee that the commitment undertaken by means of this official document does not infringe any third party rights, regardless of whether they relate to industrial or intellectual property or any other type.

b) Guarantee that the content of the work does not infringe any third party honor, privacy or image rights.
c) Take responsibility for all claims and liability, including compensation for any damages, which may be brought against the University by third parties who believe that their rights and interests have been infringed by the assignment.
d) Take responsibility in the event that the institutions are found guilty of a rights infringement regarding the work subject to assignment.

6. Institutional Repository purposes and functioning.

The work shall be made available to the users so that they may use it in a fair and respectful way with regards to the copyright, according to the allowances given in the relevant legislation, and for study or research purposes, or any other legal use. With this aim in mind, the University undertakes the following duties and reserves the following powers:

a) The University shall inform the archive users of the permitted uses; however, it shall not guarantee or take any responsibility for any other subsequent ways the work may be used by users, which are non-compliant with the legislation in force. Any subsequent use, beyond private copying, shall require the source to be cited and authorship to be recognized, as well as the guarantee not to use it to gain commercial profit or carry out any derivative works.
b) The University shall not review the content of the works, which shall at all times fall under the exclusive responsibility of the author and it shall not be obligated to take part in lawsuits on behalf of the author in the event of any infringement of intellectual property rights deriving from storing and archiving the works. The author hereby waives any claim against the University due to any way the users may use the works that is not in keeping with the legislation in force.
c) The University shall adopt the necessary measures to safeguard the work in the future.
d) The University reserves the right to withdraw the work, after notifying the author, in sufficiently justified cases, or in the event of third party claims.

Madrid, on 4 ..... of June ....., 2018

HEREBY ACCEPTS

Signed: .....

Reasons for requesting the restricted, closed or embargoed access to the work in the Institution's Repository

I declare, under my responsibility, that the project present with the title

Comparison of calculation methods for HVDC fault currents

In the ETS de Ingeniería - ICAI de la Universidad Pontificia Comillas in the academic year 2017/2018 is of my authorship, original and unpublished and has not been submittted beforehand for other purposes. The project is not another, not even partially or the information that has been taken from other documents is duly referenced.

Signed: Pablo García Mate. Date: 04/06/ 2018

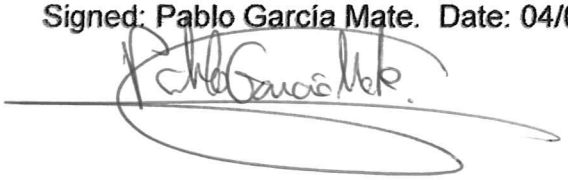

Authorized project delivery,

THE DIRECTOR OF THE PROJECT

Signed: Andreas Saçiak. Date: 04/ 06/ 2018

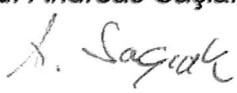

ESCUELA TÉCNICA SUPERIOR DE INGENIERÍA

(ICAI)

COMPARISON OF CALCULATION METHODS FOR HVDC FAULT CURRENTS

Autor: Pablo Garcia Mate

Director: Andreas Saçiak

Madrid

Junio 2018

RESUMEN

El crecimiento de las fuentes de energía renovables y la creciente demanda de electricidad presentan un desafío para el sistema de suministro de energía eléctrica. Estas nuevas fuentes de energía a menudo están lejos de los puntos de consumo. En estas situaciones, el transporte de larga distancia de la energía, basado en la tecnología HVAC, deja de ser técnica o económicamente razonable. En estas situaciones, la tecnología HVDC se presenta como una buena alternativa, ofreciendo también una buena controlabilidad. El diseño de estas redes debe tener en cuenta varios aspectos, siendo las corrientes de cortocircuito esperadas un factor crucial. Por el momento, a diferencia de los sistemas HVAC, los sistemas HVDC no tienen un método estándar para el cálculo de dichas corrientes, aunque existen varios estudios y métodos propuestos. Ser capaz de determinar qué método funciona mejor en cada situación sería muy beneficioso en términos de aprovechar siempre las mejores características de los métodos..

El objetivo principal de la tesis es el estudio profundo de los métodos actuales de cálculo de cortocircuitos para sistemas HVDC y la comparación de los resultados obtenidos por ellos. Por el momento, los métodos existentes solo se han estudiado de forma independiente.

La tesis será responsable de comparar dos de los métodos propuestos (doctorado de ETH y la disertación de la TU Darmstadt). Para ello, se seguirán los siguientes pasos:

• Estudio de literatura sobre métodos de cálculo existentes

• Implementación de métodos de cálculo relevantes

• Selección de escenarios de cortocircuito y creación de redes de prueba

• Comparación de los métodos de cálculo entre sí y con los resultados de la simulación

Las ecuaciones propuestas se implementarán en Matlab y se adoptará una red común para ambos métodos. El objetivo es comparar los resultados obtenidos en una amplia gama de configuraciones. Se estudiarán los sistemas punto a punto y las

redes multiterminal (MT). Los valores esperados de corriente de cortocircuito se obtendrán de simulaciones obtenidas con PSCAD.

Una vez realizada esta comparación, se obtendrán conclusiones con respecto a la elección del método y la precisión del resultado esperado. Este puede ser un paso muy importante para finalmente desarrollar un estándar que pueda ser utilizado para todas las redes HVDC. Como ambos métodos provienen de diferentes autores y diferentes universidades (lo que implica diferentes metodologías de trabajo), el primer paso es implementar una red única, en la que las ecuaciones de ambos métodos sean válidas. Ser capaz de adaptar ambos métodos a una configuración común es la única forma de compararlos. Una vez que ambos métodos se adaptan a un diseño común, este diseño debe implementarse en PSCAD. Las simulaciones de PSCAD podrán dar los resultados esperados y actuar como una referencia con la que comparar.

Una vez que se ha llevado a cabo la implementación, los parámetros del sistema (longitud de línea, valor del condensador de CC, etc.) que ya se han demostrado que son relevantes en el resultado de la simulación variarán y se discutirá la consistencia de ambos métodos. Este análisis servirá para ver qué situación es más favorable para cada uno de los métodos.

Posteriormente, los errores se compararán en todas las situaciones para las cuales haya datos disponibles y se tomará una decisión sobre la precisión de los métodos. Con los resultados obtenidos, se puede decir que las mejores estimaciones en las configuraciones punto a punto se obtienen con el método de Darmstadt, mientras que cuando las configuraciones son MT, el mejor método es el del doctorado.

SUMMARY

The growth of renewable energy sources and the increasing electricity demand introduce a challenge for the electrical power supply system. These new energy sources are often far from the consumption points. In these situations, long distance transport of the energy, based on HVAC technology becomes no longer technically nor economically reasonable. As a good alternative, HVDC technology presents itself suitable, offering also good controllability. The design of these grids has to take into account several aspects, being the knowledge of the expected short-circuit currents a crucial one. At the moment, unlike HVAC systems, HVDC systems do not have a standard for the calculation of short-circuit currents. Being able to determine which method performs better in each situation would be very beneficial in terms of always taking advantage of the best characteristics of them. However, there is currently no standard for the calculation of these currents in HVDC networks.

The main objective of the thesis is the in-depth study of the current short circuit calculation methods for HVDC systems and the comparison of the results obtained by them. For the time being, existing methods have only been studied independently.

The thesis is responsible for the proposed methods (ETH PhD and the dissertation of the TU Darmstadt). For this, the following steps will be followed:

• Literature study on existing calculation methods

• Implementation of calculation methods

• Selection of short circuit scenarios and creation of test networks

• Comparison of calculation methods with each other and with the results of the simulation

The proposed equations will be implemented in Matlab and a common network will be adopted for both methods. The objective is to compare the results obtained in a wide range of configurations. Point-to-point systems and multiterminal networks (MT) will be studied. The expected short circuit values will be obtained from simulations obtained with PSCAD.

Once this comparison is made, conclusions will be obtained with respect to the choice of method and the precision of the expected result. This can be a very important step to finally develop a standard that can be used for all HVDC networks. As both methods come from different authors and different universities (which implies different work methodologies), the first step is to implement a single network, in which the equations of both methods are valid. Being able to adapt both methods to a common configuration is the only way to compare them. Once both methods are adapted to a common design, this design should be implemented in PSCAD. The PSCAD simulations will be able to give the expected results and act as a reference with which to compare.

Once the implementation has been carried out, the system parameters (line length, DC capacitor value, etc.) that have already been shown to be relevant in the simulation result will vary and the consistency of the both methods will be studied. This analysis will serve to see which situation is more favorable for each of the methods.

Subsequently, errors will be compared in all situations for which data are available and a decision on the accuracy of the methods will be made. With the results obtained, it can be said that the best estimations in the point-to-point configurations are obtained with the Darmstadt method, whereas when the configurations are MT, the best method is the PhD one.

Index

List of figures

List of tables

CHAPTER 1: INTRODUCTION

High voltage direct current (HVDC) technology present certain characteristics that make it more attractive than High voltage alternating current (HVAC) technology in some uses. Nowadays it has been proven that this type of technology is more efficient for long-distance transmission, asynchronous interconnection (which is not possible with HVAC interconnection) and submarine cable connections.

The growth of renewable energy sources and the increasing electricity demand introduce a challenge for the electrical power supply system. These new energy sources are often far from the consumption points. In these situations, long-distance transport of the energy, based on HVAC technology becomes no longer technically nor economically reasonable. As a good alternative, HVDC technology presents itself suitable, offering also good controllability.

The design of these grids has to take into account several aspects, being the knowledge of the expected short-circuit currents a crucial one. At the moment, unlike HVAC systems, HVDC systems do not have a standard for the calculation of short-circuit currents. Being able to determine which method performs better in each situation would be very beneficial in terms of always taking advantage of the best characteristics of them.

The thesis's main objective is the deep study of the existing current short-circuit calculation methods for HVDC systems and comparison with each other. For the moment, the existing methods have only been studied independently. In this thesis, they will be tested on several scenarios with the aim on determining which conditions are most beneficial for each procedure. Once this comparison is done, solid conclusions will be taken regarding on the method’s choice and the expected result's accuracy. This can be a very important step in the path of finally developing a standard that can be used for HVDC grids.

The parameters of the system (line length, DC capacitor value, etc.) that have already been proven to be relevant on the simulation result will be varied and the consistency of both methods discussed.

As both methods come from different authors and different universities (which implies different works methodologies), the first step is to implement a unique network grid, in which both method's equations are valid. As it was said before, each method uses its own grid topology, its own parameters, etc. Being able to adapt both of them to a single one is the only way to compare them.

Once both methods are adapted to a common layout, this layout needs to be implemented in PSCAD. The PSCAD simulations will be able to give the expected results and to act as a model to compare with.

Another objective is to understand how the variation of different parameters affect the response of the system against a fault. These grid's designs are done taking into account many influencing factors, that can have beneficial or can jeopardize the stability of the system when a contingence appears.

By developing a standard method, each situation's short circuit current can be easily calculated knowing how much error should be expected and making the design of HVDC grids easier.

The thesis realization will be divided into four big blocks:

- ✓ Literature on calculation methods
- ✓ Implementation of selected procedures
- ✓ Selection of error scenarios and creation of test networks
- ✓ Comparison of the calculation methods against each other and against simulation results for the error scenarios.

This first part of the thesis consists on the study of the literature of all the calculation methods that has already been written. Having as a base the PhD and the TU Dissertation, where both methods are exposed, related papers and publications can easily be found. With a good comprehension of the already set methods and the good understanding of the previously studied scenarios, the implementation in Matlab will be much easier, focusing only on the important and delicate aspects that have already been proven to have the most influence on the final result.

Once all the literature has been selected, read and understood, the implementation of the studied algorithms in Matlab will be carried out. Two different algorithms will be created: one for the first method and another one for the second method.

The goal of this phase is to have both methods implemented and tested with the proposed ones, so it is safe to say that they are reliable. At the end, a unique set of parameters will be selected and used.

The next phase is to create a network in PSCAD that can be used for both method's equations. This PSCAD model will be compared to the previous Matlab results.

It is important to have a good selection of the scenarios that will be studied. Not all the scenarios are suitable for the comparison of both methods, and that will be an important point to take into account. Each original publication proposes its own set of different scenarios and parameter's combinations, that do not necessarily appear in both of them. As a solution, one common set of scenarios will be created and both analytic methods will be adapted to it.

The main point of this part of the thesis is to analyze in which scenarios both models can work, and which ones not.

The last part of the thesis is the comparison of the results obtained with the Matlab implementation against each other and against the PSCAD simulations.

The range of selected scenarios in the previous point have to be wide and it should include a variety in the parameters, so the robustness of both models can be tested. DC Capacitor and line length will be two of the most changed parameters due to their big influence on the system's response. Some other parameters, such as the impedance per km of the lines, number of converters, topology, etc. may also be looked at.

All these analyses will lead to conclusions. The wider the scenario's range is, the more noteworthy the conclusions will be. This last phase is the most important one, where all the previous work should lead to interesting results.

The model to implement will be done with the mathematic software Matlab (.m files). This software is sufficiently strong to cope with the analytical equations that the thesis requires for its satisfactory resolution.

Other important software for the thesis is PSCAD. This software will simulate the implemented benchmark and will get the behavior of the system current when a fault phase to ground occurs.

For the comparison of the results obtained from both softwares, Matlab will be used. For it, PSCAD data needs to be exported into Matlab.

CHAPTER 2: STATE OF THE ART

HVDC APPLICATIONS

As it was said in the introduction, HVDC lines have been recently presented as a very good alternative to certain situations. In the following paragraphs the main application for this technology will be explained.[2]

LONG DISTANCE BULK POWER TRANSMISSION

In long distance bulk-power transmission, HVDC lines present as an alternative to the HVAC lines[2]. When this application is discussed it is common to deal with the concept of "break-even distance". This concept compares the total costs that the transmission would be for HVAC and for HVDC and presents the minimum distance from which direct current lines are more economic. Although this is an interesting concept, it is not always safe to stick into that distance, as there are some influencing factors that are not taking into account such as stability limitations, required intermediate switching stations and the reactive power compensation. In the following Figure 1, it can be seen a comparison between HVDC costs against HVAC costs.

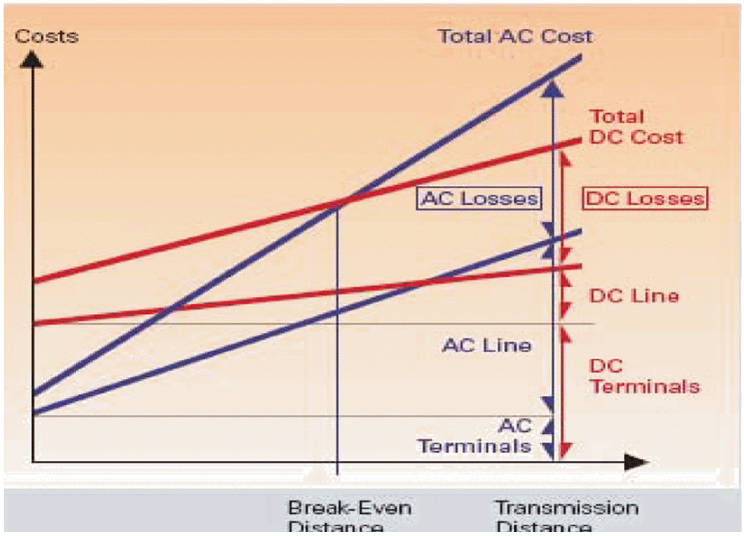

Figure 1. HVDC costs VS HVAC costs. [1, page 166]

In general terms, it can be said that as a first impression to study the decision between DC or AC grids it is a good approach. On the other hand, it is very important not to forget about the just mentioned aspects (stability, reactive power compensations, etc).

UNDERGROUND AND SUBMARINE CABLE TRANSMISSION

The main advantage of using HVDC cables for underground and submarine cable transmission relies on the reactive compensation, which is no longer needed when HVDC cables are used. Other advantages can be for instance the cost saving of the cable installations. Another very important aspect that makes HVDC more beneficial is the reduced losses that they present.

Additionally, the AC transmission cable capacity presents a reduction when the distance is increased. This problem can be solved with shunt compensation, but this is not an optimal solution for it, taking into account that it is not practical to do so for submarine cables[2].

Comparing the losses of both transmission systems, HVDC cable's losses can be half the ones presented in HVAC cables. Explanations for this is the higher number of conductors of the AC transmission systems (3 conductors, one for each phase), the reactive component of the current, skin-effect and the parasitic currents.

CONVERTER TECHNOLOGIES

In modern HVDC transmission systems, there exist mainly two basic converter technologies[2]. These two technologies are conventional line-commutated current source converters (CSCs) and self-commutated voltage source converters (VSCs). Commutation technologies are the base that sustains the direct current transmission system. A converter is a device that transforms an AC signal into a DC signal (the converters acts as a rectifier) and vice versa (the converter acts as an inverter). The following paragraphs will explain the difference between each one [2].

Line Commutated current source converter

The line commutated current source converter is the conventional transmission technology, which uses line-commutated CSCs with thyristor valves. These types of converters require a synchronous voltage source for its correct operation. Commutation is described as the transfer of current from one phase to another phase. This current transfer has to be in a synchronized firing sequence of the thyristor valves.

For its correct performance, line-commutated CSCs need to present a phase difference between the ac current and voltage. The current must lag the voltage, demanding reactive power. To fulfill this reactive power request, the system will supply it from the ac filters, shunt banks or series capacitors. These series capacitors are an integral part of the converter station. It is possible, that in some occasions the reactive power supplied does not match with the demanded one. In these cases, the ac system will provide it and fix any surplus or deficit from it. In any case, this deviation from the required reactive power value must stay within a limit, of determinate tolerance[2] and [11].

In some cases, the ac system is too weak to compensate this difference in reactive power. To solve this problem, series capacitors were connected between the valves and the transformers. These types of converters are called capacitor-commutated converters (CCCs) and provide the system some of the reactive power that was lacking. This is done automatically and it improves voltage stability. Regarding its protection to overvoltages, it is simple due to the fact that the capacitors are not

exposed to the line faults[2]. The following picture Figure 2 shows the conventional current source converter module.

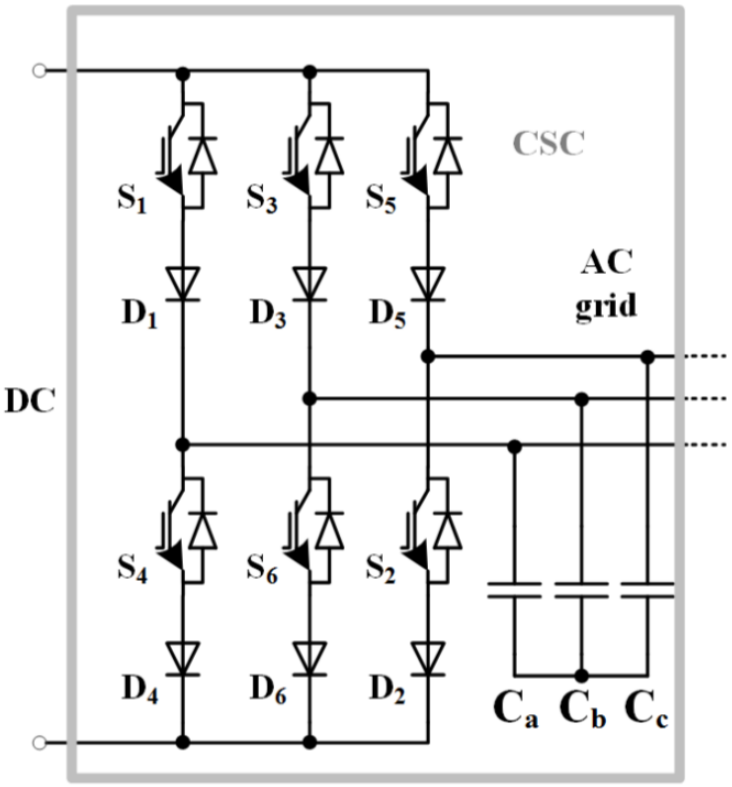

Figure 2. Conventional current source converter module. [15, page 2]

Self-commutated voltage source converter

On the other hand, self-commutated voltage source converters (VSC) with pulse width modulation were introduced in the late 1990s. These systems consist of insulated-gate bipolar transistor (IGBT) valves and solid-dielectric extruded HVDC cables/ OHL.

The main advantage of VSCs is that they can control both active and reactive power independently one from the other. The possibility of managing active and reactive power in an independent way, gives the whole converter a flexibility degree that was not possible with the line-commutated CSCs. The transfer capability is also improved with these kinds of converters. Transfer capability is directly related with the voltage stability and the transfer capability of the sending and receiving-end ac

systems. These two factors are improved due to the dynamic support that the converter presents at each terminal.

Another advantage of self-commutated VSC is that they do not demand reactive power. This lack of reactive power demand makes that the converter can manage its generation to regulate the ac system voltage, as generators do. The following picture (Figure 3) will so a schematic figure for a stand-alone VSC.

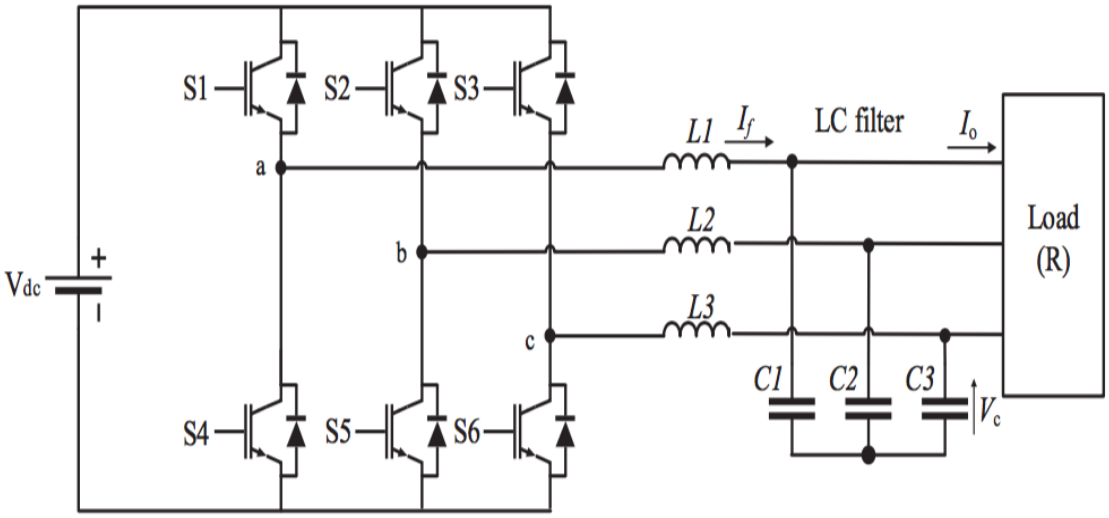

Figure 3. Power circuit schematic for a stand-alone VSC [16, page 1]

CSCs VS. VSCs

Comparing both converters and studying its influence in their applications it can be said that each one is used in different configurations and transmissions demands.

When looking at the CSCs converters, their applications are focused on point-to-point HVDC transmission. The principal strong points that this kind of converter present are good short-circuit capability, its cost-effectiveness and its high reliability of the thyristors[11].

On the other hand, for more complicated benchmarks, such as multiterminal HVDC topologies, VSCs converters show some advantages over the traditional line-

commutated converters that make them much more efficient. The main benefits of VSCs are [ETH]:

- The possibility to control active and reactive power independently
- Commutation trustworthiness
- Dynamic response
- Improvement in AC network short circuit capacity
- No reactive power demand
- Black-start capability

All these characteristics make voltage source converters a better option when multiterminal networks are being treated. A multiterminal network is composed with different branches. These branches have different performances regarding its configurations and operation modes. The different possibilities that exist are:

- Asymmetric monopole
- Symmetric monopole
- Bipolar
- Combination

Asymmetric monopole

This kind of configuration is the simplest one, and as a result the less expensive one. The requirements for these kinds of configurations are one converter per terminal and one full insulated high voltage conductor. The disadvantage of this high voltage conductor is that a constant DC current flows through ground. This current can cause corrosion with all its implications, as damaging the transformers due to saturation. Figure 4 shows an asymmetric monopole configuration.

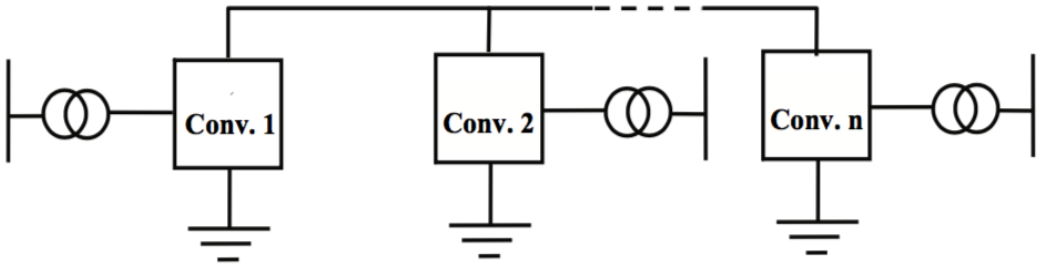

Figure 4. Asymmetric Monopole configuration. [11, page 16]

Symmetric monopole

As differences from the asymmetric monopole configuration, no ground currents flow during normal operation. Another important difference is the flexibility that it offers. The two poles cannot operate in an independent way, but this configuration allows to carry potential of opposite polarity. Figure 5 represents a symmetric monopole configuration.

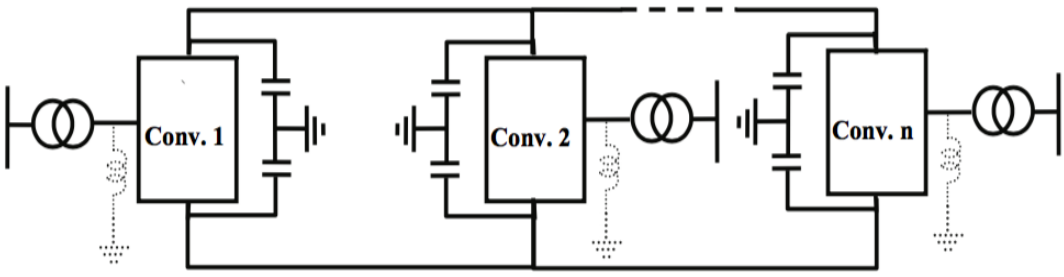

Figure 5. Symmetric Monopole configuration. [11, page 17]

Bipolar

The highest transmission capacity is achieved with a bipolar configuration. Both poles can be controlled in an independent way, which offers big possibilities such as working as an asymmetric monopolar configuration with a reduction in the transmission capacity. Figure 6 represents a bipole configuration.

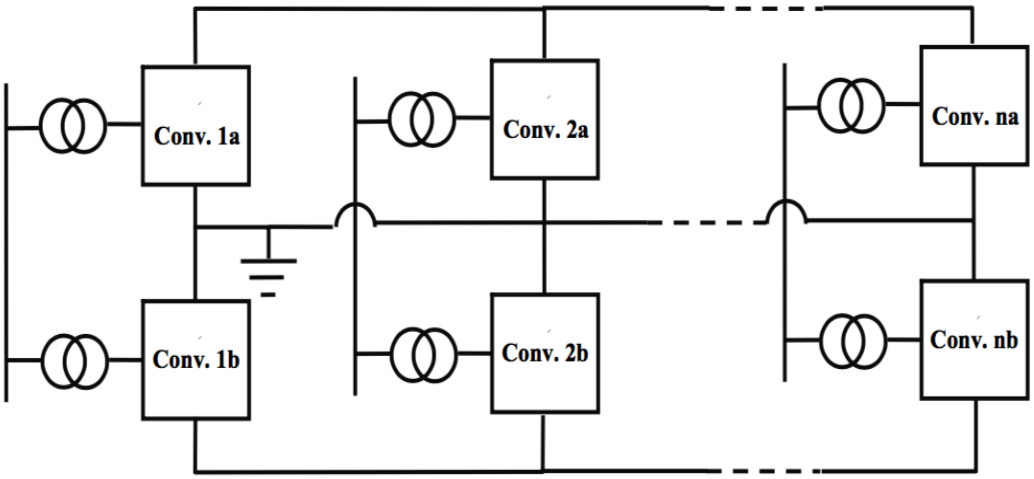

Figure 6. Bipole configuration. [11, page 17]

Combination

The last possibility is that in a multiterminal HDVC network, not all the branches work in the same way and more than one configuration appear in the network, being in this case a combination of various configurations. Figure 7 shows a combinations of all three last configurations.

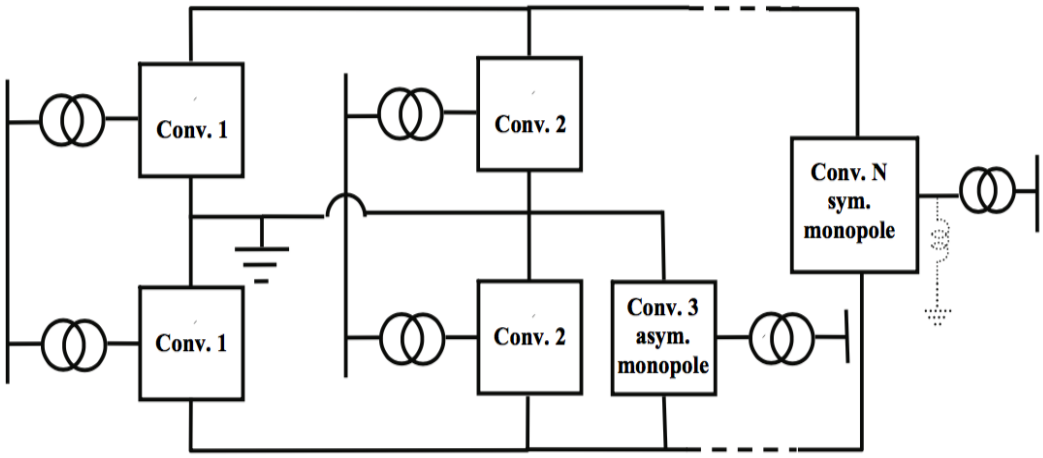

Figure 7. Combination of the configurations [11, page 18]

STATION LAY-OUT

CONVENTIONAL HVDC

Conventional HVDC's stations depends on numerous factors such as DC system configuration, AC filtering and the reactive power compensation requirements. The station itself consists of the following elements:

- Converter
- DC equipment
- Converter transformer
- Reactive power elements
- Harmonic filters

The thyristor valves are air-insulated, water cooled and they are normally enclosed in a converter building, which receive the name of valve hall[2].

With the objective of making the most compact possible design, converter transformers are sometimes placed neighboring the valve hall. Valve arresters must be placed immediately next to the valves. Regarding to the cooling systems, closed-

loop valves are used to circulate the cooling medium, which can be deionized water or a mix of water and glycol, through the indoor thyristor valves. The AC system voltage and the reactive power compensation requirements have big influence on the area requirements. Each system requirements have its reactive power exchange and its maximum voltage step. These requirements for each system makes that each individual bank rating is limited by these conditions. In terms of the total space used, the AC yard with filters and shunt compensation can cover up to three quarters of the total area requirements. The following Figure 8, will show a conventional HVDC station layout.

VSC-BASED HVDC

In these type of converters, the transmission circuit is formed by a bipolar two-wire HVDC system. The presence of the DC capacitors is to provide a stiff DC voltage source. AC phase reactors and power transformers are used for the coupling of the converters to the AC system. Harmonic filters are located between the phase reactors and power transformers, which is not common in most of the conventional converters. This is done so that the transformers are not exposed to DC voltage stresses or harmonic loading.

A set of series-connected IGBT positionsform the IGBT valves which are used in

Figure 8. HVDC Conventional Station layout. From [2, page 41].

VSC converters. Each complete IGBT position consists of:

- IGBT
- Antiparallel diode
- Gate unit
- Voltage divider
- Water-cooled heat sink

Each gates unit includes gate-driving circuits, surveillance circuits and optical interface. The gate driving electronics control the gate voltage, as well as the turn-on and turn-off of the current. The goal of this control is to achieve optimal turn-on and turn-off processes of the respective IGBT.

In case that the switching voltage needs to be higher than the rated voltage of one IGBT, more positions are connected in series in order to achieve higher voltage values. If this series connection is required, it is important to bear in mind that all IBGTs must turn on and off at the same moment to achieve a uniformly distributed voltage across the valve.

When the current is the limiting factor, and higher currents are required, the solution comes from the paralleling of IGBT components or press packs.

For VSC converters, AC filters no longer needs the space needed in conventional converters and are not required for reactive power compensation. All the equipment needed for the converter stations is located indoors, expect for the transformer, the high-side breaker and the valve coolers. The next figure (Figure 9) will show the HVDC station layout for VSC converter.

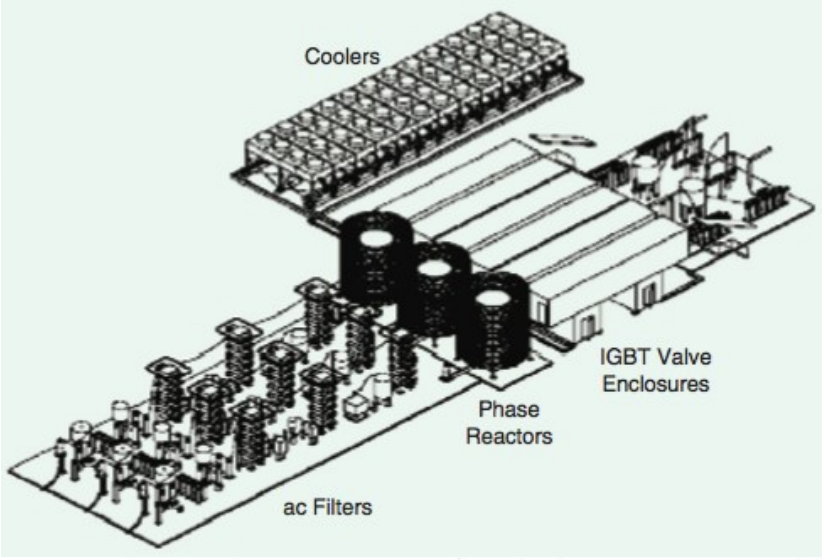

Figure 9. VSC HVDC Station Layout. From [2, page 41]

TYPES OF FAULTS

In HVDC systems there are several types of failures on lines, which will lead to a short circuit in the scheme. These type of faults are the following:

- Pole-to-ground faults
- Pole-to-pole faults

The thesis will put its focus on the pole-to-ground faults as they are considered to be significantly more frequent than the pole-to-pole faults[11]. The main reasons that lead to a pole-to-ground fault are the aging of the cable's main insulation or external damages. These situations provoke the breakdown of the cable insulation and afterwards, that might lead to the pole-to-ground fault.

Once the breakdown has occurred in the cable insulation, an arc burns between the pole and the sheath of the cable. Also, a ground loop through the sheath and the next grounding point is established.

The current that flows through the arc experiments an increase in its value at high speed. This increase in the current is the responsible for the destruction of the cable at ground fault location. Once the cable is destructed, the arc now burns between the pole and the ground. This arc is characterized by being a low-ohmic path for the current.

On the other hand, after the ground fault occurs, the voltage behavior is different to the current's. In this case, the value of the voltage decreases to a level determined by the fault resistance, the fault current and the characteristics of the soil. This drop in the voltage is quick, but not instantaneously, which can be explained by the voltage supporting of the distributed cable capacitance and the inductance in the fault[11], [12] and [13].

MULTITERMINAL SYSTEMS

The majority of HVDC systems are used in point-to-point configurations. These transmission systems are defined as two converter's stations configurations, each station located at each end of the line.

Historically, the idea of using HVDC systems not only for point-to-point connections, but also for multiterminal networks has raised in several occasions. In these networks, the power is exchanged at least between three power converters. The first multiterminal networks that were connected via HVDC systems were implanted in the 1980s and 1990s in Italy and Canada. These systems were based on the previously discussed line-commutated converters. Due to the behavior of these converters, the operation of the DC networks could not be done or only with great effort.

The new generations of self-commutated power converters, makes the operation in multiterminal networks possible due to its multiple advantages compared to the line-commutated converters.

CURRENT EXISTING METHODS

At the moment two methods have been proposed with the objective of advancing into a more standardized way to face the study of short-circuits in HVDC grids. In both cases, the results obtained with the analytical equations proposed have been compared with PSCAD simulations. PSCAD stands for Power System CAD and it is a tool which allows to simulate the electrical behavior of a certain circuit. Besides these two methods, a standard method exists for short circuit in DC grids.There have also been other publications, which have helped the following publications such as: [3],[4],[5],[6],[7],[8],[9] and [10]. Some of these public publications were written by the authors of the methods which are going to be compared. This previous work helped them to get a better understanding of the transient process of the current when a short circuit occurs. These previous publications are related to the understanding of short circuit current transient. Also, different types of converters are studied (six pulse bridge, two-level converters).

STANDARD IEC 61660

IEC 61660 is a calculation method for short circuit currents in DC auxiliary installation of power plants and substations. This standard proposes a time course current divided in two periods. These two periods are separated by the time to peak current (first period before reaching t_p and second period after t_p). The proposed equations in [5] are the following ones:

$$i\,(t) = \begin{cases} i_1(t) = i_p \cdot \dfrac{1 - e^{\frac{-t}{\tau_1}}}{1 - e^{\frac{-t_p}{\tau_1}}} & ,0 \le t \le t_p \\ i_2(t) = i_p \left[\left(1 - \dfrac{I_k}{i_p}\right) \cdot e^{-\frac{t-t_p}{\tau_2}} + \dfrac{I_k}{i_p} \right] & ,t \ge t_p \end{cases} \quad 0.1$$

This current is composed of four different contributions, which are:

- Rectifiers
- Smoothing capacitors
- Stationary batteries
- DC motors

By doing an extrapolation of this method to HVDC systems, some changes must be done. Short circuit current in HVDC systems is not affected by stationary batteries and DC motors, so these two contributions will not be counted for such systems.

IEC 61660 has been proven in classic HVDC models (CSC) and in VSC HVDC models. In [5], two-level converter models are used. This standard proposes equations to calculate the current of each one of the contributions, being different for CSCs models and VSCs models.

The results obtained from the proposed equations are compared to a time domain signal obtained in PSCAD. In these calculations, the lines of the network are simplified to lumped frequency-independent series impedances. This assumption is only valid under certain circumstances, which are: medium voltage network, short

interconnections and small line capacitances. In HVDC systems, these circumstances are not real, and for instance, the capacitance cannot be neglected [11] and [5].

Taking all these into consideration, this comes to achieve reliable results only con certain circumstances, which are the following ones: lines are relatively short, and the DC capacitor and pole reactor are high[11]. Under these circumstances, the lumped element become dominant over the frequency-dependent distributed line parameters. As the goal of a standard for HVDC systems is the good performance of the model in every situation, the IEC 61660 is dismissed for the purpose.

PHD OF ETH ZURICH

This PhD [11]studies transient fault currents in HVDC VSC Network during pole-to-ground faults. It proposes analytic approximation of fault currents from the different contributions of the system.

The network model, which is going to be used, consists of a converter, a DC capacitor and a busbar, which gathers the different lines that converge at that point. Figure 10 shows the network. All these elements in the system have an influence on the short-circuit current and are considered in different equations.

The author divides the short-circuit current into different contributions. One of the contributions are the capacitive sources and the other one the AC Network contribution.

It is important to notice the influence that both contributions have on the total current. The short circuit current during the first few ms after the fault has occurred is dominated by the capacitive sources. In this period, the AC side can be neglected, due to its weak influence[11].

Once this period is over, the next period's behavior is the opposite that the one seen before. The period begins with little influence of the capacitive sources, being the steady-state short circuit exclusively fed by the AC network contribution.

Further variations on different parameters of the system such as fault resistance, DC capacitors, network topology or impedances are done in order to see the parameter's influence.

Capacitive Sources

For the capacitive sources contribution, the equations proposed are obtained based on the planar skin effect and the individual surges. These equations are proven on cable networks, but they can also be applied to OHL configurations.

The chosen configuration to test the capacitor contributions consist of:

- Converter
- DC Capacitor
- Busbar
- Converter
- Faulted line

In this network (Figure 10), a solid pole-to-ground fault occurs.

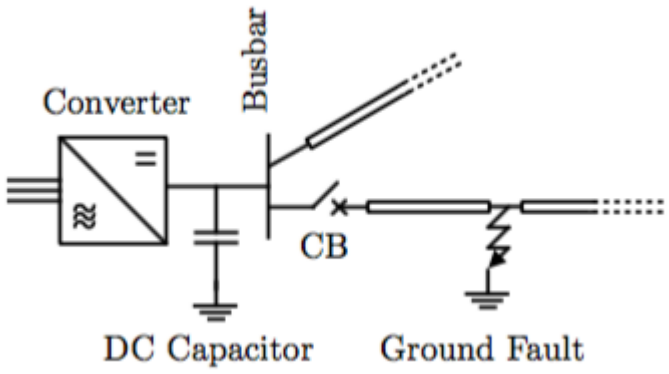

Figure 10. PTP Topology. From [11, page 84]

The faulted line is connected to the busbar. The busbar is also connected to an adjacent feeder, simulating a meshed DC grid. The DC capacitor is between the converter and the busbar and the converter's configuration is a full bridge one. The full bridge converters are blocked immediately after the detection of the fault. For this reason, they can be omitted for the capacitor contributions, being only the DC

capacitor and the adjacent feeder the elements that contribute to the short circuit current.

The capacitive sources contributions also include a division and studies all the elements that belong to them. In the studied system, the DC capacitor and the adjacent feeder are the components which are going to be studied.

The short circuit current that the DC capacitor adds to the system is derived from the voltage that the capacitor experiments. This voltage can be defined as the sum of the forward and reflected, backward travelling wave. The voltage value, the length at which the fault occurs, the reflection coefficient and the travelling wave determine the voltage in the DC capacitor in the Laplace domain.

As the voltage and the current fulfill this equation in the time domain, the voltage should be transformed into this domain. This transformation can be done in two different ways: the first one is an exact transformation and the second one is an approximation. For the thesis purposes, the approximation method satisfies our requirements and the formulas obtained are used.

The adjacent feeder contribution is referred to the transmission through the busbar into the neighboring feeder of the incident negative voltage surge. This surge is initiated at the ground fault location. The neighboring feeder is, thus, discharged, contributing in this way to the total fault current in the CB.

Unlike the DC Capacitor short circuit current, the adjacent feeder short circuit current is calculated with the help of the travelling wave directly in the Laplace domain. With the supposition of the adjacent feeder being infinitely long, there is no backward travelling wave to be considered. This current must also be transformed, in order to be able to work with both contributions in the same domain. Again, two different alternatives are presented: exact transformation and approximation. For the same reasons explained before, the approximation formulas are accurate enough to use them. These equations were proposed in [11], [12] and [13].

$$v_c(t) = V_0 \cdot erfc\left(\frac{\alpha\,\tau}{2\sqrt{t-\tau}}\right) \cdot \left(e^{-\frac{2}{CR_0}(t-\tau)} - 1\right) \cdot \sigma(t-\tau) \qquad (0.2)$$

$$\begin{aligned} i_c(t) = & -C\frac{dv_c}{dt} \\ & = -V_0 \\ & \cdot \left[\exp\left(-\frac{\alpha^2\tau^2}{4(t-\tau)}\right) \cdot (t-\tau)^{-3/2} \cdot \left(e^{\frac{-2}{CR_0}(t-\tau)} - 1\right)\right. \\ & \left. - \frac{2}{CR_0} \cdot e^{\frac{-2}{CR_0}(t-\tau)} \cdot erfc\left(\frac{\alpha\tau}{2\sqrt{t-\tau}}\right)\right] \cdot \sigma(t-\tau) \end{aligned} \qquad (0.3)$$

Once both contributions have been transformed into the time domain, the sum of both of them represent the short circuit current that flows through the circuit breaker when a fault line to ground occurs.

The implementation of these formulas into Matlab leads to time domain signals, which represent the behavior of the current and voltage in the transient period of the short-circuit.

AC Network contribution

This second contribution is responsible of the AC Network infeed. It is noteworthy that not both contributions have their highest impact at the same time. On the one hand, the just discussed capacitor sources have their highest impact during the first few ms of the transient period. Once this period is over, the AC network contribution takes over and becomes the one that defines the total short circuit current. In fact, it can be defined as a gradual process, where the AC infeed starts with almost none importance, at the time when the fault occurs, and gains importance over the capacitive sources the following ms. In the steady state, the short circuit current is only fed by the AC Network contribution.

The publication proposes new analytical expressions, also for this second period in point-to-point connections and multiterminal DC systems. The author reached the conclusion that the, until the time, existing equations that defined the transient process were not accurate enough and only applicable to certain situations.

The presented equations are valid regardless the line configurations (both cable and OHL achieve good results) and the type of fault (pole-to-ground or pole-to-pole). Nevertheless, in his publications, only cable pole-to-ground faults results are presented.

The study makes a difference for the different configurations that the grid can have. The network can consist only of two nodes, which is represented as a point-to-point configuration or it can have more nodes, being in this case a multiterminal network. As it was already said, equations for both situations are provided.

In a pole-to-ground fault, the steady state short circuit current can be calculated by the Ohm's law. These formulas are provided by [12] and [13].

$$I_0^{\text{avg}} = \frac{3}{\pi} \cdot \frac{\sqrt{\frac{2}{3}} \cdot N \cdot V_{\text{ac}}}{\sqrt{R^2 + X^2}} \tag{0.4}$$

$$R = N^2 R_{\text{ac}} + \frac{2}{3} R_{\text{f}} + \frac{2}{3} R_{\text{dc}} \tag{0.5}$$

$$X = \omega\, N^2 (L_{\text{ac}} + L_{\text{t}}) + \omega\, L_{\text{t}} + \frac{1}{2} \omega L_{\text{arm}} \tag{0.6}$$

To do so, the voltage will be divided by the impedance in the steady state and the result will be the resulting current. The phase-to-phase voltage is V_{ac}, the reactances that have an impact on this state of the transient are the transformer reactance L_t, the phase reactor L_S and the armature reactance. The inductances in the DC side can be omitted for the calculation of this current. AC and transformer reactances will need to be multiplied by the transformer turns ratio to the power of two. The resistances used in the formula are the resistance of the faulted cable R_{DC}, and the fault resistance. As well as AC inductance, the AC resistance will also be multiplied by the transformer turns ratio to the power of two.

As it was exposed before, the systems which are going to be studied will be point-to-point and multiterminal configurations. The formulas for the multiterminal networks were not provided by[12], but the Phd [11] derives the formulas for these situations.

STEADY STATE CURRENT

- The point-to-point configurations can be derived in a similar way than (0.4). With the help of Kirchhoff's Current Law (KCL), the following equations are proposed. In a situation, where the fault resistance is zero, equations (0.4) and (0.7) are equivalent.

$$I_0^{\text{avg}} = \frac{\frac{3}{\pi}\cdot\sqrt{\frac{2}{3}}\cdot N_1\cdot V_{\text{ac1}}\left(Z_2+\frac{2}{3}R_{\text{f}}\right)-\frac{3}{\pi}\cdot\sqrt{\frac{2}{3}}\cdot N_2\cdot V_{\text{ac2}}\cdot\frac{2}{3}R_{\text{f}}}{Z_1Z_2+\frac{2}{3}R_{\text{f}}Z_1+\frac{2}{3}R_{\text{f}}Z_2} \qquad (0.7)$$

$$Z_i = j\omega\left(L_{\mathrm{ac},i}N_i^2 + L_{\mathrm{t},i}N_i^2 + L_{\mathrm{s},i} + \frac{1}{2}L_{\mathrm{arm},i}\right) + R_{\mathrm{ac},i}N_i^2 + \frac{2}{3}R_{\mathrm{dc},i} \quad , \; i = 1,2 \tag{0.8}$$

- On the other hand, when handling with multiterminal topologies, the approach to reach the steady state short circuit current is not exactly the same. For the treatment of it, it is expressed a system of linear equations. The topology is divided by the number of terminals present in the configuration. For a *l*-terminal system, l +1 linear equations will be studied. The additional linear equation, comes from the ground fault.

$$\left[Y_{\mathrm{dc}} + \frac{2}{3}Y_{\mathrm{ac}}\right] \cdot \begin{bmatrix} v_{\mathrm{dc},1} \\ v_{\mathrm{dc},2} \\ \cdots \\ v_{\mathrm{dc},n} \\ v_{\mathrm{f}} \end{bmatrix} = \frac{3}{\pi} \cdot Y_{\mathrm{ac}} \cdot \begin{bmatrix} v_{0,1} \\ v_{0,2} \\ \cdots \\ v_{0,n} \\ 0 \end{bmatrix} \tag{0.9}$$

The elements of these matrixes can be calculated following the next equations(0.10)-(0.12).

$$Y_{\mathrm{dc},ij} = \begin{cases} y_{\mathrm{dc},ii} + \sum_{i \neq j} y_{\mathrm{dc},ij} \text{ if } i = j \\ -y_{\mathrm{dc},ij} \text{if } i \neq j \end{cases} \tag{0.10}$$

$$Y_{\mathrm{ac},ii} = [N_i^2\left(j\omega L_{\mathrm{ac},i} + j\omega L_{\mathrm{t},i} + R_{\mathrm{ac},i}\right) + j\omega\left(L_{\mathrm{s},i} + \frac{1}{2}L_{\mathrm{arm},i}\right)]^{-1} \quad (0.11)$$

$$v_{0i} = \sqrt{\frac{2}{3}} N_i \cdot V_{\mathrm{ac},i} \quad (0.12)$$

Y_{dc} matrix represents the admittance matrix of the DC part of the topology, which includes the faulted node and has (n+1)x(n+1) dimensions. Y_{ac} matrix represents the admittance matrix of AC part of the network. In this case, the faulted node is also included, having, thus, the same dimensions as the previous matrix. As Y_{ac} represents the AC side of the topology, the elements of it corresponding the fault node will be zero.

TRANSIENT CURRENT

For the transient current it is important to consider as a start point that the exact time development from all the transient contributions cannot be exactly represented analytically and the formulas that are proposed in [11] are derived from the peak value.

The two contributions studied in this PhD have the peak values at different points and the dimensioning criteria which is used for the derivation of the following equation is that the peak current for the capacitor contributions occur at 2 ms and the peak current for the AC infeed at 13 ms. Assuming this and with the help of the solution of an underdamped, oscillating second order system, the following time domain current equation is proposed:

$$i_{\mathrm{cb}}(t) = \frac{\pi}{3} \cdot I_0^{\mathrm{avg}} \left\{ 1 - \mathrm{e}^{-\varsigma_{MT}\omega_{\mathrm{T1}}(t-T)} \cdot \left[\cos\left(\omega_{\mathrm{MT}}(t-T)\right) + \frac{\varsigma_{\mathrm{MT}}}{\sqrt{1-\varsigma_{\mathrm{MT}}^2}} \cdot \sin\left(\omega_{\mathrm{MT}}(t-T)\right) \right] \right\} \cdot u(t-T) \quad (0.13)$$

$$T = \frac{l}{c} \quad (0.14)$$

$$c = \frac{1}{\sqrt{LC}} \quad (0.15)$$

For the calculation of the damping factor, the method exposed in [11] will be used and the equations required are the following ones (0.16)-(0.25)

$$\varsigma_{\mathrm{MT}} = \varsigma_{\mathrm{T1}} \cdot \frac{\alpha_{\mathrm{T1}} + \alpha_{\mathrm{MT}}}{\alpha_{\mathrm{T1}}} \quad (0.16)$$

$$\alpha_{\mathrm{T1}} = \frac{R\omega}{X} \quad (0.17)$$

$$\alpha_{\mathrm{MT}} = \frac{R_{\mathrm{eq}}}{L_{\mathrm{eq}}} \quad (0.18)$$

$$\varsigma_{\mathrm{MT}} = \varsigma_{\mathrm{T1}} \cdot \frac{\alpha_{\mathrm{T1}} + \alpha_{\mathrm{MT}}}{\alpha_{\mathrm{T1}}} \tag{0.19}$$

$$R_{\mathrm{eq}} = \left[\frac{1}{R_{1\mathrm{f}}} + \frac{1}{R_{13} + \left(\frac{1}{R_{23}} + \frac{1}{R_{34}} + \frac{1}{R_{24}} \right)^{-1} + R_{2\mathrm{f}}} \right]^{-1} + R_{\mathrm{f}} \tag{0.20}$$

$$L_{\mathrm{eq}} = \left[\frac{1}{L_{1\mathrm{f}}} + \frac{1}{L_{13} + \left(\frac{1}{L_{23}} + \frac{1}{L_{34}} + \frac{1}{L_{24}} \right)^{-1} + L_{2\mathrm{f}}} \right]^{-1} \tag{0.21}$$

$$\varsigma_{\mathrm{T1}} = \sqrt{1 - \frac{\pi^2}{\pi^2 + \left(\ln\left(\frac{I_{\max}^{\mathrm{T1}} - I_0^{\mathrm{T1,avg}}}{I_0^{\mathrm{T1,avg}}} \right) \right)^2}} \tag{0.22}$$

$$\omega_{\mathrm{T1}} = \frac{\pi}{\frac{2\phi_{\mathrm{T1}}}{\omega} \cdot \sqrt{1 - \varsigma_{\mathrm{T1}}^2}} \tag{0.23}$$

$$\phi_{\mathrm{T1}} = \arctan\left(\frac{X}{R} \right) \tag{0.24}$$

$$\omega_{\mathrm{MT}} = \omega_{\mathrm{T1}} \sqrt{1 - \varsigma_{\mathrm{MT}}^2} \tag{0.25}$$

TU DARMSTADT DISSERTATION

In this dissertation[14], the author proposes equations for different parameters of the short-circuit transient current response after the fault. These parameters are time to peak, steady state short-circuit current, short-circuit current initial slope and current peak.

Unlike the PhD from Zurich, this dissertation studies four different converters:

- Six-pulse bridge
- Twelve-pulse bridge
- Two-point converter
- Modular multi-level converter

All of these converters are studied for monopolar and bipolar configurations, so equations for eight different configurations are provided.

Another difference that can be easily found between the two studies is that the TU Darmstadt's formulas give special point of the time course, while the PhD from Zurich gives time domain signals as results. In the future comparison, these characteristic points from the current (steady state and peak current) will be obtained from the time course result of the PhD and compared to the values from the TU Darmstadt method.

The goal of the thesis is to compare both methods and see which one yields better results for different situations. To achieve that goal, only the configurations that can be compared in both methods will be implemented. In this case, only two-level converter configuration will be studied.

The two-point converter is one of the self-commutated converters with switch-off IGBTs that are connected in anti-parallel to diodes. In the event of a short-circuit

on the DC side, these IGBTs are blocked within a few microseconds. The corresponding equivalent circuit diagram is the following one (Figure 11).

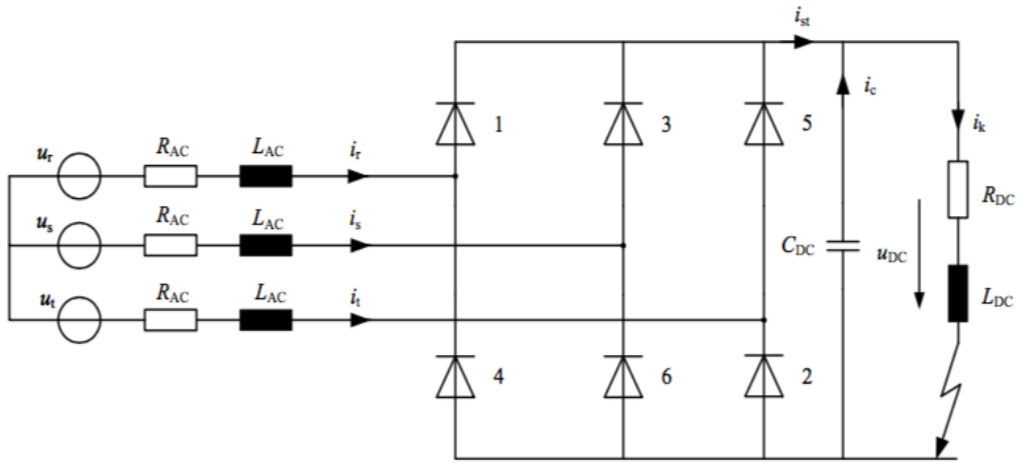

Figure 11. Two level converter's equivalent circuit. From [14, page 132]

This kind of converter's main characteristic is the fact that the output voltage is limited to two voltage levels. Another important point in these converters is the importance that the dc capacitor has. Before the short-circuit occurs, the capacitor is charged to the voltage u_{DC}. If the capacitor is neglected, the equivalent circuit diagram of the two-point converter corresponds to the six-pulse bridge. For these converters, capacitor's and dc infeed's contributions can be easily distinguished, existing a current's peak for both contributions.

Two-level converters can be applied to monopolar and bipolar configurations (these configurations were explained previously in 0). In the case that concerns the thesis, only bipolar configurations will be studied.

As it was said before, the first step is to adopt the benchmark that the TUD Dissertation gives to implement the formulas and check their reliability. Luckily, the publication presents a wide range of different parameters that makes it easier to build a robust model.

The formulas provided provide some of the characteristic point the transient period of the short circuit current. The formulas provided are the following ones:

$$I_{\mathrm{k}} = \frac{\hat{u}}{\sqrt{\left(R_{\mathrm{AC}} + \frac{2}{3}R_{\mathrm{DC}}\right)^2 + (\omega L_{\mathrm{AC}})^2}} \quad (0.26)$$

$$i_{\mathrm{pC}} = \frac{U_{\mathrm{DC}}}{\omega_{\mathrm{res}} L_{\mathrm{DC}}} sin\left(\omega_{\mathrm{res}} \cdot t_{\mathrm{p}}\right) \cdot \mathrm{e}^{-\delta t_{\mathrm{p}}} \quad (0.27)$$

$$t_{\mathrm{p}} = \frac{1}{\omega_{\mathrm{res}}} \cdot \arctan\left(\frac{\omega_{\mathrm{res}}}{\delta}\right) \quad (0.28)$$

$$i_{\mathrm{p,6PB}} = \kappa \cdot I_{\mathrm{k}} \quad (0.29)$$

$$\kappa = 1 + \sin(\gamma) \cdot \mathrm{e}^{-t_{\mathrm{p}}/\tau} \quad (0.30)$$

$$i_{\mathrm{p}}^{*} = i_{\mathrm{p,6PB}} + 0.2\, i_{\mathrm{pc}} \mathrm{e}^{-\frac{R_{\mathrm{AC}}}{X_{\mathrm{AC}}}} \quad (0.31)$$

$$i_{\mathrm{p}} = max\left\{i_{\mathrm{pC}}, i_{\mathrm{p}}^{*}\right\} \quad (0.32)$$

$$\delta = \frac{R_{\mathrm{DC}}}{2L_{\mathrm{DC}}} \qquad (0.33)$$

$$\omega_0^2 = \frac{1}{L_{\mathrm{DC}}C_{\mathrm{DC}}} \qquad (0.34)$$

CHAPTER 3 : IMPLEMENTATION

PHD METHOD

The implementation of the formulas proposed in the ETH PhD, was done in Matlab, with ".m" files. The thesis proposes formulas for the different contributions of the electrical system. The procedure followed here was the following:

- Independent implementation for the different contributions
- Checking the reliability of the formulas with PSCAD simulations
- Superposition of the contributions
- Comparison with PSCAD simulations

INDEPENDENT IMPLEMENTATION FOR THE DIFFERENT CONTRIBUTIONS

This is the first part of the process. Here, the proposed formulas in the PhD are studied and implemented in Matlab. The different contributions that the author proposes are: Capacitive sources contributions and AC Network contribution.

Capacitive sources contributions are subdivided into DC capacitor's current and the adjacent feeder's current contribution, while AC network contribution is just one equation.

At this point, the benchmark and the system parameters were the same proposed in the original publication. By selecting the same parameters, the graphics obtained could be compared to the ones in the PhD.

The formulas given in the thesis [11], were not the correct ones, as the results were not the expected ones, and the calculations of the right formula was done.

The new equation provided results much more accurate and similar to the provided ones. This equation is the following:

$$
\begin{aligned}
i_c(t) = & -C\frac{dv_c}{dt} \\
& = -C \\
& \cdot \left[-\left(2V_0 exp\left(-\frac{2t-2\tau}{CR_0} \right) \cdot erfc\left(\frac{\alpha\tau}{2\sqrt{t-\tau}} \right) \right) \cdot \frac{1}{CR_0} \right. \\
& + V_0 \alpha\tau \cdot exp\left(-\frac{\alpha^2\tau^2}{4(t-\tau)} \right) \cdot exp\left(-\frac{2t-2\tau}{CR_0} - 1 \right) \\
& \left. \cdot \frac{1}{2\sqrt{\pi}(t-\tau)^{3/2}} \right]
\end{aligned}
\qquad (0.1)
$$

The new equations, including the corrected one, were tested on different networks, with different line parameters. The most influencing factors are the DC capacitor and the line length. The studied layouts were the following ones:

Table 1: Different layouts system's parameters

Parameters	Layout 1	Layout 2	Layout 3
C_{DC} [µF]	100	100	1
x [km]	10	100	100

CHECKING THE RELIABILITY OF THE FORMULAS WITH PSCAD SIMULATIONS

The next step is to look at the signals obtained and compare them with PSCAD simulations. To do so, the same network used for the analytical equations is implemented in the software PSCAD. The network consists in a point-to-point connection, where the parameters shown in Table 1 are used. The rest of the parameters of the systems are the following ones:

Table 2. System's parameters

Parameters	
Rated converter power	450 MW
DC Voltage	320 kV
AC Voltage	400 kV
SCR of AC Network	20
X/R of AC Networks	10
Transformer leakage reactance	0.1 p.u
Transformer Turns Ratio	270/400
Converter Phase Reactor	0.05 p.u
C_{DC}	10 – 100 μF
R_f	0 – 4 Ω
Line length	10 – 100 km

These different systems lead to the following current waveforms in the time domain. In the original publication [11], the author describes a correction factor that is applied to the different contributions. This correction factor is visually estimated and set to 0.88. In the simulations done, three different factors were tested in order to compare which one lead to a better performance. The three different factors were 0.75, 0.88 and 1. In the following pictures the results are shown with the best correction factors, which were 0.88 and 1. It has been proved that the best result was when the factor of 0.88 was used, as the author described in the original thesis.

Due to this, the figures will show the behavior of the current when this factor is applied (Figure 12-Figure 14). The selected layout is the third one, where the values

of the parameters are C_{DC} = 1 μF and x = 100 km. The rest of the simulations for the layout 3 can be seen in the appendix Figure 35- Figure 40.

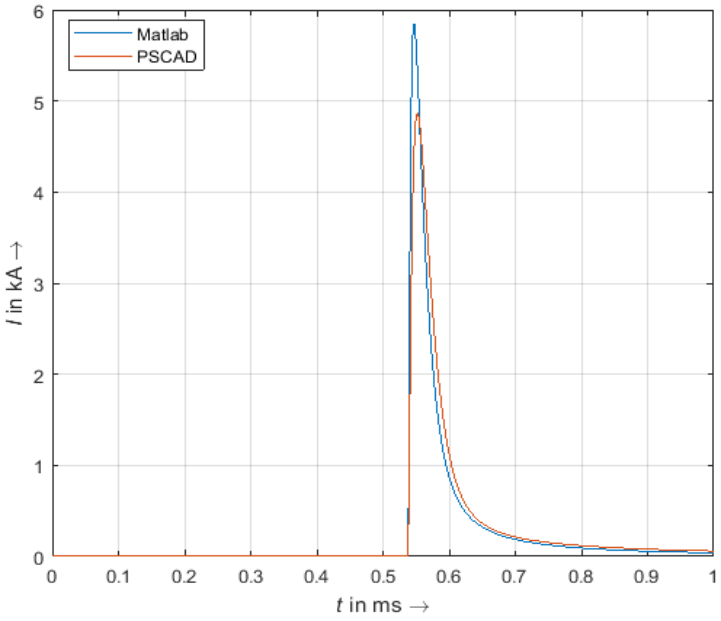

Figure 12. Current capacitor contribution for Layout 3 and CF 0.88

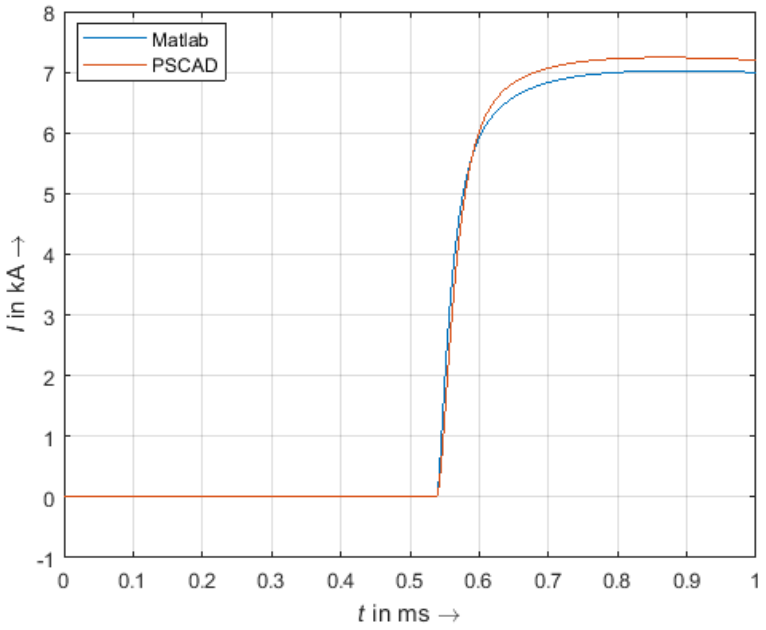

Figure 13.Current adjacent feeder contribution for Layout 3 and CF 0.88

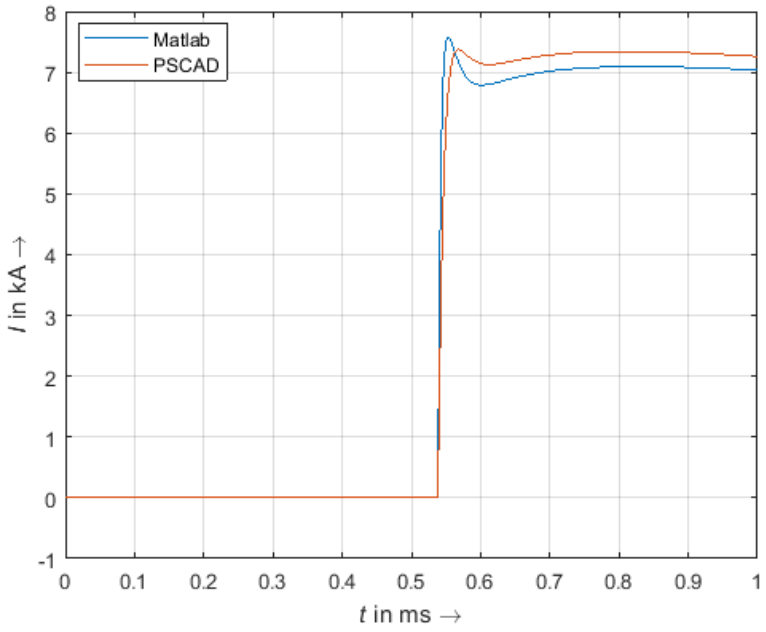

Figure 14. CB Current for Layout 3 and CF 0.88

In this layout, the objective is to check how the systems behaves when the value of the DC capacitor is very low (1 μF) and the distance to fault is 100 km. Observing the three previous figures, it is seen that the current capacitor contribution is almost 1 kA higher in the peak moment, while in the rest of the time course both waves match accurately.

On the other hand, the Matlab simulation is slightly lower for the adjacent feeder contribution in the peak value. Overall, when both contributions are superposed, the CB current present a very good behavior and the time domain signal can be said to be reliable.

The figures of the first and the second layout are attached in the appendix of the thesis. The observed behavior of those two layouts will be described in the following paragraphs.

In the first layout, the distance to the fault location is 10 km and the DC capacitor has a value of 100μF. With these conditions and a correction factor of 0.88the obtained results are shown for the first ms. In the simulation it was be observed how the number of surges seen in the PSCAD simulations are 9 for the specified time, while the Matlab analytic simulation only represent one. The original PhD proposes a formula for the subsequent surges, but it is only valid for the first two-three surges, and afterwards does not give reliable results. This situation is also attached in the appendix Figure 41.

Furthermore, the PSCAD model stablished to obtain these results (in this layout) is not a realistic one and the future topologies and parameters will not lead to these results (more than one surge and currents of 60 kA).

On the other hand, the second layout yield to more realistic results than the first one. In this case, the distance to the fault is 100 km and the dc capacitor value is 100μF. These contributions can be seen to be important only in the first few ms. That is the reason that the simulated time for these simulations is only 1 ms. In this layout, with the set of parameters chosen, the current capacitor contribution experiments an error of about 2 kA, while the current adjacent feeder contribution follows better the expected value of current.

Analyzing the simulations and comparing them to the original and PSCAD simulation ones it can be said that the implementation of the capacitive sources currents is done correctly.

The next step is to implement the AC infeed contribution. To do so, another system is implemented in PSCAD, where the other contributions have no influence on the system. This is not a situation, which is normally seen in reality, but it is done to be able to compare both analytic and PSCAD simulations in the most independent way.

In this case, the obtained result was the following one (

Figure 15):

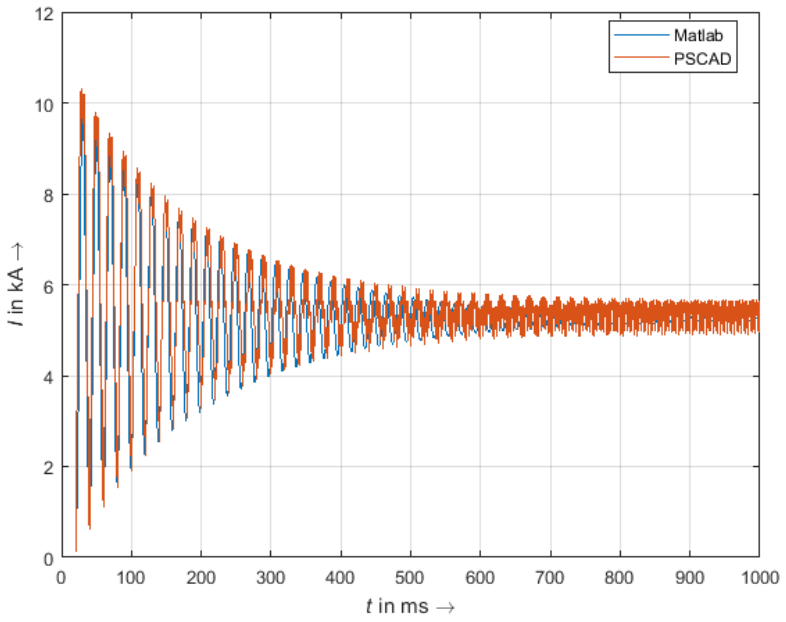

Figure 15. AC Network contribution's comparison

This figure compares the PSCAD simulation with the Matlab analytic behavior in the time domain. When the total system is studied, the AC system infeed will have its most influence after the capacitor contributions are extinguished. It is also important to notice that this behavior is not the expected one for the AC infeed when all the contributions are connected to the system, and this simulation is only done to compare the trustworthiness of the proposed equations.

As it can be seen the analytic solution matches good with the PSCAD solution both in the first part of the transient and in the final steady state current, which will determine the steady state of the complete system. When all the contributions are connected in the system, the AC network contribution will also be studied and analyzed to monitor and control that its contribution is also correct under those circumstances. The damping factor applied to it is one of the most decisive parameters in the behavior of the system and needs to be constantly reviewed.

SUPERPOSITION OF THE CONTRIBUTIONS

Once all the contributions have been separately implemented and calculated, the next step is to overlay the different contributions to have the real total current response when a fault phase to ground happens.

The superposition will be done in two steps: first all the capacitive sources will be superimposed and afterwards, the result from the capacitive sources will be overlaid with the AC network contribution.

For the capacitive sources the number of surges needs to be taken into account, using the following formula and being N the number of surges. The following formula (0.2) ,is the one applied for the superposition of the capacitive sources:

$$i_{\mathrm{cb}}(t) = \left[\sum_{m=0}^{N-1} i_{\mathrm{f}}(t - 2\tau m) + i_{\mathrm{c}}(t - 2\tau m)\right] \qquad (0.2)$$

Subsequent surges are observed, but as it has been proven empirically, this equation is only valid for the first few instants (0-0.2 ms) of the simulation.

COMPARISON WITH PSCAD SIMULATIONS

The last part of this method implementation and study is to compare the total current with PSCAD simulations for the whole system contributions and in different situations.

At this point it is crucial to evaluate the parameters that are going to be selected for the system, as conclusions are going to be obtained from these graphics and time courses. Unlike the previous points of this method, it is not necessary to select the same benchmark as it was in [11]. The equations have already been proved to work and this gives more freedom in terms of a wider range of parameters values to choose and, as a result, more interesting conclusions can be obtained.

As it was said before, the objective of this procedure is to study the accuracy of the method in, as many different configurations as possible. To do so, it is interesting and important to look at point-to-point configuration and also at multiterminal networks. Taking into account, that equations are provided for both configurations, the comparison can be calculated both for point to point and multiterminal networks.

The point to point configuration consists of two converters, which are connected with a cable. At one point in that cable, the fault occurs. On the other hand, when looking at a multiterminal configuration, more than two converters will form the network. The system selected will consist of 4 different nodes, with 4 converters and different lines connecting the nodes. The multiterminal topology used, is the same that the one implemented in [11]. This decision was made, due to the fact that the equations proposed included equations to calculate the equivalent resistances, that were only applicable to that topology. In the following figure (

), it is shown:

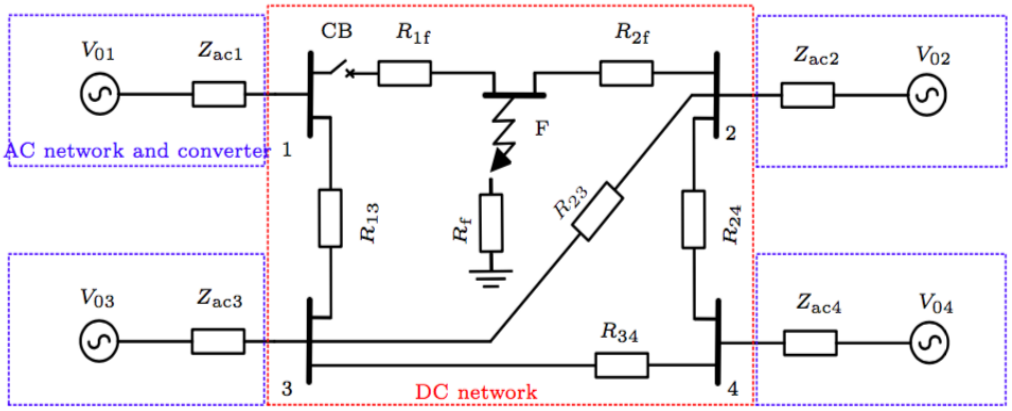

Figure 16. Multiterminal topology selected. From [11, page 110]

In the next steps, the results obtained will be presented and studied:

Point to point configuration

To get as many conclusions as possible a wide range of different parameters were set up to analyze the outcome of the system transient behavior. In the thesis it has already been proved that the main parameters which affect the transient response of the system are:

- Line length
- DC Capacitor
- Ground resistance
- DC inductance
- Converter inductance
- AC impedance

In the following chapters, the parameters which are going to be studied are the line length, the DC capacitor and the ground resistance.

These three parameters determine mostly the transient current and times, even though there are other parameters that also affect the transient, which can be related to the converter (SCR, power, resistance and inductance values, etc.). In this thesis, converter's parameters will be considered constant, and the only changes, which will be considered are the mentioned ones.

The first parameter to be studied and changed is the line length. Five different line lengths will be analyzed, which will cover the range from shorter lines (10 km) to longer lines (100 km). In-between those to values, other line lengths such as 30, 50 or 70 km are to be considered. This selection of the line lengths was done to cover the different possibilities that the behavior of the current could have. For short lines (10 km and less), the DC capacitor's influence is higher than the converter's influence on the short circuit current. In these cases, the total peak current is determined by the DC capacitor. With an increase on the length, the influence of the converter increases to the detriment of the influence of the DC capacitor, being the total peak determined no longer by the DC capacitor, but by the AC infeed. The maximum line length which is studied is 100 km, because the behavior that the current has does not change qualitatively (it does change quantitatively). For the study of the lines, groups of line lengths are made considering the behavior that the transient current experiments.It has been proven that short lines (10 km) behave differently that medium lines (30, 50 and 70 km) and longer lines (100 km).

For each of those distances, the DC capacitor (C_{DC}) and the ground resistance (R_f) will be varied in order to see which the most relevant changes and which parameters are affect the most. The C_{DC}will cover the range from 10 μF to 100 μF, having intermediate values (30, 50 and 70 μF) and the R_f will take three different values which are 0, 2 and 4 Ω.

With all these different variations, the objective is to analyze if the change produced by the DC capacitor's and the ground resistance's variation is the same independently of the line length or if, on the other hand, it affects more at some values of line lengths.

Line length: 10 km

This is the shortest line length that will be discussed in the thesis and significant changes can be appreciated when the results are compared to a 100 km line. One of the most relevant aspects that can be concluded is that the line length has an important influence on the capacitor contribution current's peak. Maintaining the C_{DC} and the R_f constant, it can be observed that the capacitor contribution current's peak (i_{cp}) decrease with an increase on the line length. This is explained because for short distances to the fault, the converter component is relatively low and the short circuit current is determined by the capacitor current. When the fault location is at higher distances, the opposite behavior occurs.

For this length, the waveform that the current has is the following one (Figure 17). As it can be read in the legend, the blue signal represent the Matlab result for the proposed method, while the red and the yellow signals were obtained with PSCAD.

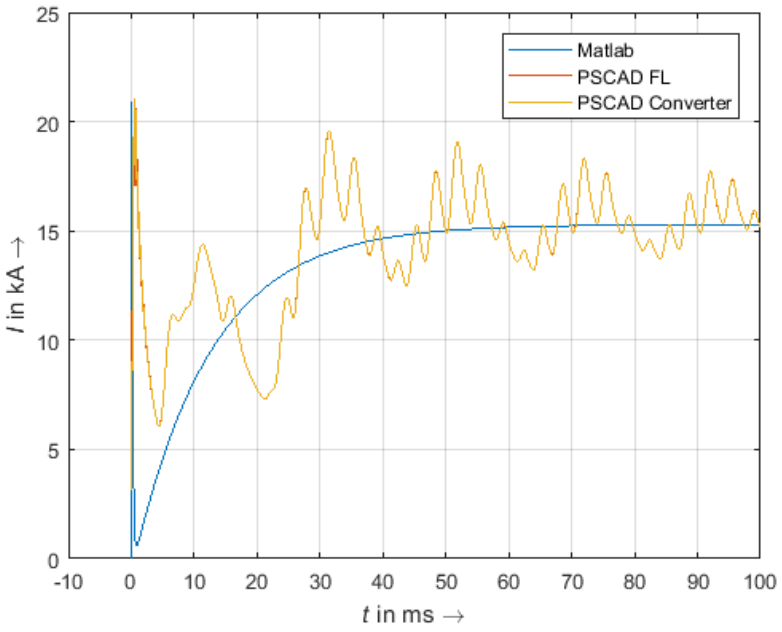

Figure 17. PSCAD- Phd method Current behavior comparison (10 km, 10 μF, 0 Ω)

The difference between both of them is that the red signal is the current measured at fault location, while the yellow one is the current measured just after the converter.

Even though the difference is almost not appreciated, the PhD method was developed for the current after the converter and the TUD dissertation was developed for the current at fault location.

As it was said before, for shorter lines, the DC capacitor has more influence than for longer lines, and in this case, the total peak current of the transient (i_p) matches with the capacitor contribution current's peak (i_{cp}).

The next step is to analyze how the behavior changes for alterations in the C_{DC} and the R_f.

First, the R_f will be kept constant to a certain value (0 Ω for example), and the relative and absolute error in the peak and steady state current will be measured for different values of the C_{DC}. Afterwards, the procedure will be done the other way around, keeping constant the DC capacitor and making variations in the ground resistance. In this figure Figure 18, the absolute error for the PhD method can be seen for different values of C_{DC}, when the R_f is kept constant.

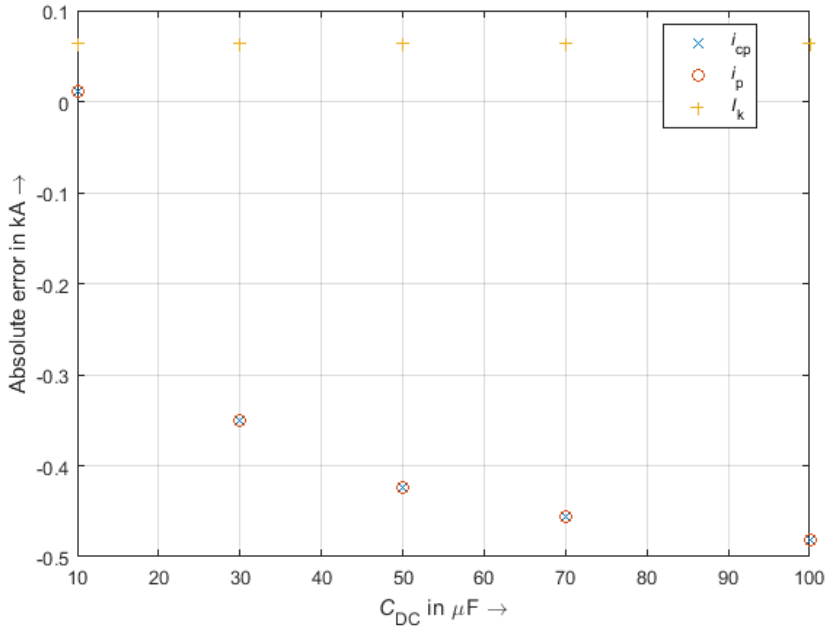

Figure 18. Absolute error for PTP x = *10 km,*R_f = *0* Ω *and variation in* C_{DC}

Errors from three different points are measured (capacitor contribution current peak (i_{cp}), total current peak (i_p) and steady state current (I_k)). These points are taken and measured from the time course current that the equations provide.

Analyzing the three different characteristic points, it is interesting to see, how I_k does not experiment any variation when the C_{DC} is modified. As it was explained before, this is because the C_{DC} has its influence in the first part of the transient, and not in the last part, when the steady state current is determined. In the next chapters, it will be seen how this steady state current varies depending on the line length and the ground resistance, but remains unchanged for different values of C_{DC}. This is explained, due to the fact that the contribution of the C_{DC} is extinguished in the last part of the transient, where the steady state current is determined. For the exposed configuration, the absolute error is lower than 0.1 kA.

Another interesting point to see, is that for short lines, the peak current matches with the capacitor contribution's peak.

This current peak's error reaches its minimum value for very low capacitors, being almost 0 for 10 μF. An increase in this value, makes the error increase, reaching its maximum value for 100 μF, 0.5 kA.

In the next figure (Figure 19), the relative error for the PhD method can be seen for different values of C_{DC}, when the R_f is kept constant.

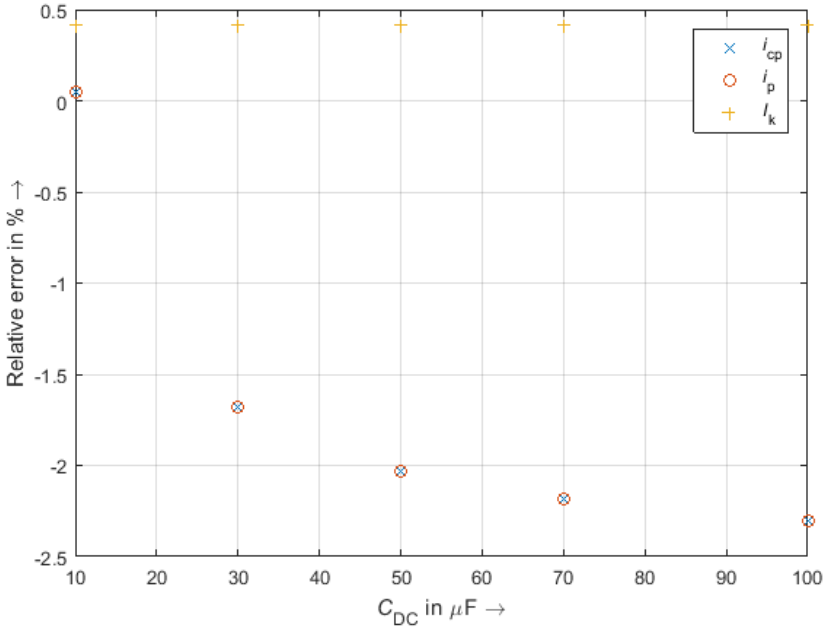

Figure 19. Relative error for PTP x = *10 km,* R_f = *0* Ω*and variation in* C_{DC}

It is also important to check the errors in a relative way, due to the fact that an error of 1 kA is not equally critical when the expected value is 2 kA or 20 kA. In the case of PTP configurations, for a 10 km line and ground resistance of 0 Ω, the relative error for the peak current varies between almost 0 %, for low DC capacitors, and -2.5 % for the highest DC capacitors. Taking a look at the steady state current, the relative error is slightly below 0.5% for all the values of C_{DC}.

The next figures (Figure 20 and Figure 22) will show the absolute and relative error for steady state, and peak current in a configuration where the C_{DC} remains unchanged (10 μF) and the R_f changes from 0 to 4 Ω.

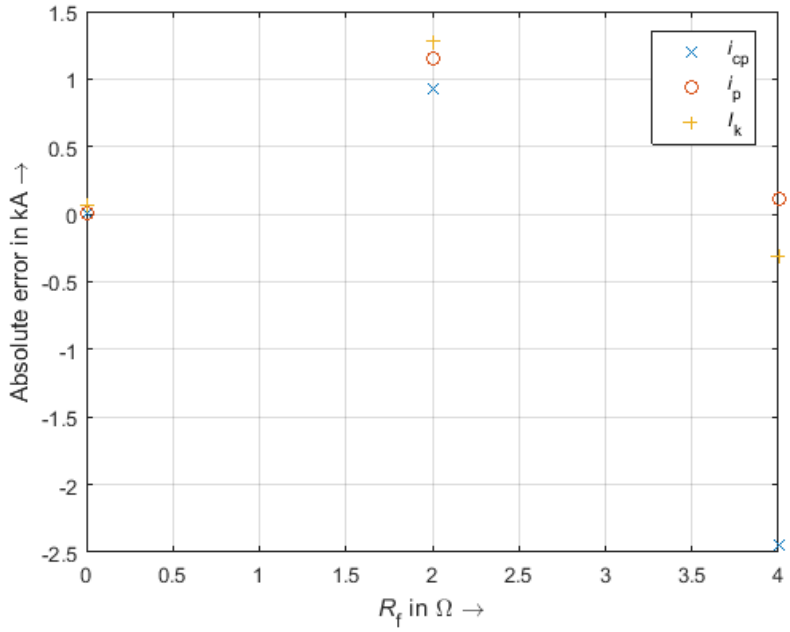

Figure 20. Absolute error for PTP x *= 10 km,* C_{DC} *= 10 µF and variation in* R_f

In configurations, where the ground resistance varies, the steady state current remains no longer constant, but experiments changes. It is also interesting to observe that the peak current of the transient no longer occurs due to the capacitor contributions, but it occurs in the period where the AC infeed is the most influencing contribution. This fact is represented in the following figure (Figure 21), which represents the Matlab simulation, and the PSCAD values in the fault location (PSCAD FL) and in the point next to the converter (PSCAD Converter).

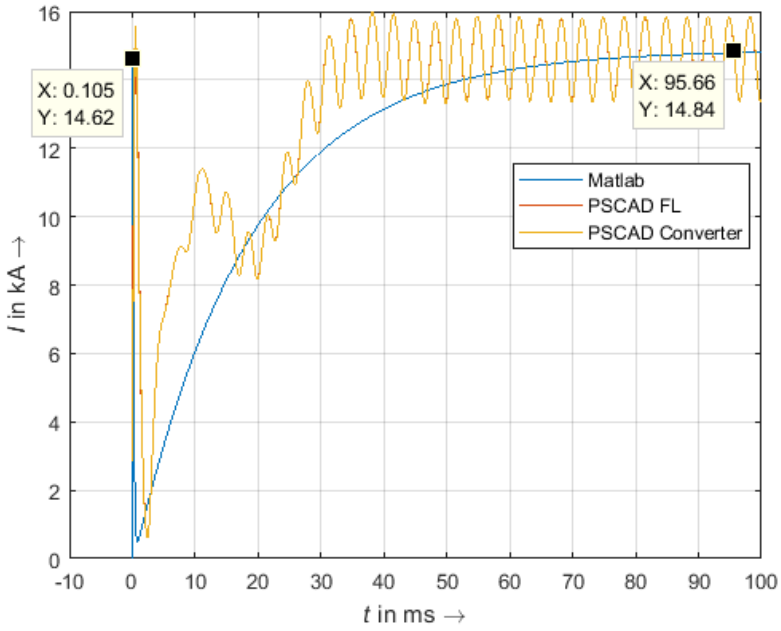

Figure 21. PSCAD- Phd method Current behavior comparison (10 km, 10 μF, 2Ω)

As it can be seen in the figure, the highest value of the current in the transient process is no longer the peak at the beginning, but the steady state current.

Back to Figure 20, i_{cp} experiments it highest error for the highest value of R_f (4 Ω), while its minimum errors is reflected for a configuration where no ground resistance exists (0 Ω).

On the other hand, both I_k and i_p present very accurate results for 0 Ω and 4 Ω, while for an intermediate value of ground resistance, the error is higher. Due to this situation, the impact of the ground resistance on steady state current and total peak current must be analyzed in further configurations to get better conclusions.

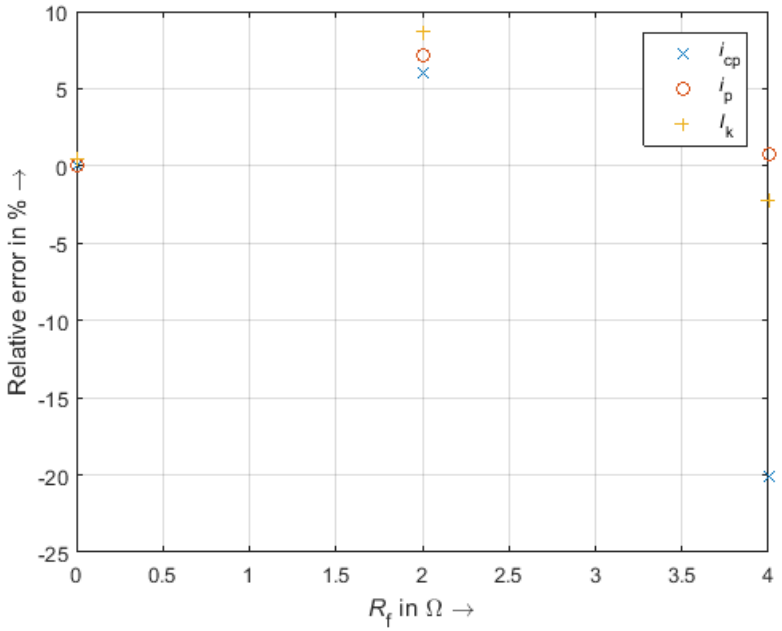

Figure 22. Relative error for PTP x = *10 km,* C_{DC} = *10 μF and variation in* R_f

Looking at the relative errors, instead of the absolute ones, it can be observed that for ground resistance equal to zero, the relative error is between 0-1 %, being the most reliable results. When the ground resistance increases to 2 Ω, the relative error for the three characteristic points is between 5 and 10%. At last, the highest ground resistance analyzed is 4 Ω, and it leads to very low relative errors for the steady state and the peak current (below 2.5%), but a very high error for the peak capacitor current, being around 20%.

Line length: 30 km, 50 km and 70 km

In this new chapter, intermediate line lengths will be discussed. As it was said before, the longer the line, the lower the capacitor contribution's peak will be, due to the relative importance that the converter and the DC capacitor have on the transient current (for shorter lines, the DC capacitor has more influence than for longer lines). As a point to start, for these line lengths, the capacitor contribution's

peak will no longer match with the total peak of the transient period. In these cases, the global peak of the current will be due to the AC infeed.

In the appendix, Figure 42 and Figure 43 show the time domain signals for 30 km and 70 km (C_{DC} = 10 μF and R_f = 0 Ω).

It is important to check if the changes of the parameters (C_{DC} and R_f) affect in the same way to medium line lengths systems than to short line lengths systems. To do so, the same procedure will be followed, maintaining in one case the C_{DC} constant and applying changes to R_f, and in the other case the other way around.

The variables to study are the same ones that were studied before: peak currents (both contributions) and steady state current. Results from the three line lengths were obtained and it can be said that the system behaves the same for the different line lengths, so it makes sense to make an aggrupation of medium lines for the analysis.

As it was done before, first the ground resistance will be set to a certain value (0 Ω) and it will be kept constant. It is observed that a change in the DC capacitor does not have much influence in the % of error that the method presents. There are very few variations between different values of C_{DC} in the three of the variables. These figures can be seen in the appendix Figure 44 and Figure 45.

i_p remains unchanged for the different values of C_{DC} This is because the total peak of the system occurs once the capacitor contribution is extinguished and the dc capacitor does not have any influence.

When looking at i_{pc}, the error that it presents is practically constant, but experiments a slight tendency to increase the error, as the value of the DC capacitor increases.

The steady state current error is also constant, for the same reason that the total peak current remains unchanged.

To sum up, the steady state and the peak current errors remain unchanged when the C_{DC} is changed, while the capacitor contribution current peak's error slightly presents a tendency to increase with an increase in the C_{DC}.

Now, the ground resistance will be the changing parameter, while the C_{DC} remains constant. The Figure 46 and Figure 47 are attached in the appendix.

For these analysis, it is helpful to analyze each of the characteristic points of the current in an independent way, as a change in R_f does not have the same influence in the total peak current, the steady state or capacitor contribution's peak current.

First, the steady state current will be studied. Contrary to the previous change in the DC capacitor, the ground resistance does have big influence on the steady state current. Even though, the value of the steady state current changes with a variation of the ground resistance, the relative error of this characteristic point of the current remains always very low, increasing slightly with an increase in the ground resistance.

When the characteristic value studied is i_{cp}, the system does not behave in a linear way, and no clear tendency can be obtained. The only aspect that is repeated constantly for the different line lengths is that the method usually overestimates the value for low and high values of ground resistance and underestimates the peak for intermediate values of ground resistance.

Finally, the total peak value of the current experiments better results for higher values of ground resistance.

Line length: 100 km

The longest line lengths analyzed are the 100 km ones. In these lines, the difference of the capacitor contribution's peak and the peak of the ac infeed is the highest in the studied cases. The following picture (Figure 23) will show the PSCAD time waves from a 10 km and a 100 km line length superposed.

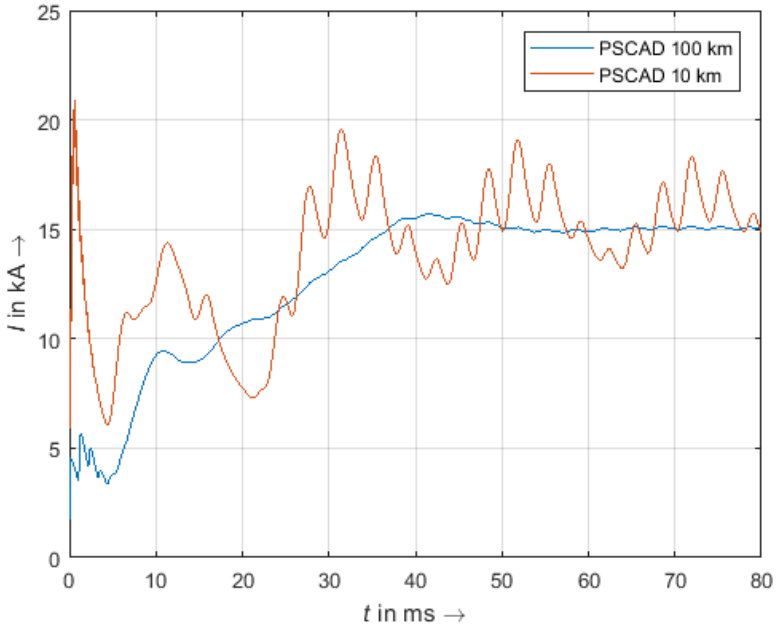

Figure 23 . PSCAD comparison (10 km – 100 km)

The previous figure superpose the PSCAD results for two different PTP configurations, with the same parameters, only changing the line length (10 km and 100 km). As it was said before, it is interesting to observe how the capacitor contribution influence decrease with the increase of the line length, while the steady state current value does not present big changes in the value, but in the ripple it has, being higher for shorter distances.

Regarding to the errors variations due to a change in the parameters, it is noteworthy having in mind that 1 kA will affect much more to the relative error of the longer lines. This is why, even though the absolute error variation for different ground resistances or DC capacitors is the same, the relative errors increase with an increase in the distance.

To gather everything up, regarding to the PTP configuration and the PhD method it is important to bear in mind that two groups can be made in this case.

The first group would consider short lines (10 km), where i_{cp} is the same as i_p of the transient period (almost for all configurations of 10 km the capacitor contribution's peak represents the total peak). In these cases, the peak error increases with an

increase of the DC capacitor, while it does not behave in a uniform way with a change in the ground resistance. Hence, no reliable conclusions can be obtained for a change in the ground resistance. On the other hand, the steady state current presents no change against variations in the DC capacitor, and it presents very good results for low and high values of ground resistance, being slightly worse for intermediate values.

The second group would be the configurations where the capacitor's peak does not represent the total current's peak. Some configurations of 10 km line lengths and the totality of longer lines belong to this group. For this group, three different characteristic points must be taken into account. First, the steady state current's estimation deteriorates with increasing values of ground resistance, while it remains unchanged for different values of DC capacitor. Secondly, the total peak current's error decreases with an increase in the value of ground resistance and remains unchanged for different values of DC capacitor (as when the total peak occurs, the influence of the capacitive sources is already extinguished). Finally, the current's capacitor current does not present clear results in order to achieve a good conclusion. It is noticeable that it tends to underestimate the real value for low and high ground resistance's values and to overestimate for intermediate values.

The last analysist that will be done for this method in the PTP configurations will be regarding to the line lengths. To do so, ground resistance's and dc capacitor's values will be kept constant (10 μF and 0 Ω). The results can be seen in the appendix in Figure 48 and Figure 49.

Analyzing the three different characteristic points for different distances interesting conclusions can be taken.

The behavior of the steady state current is very good, remaining the relative error for the five distances below 2%. There is a slight tendency for this error to increase with the distance.

The total peak estimations present its minimum value for 10 km, where this peak is the same as the capacitor's contribution peak current. If this value is omitted, the error decreases with an increase of the distance, being in all cases the value overestimated.

Multiterminal configuration

The multiterminal topology is the one shown in

. As it was said before, the topology was copied from the PhD in order to be able to use the formulas proposed for that specific layout. If the node topology is changed, these formulas would be no longer valid, so the variations done for this configurations are the same that were applied to the PTP:

- The distance from the converter to the point where the fault occurs is varied from 10 to 100 km covering intermediate values.
- The DC capacitor will also adopt the same values than in the PTP configuration (10, 30, 50, 70 and 100 μF)
- The ground resistance will be changed and, 2 and 4 Ω systems will be studied.

In the MT network, the fault occurs between node 1 and 2 and the distance to node 1 will be changed from 10 to 100 km. Unlike, the PTP configuration, where big changes could be appreciated when the distance was changed from 10 to 100 km, in a multiterminal network, where there are other lines implied in the system, and many other parameters which influence the result, the changes that will be appreciated are much smaller.

Line length: 10 km

The first difference that can be noticed for the multiterminal configuration, is that, with the selected layout, no matter the changes applied to the parameters, the values for the characteristic current points (capacitor's contribution current, total peak current and steady state current) will no change significantly.

The wave form that the transient current will present for this multiterminal configuration is the following one Figure 24:

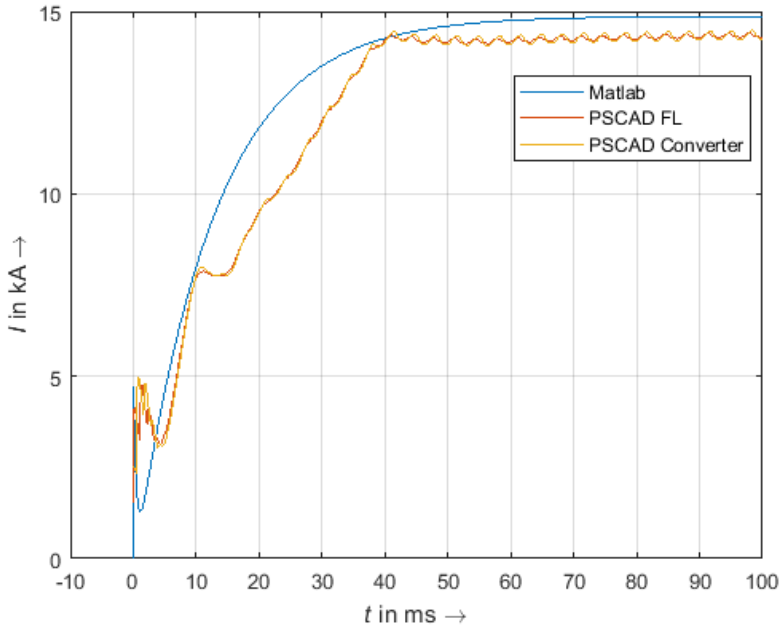

Figure 24. PSCAD- Phd method Current behavior comparison (10 km, 10 μF, 2Ω)

The three important points will be also discussed for the multiterminal configuration and how do they change with the DC capacitor and ground resistance.

The first changes will show how the error changes when the ground resistance is constant and the DC capacitor varies its value. The figures (Figure 25 and Figure 26) can be seen in the appendix and show the described behavior.

Analyzing how the error changes with a change in C_{DC}, the conclusion can be quickly obtained by looking at Figure 25 and Figure 26.

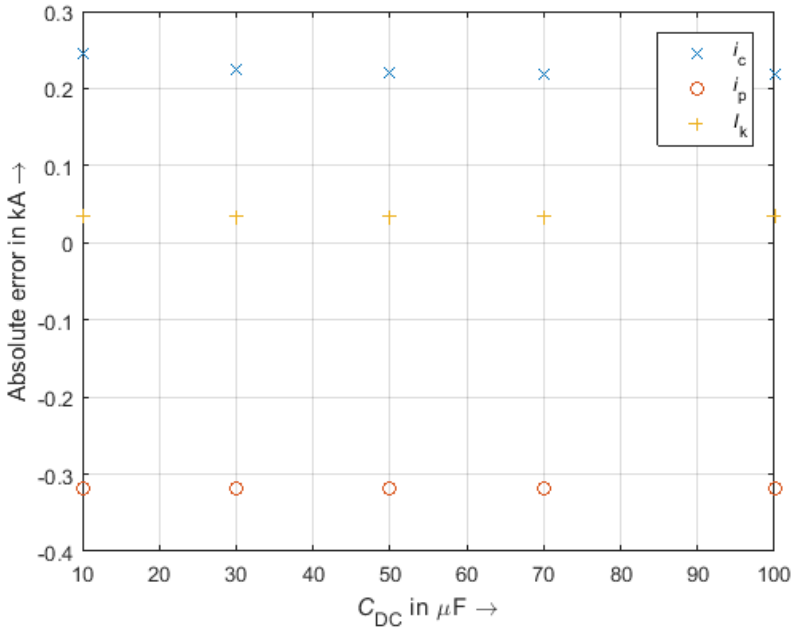

Figure 25. Absolute error for MT x *= 10 km,* R_f *= 2* Ω *and variation in* C_{DC}

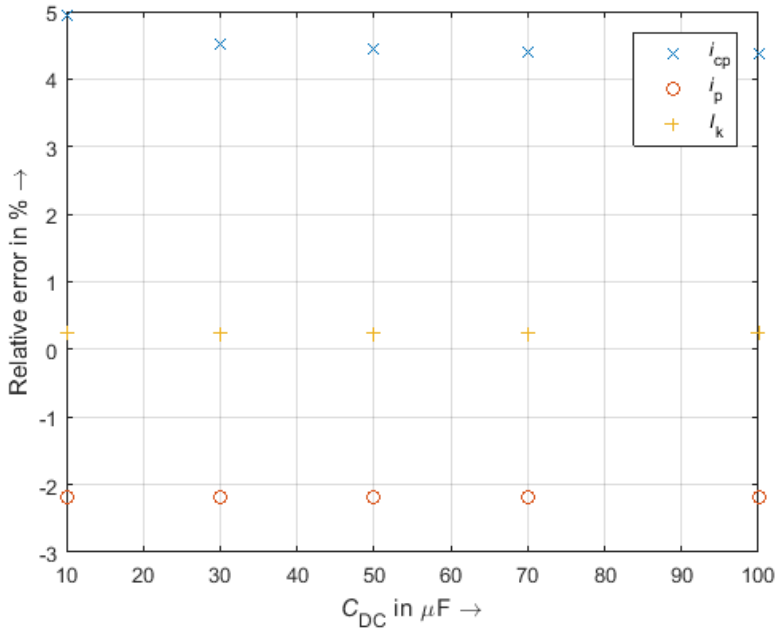

Figure 26. Relative error for MT x *= 10 km,* R_f *= 2* Ω *and variation in* C_{DC}

In this case, the DC capacitor does not have any influence on the presented error and it remains practically unchanged. In the steady state current and peak current, in fact, it does not change at all, due to the fact that the DC capacitor has an influence in the first part of the transient and then it extinguishes. Once the influence of the DC capacitor is extinguished, the AC infeed is the one that determines the value of total peak and steady state current. The capacitor current's peak presents slight changes, with differences lower than 0.5%.

Once the influence of the DC capacitor is tested, the ground resistance is the parameter to look at. C_{DC} will be set to 10 μF and R_f will change in order to try to find a tendency in the way the method works for different values of resistances.

The figures (Figure 50 and Figure 51) show the absolute and relative error that the system has when the ground resistance is changed. As it can be seen, the capacitor current contribution's peak error and the steady state current's error is not affected by a change in the resistance, while the peak of the system's error does change. In this case, the error increases by almost 1%.

Line length: 30, 50 and 70 km

The next line lengths to be analyzed are the medium lines. For these lines, the behavior against a change in the DC capacitor is the same as for short lines (10 km).

If the parameter kept constant is the C_{DC} and the R_f changes, the behavior of the i_{cp} is the same that the one seen in short lines. On the other hand, I_k and i_p error have a different variation when analyzing medium lines. To do the analysis, the following figures will be useful. The results are in the appendix (Figure 52 and Figure 53)

The conclusion that can be obtained from the data taken is that the method tends to underestimate the values for lower ground resistances and overestimate for higher values of ground resistance, being the error very low in both cases and below 4%.

Line length: 100 km

The estimations for long line lengths present the same error variation that medium line lengths.

The last analysis to do for multiterminal configurations is how the distance to fault affects the current estimations. For it, the DC capacitor and the ground resistance will be set to 10 μF and 2 Ω respectively. The figures can be seen in the appendix (Figure 54 and Figure 55)

For the steady state current, the best results are obtained for short distances (less than 0.5% of relative error), while for medium and long lines the error stabilizes in 3.5%.

When the point to be studied is the total peak current, it can be seen how the error is also slightly better for short lines (around 0.5% better) than for medium and long lines.

To finish with the characteristic points, the capacitor current contribution's peak is the only value which presents worse results for short than for medium and long lines. In this case, the difference is higher than before, and it is of almost 4% worse for short lines.

Knowing how the three values change and where does these currents come from, it can be concluded that the capacitor contributions lead to better results in medium and long lines, while the AC infeed contribution has slightly better estimations for longer lines.

Conclusion

Once the influence of the parameters has been studied (both in PTP configurations and MT networks, an explanation to the errors in the steady state current and in the peak currents is provided.

The differences observed for the steady state current are due to the simplified calculations that have been used. In these calculations, only the sixth harmonic was considered, and not the rest of the harmonics which are present in the simulations.

On the other hand, the error which is observed on the peak values are due to the estimations errors in the single terminal damping ratio (ς_{T1}). The value of the single terminal damping ratio is estimated in the first place. This estimation leads to error in the peak currents.

After these four steps, the PhD equations are totally executed, and the results are ready to be compared with the TUD Dissertation method.

TUD DISSERTATION'S METHOD

This second method to study the system behavior was developed in TU Darmstadt in 2016. Unlike the first method already discussed, this one does not provide a time domain signal, but it gives some key values in the current response to a phase to ground fault. These values are:

- Time to peak
- Steady state short circuit current
- Peak short circuit current
- Short circuit current initial slope

The given values correspond to the values experimented by the total current, taking into account all the superpositions.

The work methodology applied to this method will be the same one applied to the first one, and will be the following one:

- Equations implementation
- Checking the reliability of the formulas with PSCAD simulations

In this case, unlike the first method, the equations provided are directly considering all the superposition of the different contributions (capacitive and AC infeed contributions) and that step can be skipped.

To proceed in that way, the benchmark and the parameters selections proposed in the dissertation will be taken and used for the Matlab simulations.

As it was said before, the aim of this part of the thesis is to be sure to implement the formulas correctly, so that the results can be treated with a high level of reliability. To do so, all the given parameters combinations will be tested and compared.

As happened with the PhD from Zurich, the input parameters in these formulas are the AC and DC impedances, the converter parameters and the voltages of the system.

Two of the most important relations that are observed to have a big influence on the output are the R_{DC} and R_{AC} relation, as well as L_a and L_{AC} relation. With different values for these relations, diverse output signals are observed, and the robustness of the equations are tested. There can be big difference between a very low and a very high parameter's relation.

To be sure that the equations proposed in the dissertation were correct and that the implementation done in Matlab was also satisfactory, these equations are implemented in Matlab and the results are compared to the expected ones.

The original dissertation provides a wide range of parameters and its respective results of steady state current, peak current, initial slope and time to peak. By adopting the same parameters choice, the results obtained should be the same. By doing this test, it can be proven that the equations are correct and the implementation in Matlab is also adequate. Once this step is done, the parameters selection can be changed and other conditions can be studied.

The comparison lead to some interesting results. The results obtained for the characteristic points were accurate and in very few cases the results were slightly different. Not even for the highest error, the difference was so big, that the implementation could be categorized as wrong.

Once the formulas are implemented and compared to the proposed graphics of the original publication, it can be said that the implementation of this publications is

also completed. The next step is the comparison to PSCAD simulations in different situations.

Comparison with PSCAD simulations

For the TU Darmstadt Dissertation method, also two different topologies were studied. First, PTP configurations will be studied. The range of variations in the parameters is the same that it was applied in the previous method.

A distinction between line lengths is done, where the distances simulated are 10, 30, 50, 70 and 100 km. The parameters which affect the behavior of the system are the same (C_{DC} and Rf). For each distance, five different values of DC capacitor (10, 30, 50, 70 and 100 μF) and three different values of ground resistance (0, 2 and 4 Ω) values are tested.

Once the PTP configuration is studied and analyzed, the next topology is a multiterminal network. In this case, the topology which will be adopted is the one that was used for the PhD method and it can be seen in

. By making this decision, a comparison for the same configurations and topology is possible between the two methods. The changes that will be applied to the topology are related to the distance from the converter to the point where the fault occur, the DC capacitor value and the ground resistance value.

Point to point configuration

Line length: 10 km

The first line length to analyze is 10 km, which will be the shortest distance to be taken into account. With this line length, if the ground resistance is 0 Ω, the capacitor's current peak will be the total peak of the transient system. For higher values of ground resistance, the peak current of the AC infeed contribution is slightly higher. This aspect will be noticed in the following figures (Figure 27).

To analyze as deeply as possible how the variations affect the result, the process will be separated in two parts. First, R_f will be kept constant, and C_{DC} will change between five different values (10, 30, 50, 70 and 100 μF). Afterwards, the DC capacitor will be the parameter set to a fixed value and the ground resistance changes. The relative error will be represented in Figure 27.

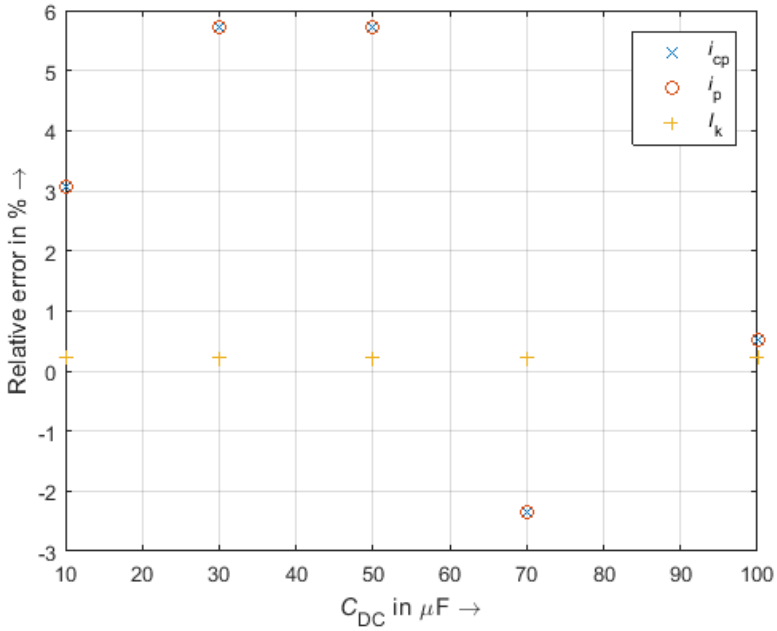

Figure 27. Relative error for PTP x = *10 km,* R_f = *0* Ω*and variation in* C_{DC}

Looking at the relative error of the three characteristic points of the current it can be said that the results obtained are consistent for a value of ground resistance equal to zero. The highest recorded error is below 6%, which matches with the expected error for this method. The original publication [14]does not show the errors for this exact parameter set-up, and uses other parameters. The results obtained with similar parameters are comparable to ones showed in the thesis.

The DC capacitor does not have an influence in the steady state current, thus the error remains constant, and below 0.5%. On the other hand, C_{DC} has a big influence on the peak values, especially in this situation where the capacitor contribution's peak is also the total peak of the current. Unfortunately, the error does not present any tendency for the capacitor change, and it varies between -2% and 6% for the

different values. The only conclusion that it can be obtained is that a change in the DC capacitor does not jeopardize the results of the method, nor makes them better.

The next figures, (

Figure 28 and Figure 29) show the influence that the ground resistance has when the DC capacitor remains unchanged.

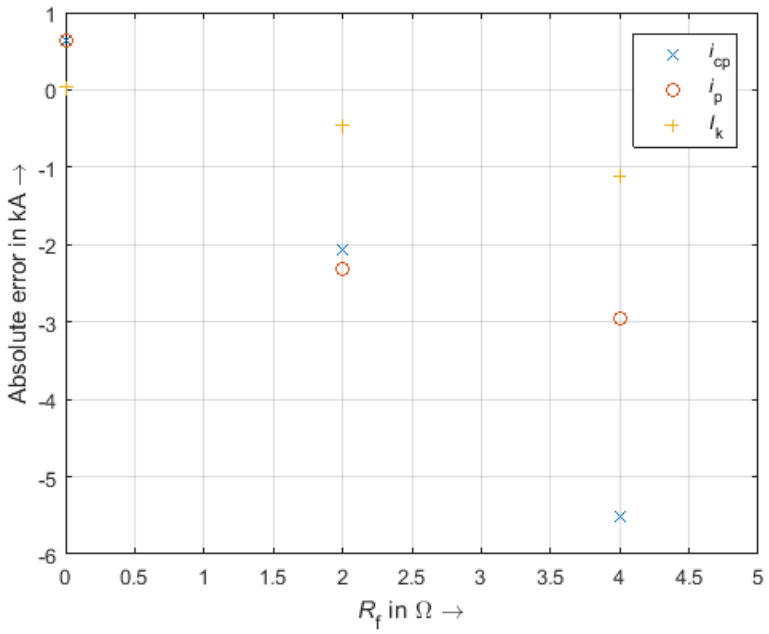

Figure 28. Absolute error for PTP x *= 10 km,* C_{DC} *= 10 μF and variation in* R_f

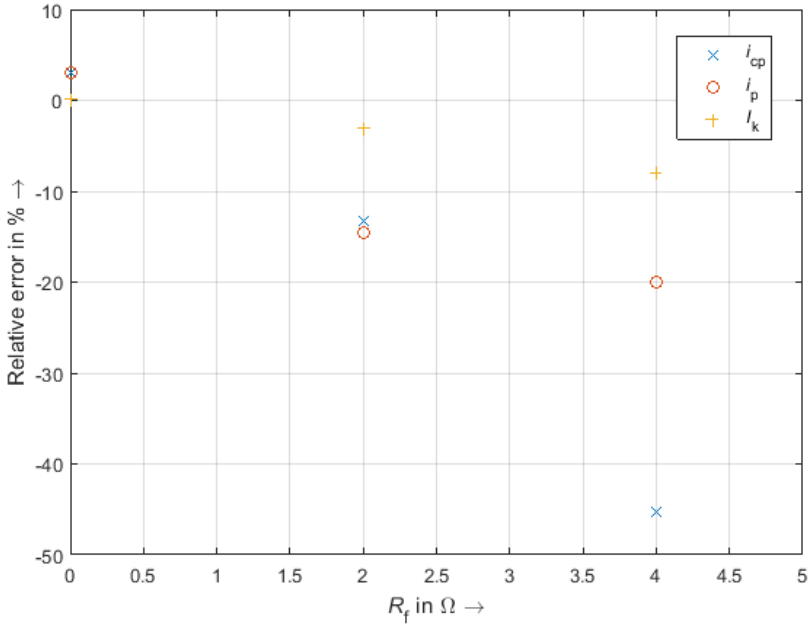

Figure 29. Relative error for PTP x = *10 km,* C_{DC} = *10 μF and variation in* R_f

When the parameter to be modified is R_f, the tendency shown in the values is clear and in the three cases an increase in the ground resistance imply an increase in the error made. The most affected point is the capacitor contribution's peak, whose error reaches around 45 % for a ground resistance of 4 Ω. The total peak current is also affected by an increase in the ground resistance and its error reaches 20% at its maximum. The steady state current is the less affected point, being its error always below 10%.

Line length: 30, 50 and 70 km

The methodology to follow in intermediate line lengths is the same as the one followed for shorter lines. First, the ground resistance will be set to a certain value (0 Ω) and the DC capacitor will adopt different values (10, 30, 50, 70 and 100 μF). Once, the influence of the capacitor is studied, the ground resistance will be the parameter that changes. It is also very important to check if the behavior observed for the different line length is the same or not.

For a ground resistance set to 0 Ω, it is safe to assure that the change in the DC capacitor affects the same way all the line lengths (30, 50 and 70 km). In this case, no significant change is appreciated for any of the distances and values of the DC capacitor. The error for the three characteristic current's points remains unchanged.

The figures attached in the appendix (Figure 56 and Figure 57) will serve as an example for the intermediate line lengths. It represents a 50 km line length, which qualitatively has the same behavior as the 30 and 70 km lines.

When the parameter changed is the ground resistance, the errors vary much more than before. That is to say, a ground resistance variation makes the method much more vulnerable than a DC capacitor variation. The results can be seen in the appendix (Figure 58 and Figure 59).

As it was said before, prior to reach to any conclusion for intermediate line lengths, it is important to see if a change in the ground resistance affects the same way every line in this group. This aspect was checked and it is confirmed that the three line lengths react the same way to changes in the ground resistance.

First, the steady state current is examined. This is the value that has less variation, and the maximum variation for extreme values is around 5%. Further, higher values of R_f increase the error in the estimated value.

The capacitor contribution's peak also experiments big changes for different values of ground resistance and has better performance for intermediate than for extreme values.

The last value to look at, is the total peak current, whose tendency is the same as the steady state current. The best performance comes when the ground resistance is zero, while an increase in the resistance makes the result worse. An increase of 4 Ω can affect around 10% in the final result.

Line length: 100 km

For long lines, the behavior that is observed is similar than for intermediate line lengths, with slight differences.

First, the influence of a variation in the DC capacitor is studied, remaining the ground resistance fixed to 0 Ω. As it happened with intermediate lines, C_{DC} has almost no influence in the error variation in none of the current characteristic points. Even though, the values change, the error that the system presents are constant when it is compared to PSCAD simulations.

The second parameter to change its value is the ground resistance. As happened before, when R_f varies, the method behaves better for certain situations.

The only difference in this point is in I_k. For this length of line, the steady state current's estimation improves its performance with an increase in the ground resistance, while for short and medium lines it was the other way around. The peak currents vary the same way that they did for medium lines.

Once the influence of the different parameters is tested for short, medium and long lines, the last point to test for PTP configurations is compare how does the error react to different line lengths when the same parameters are set to the system. The parameters, which will be used for the comparison are 10 μF and 0 Ω. The figures attached in the appendix (Figure 60 and) will show the absolute and relative error measured for the different lengths.

This is one of the most important analysis that will be done, as it can be compared the performance of the method for different line lengths. It is very important to check the method's robustness. A good method will not present a lot of differences between shorter and longer distances.

In the figures in the appendix, (Figure 60 and) it can be observed that the error does not vary much from the shortest distance to the longest one. The maximum variation experimented is around 5%, which in absolute value represent less than 1 kA. Taking a deeper look and analyzing the three different characteristic points, three different behaviors are observed.

First, the steady state current has its better results for short lines, increasing the error for intermediate and long lines. In all the cases, the recorded relative error is below 5%.

The total peak current's performance is different and reaches relative errors below 1% for intermediate distances, while this error increases both for short and long lines, being the maximum error 3%.

Last, the capacitor's current does not present a clear tendency in the presented error. When the capacitor current peak matches with the peak current, the error reaches its minimum value (3%), but when this peak no longer represent the total peak of the transient period, the relative error can reach values of almost 12 %. The only conclusion that can be extracted from these analysis is that for short lines, when the peak represents the total peak of the transient period the estimated value is much better than for longer lines, when this peak is only a relative maximum and not the absolute.

Multiterminal configuration

The next step is to check if the results present the same grade of accuracy when more nodes are added into the system. The multiterminal network which is going to be tested is the same one that it was used for the PhD method. This configuration is adopted for the same reasons given before and also to be able to compare both methods afterwards and observe which one presents better results in the different situations.

The parameters which are going to be changed for this configurations are: the distance to the fault location from the converter, the value of the DC capacitor and the ground resistance. The lines will be divided into three different groups: short lines (10 km), intermediate lines (30, 50 and 70 km) and long lines (100 km).

Line length: 10 km

For the three groups of lines, the procedure to follow is the same as the one done in the previous chapters. First, the ground resistance will be kept constant and the influence of a variation in the DC capacitor in the absolute and relative error will be studied. Later, the influence of the ground resistance will be one tested when the

DC capacitor value is constant. The results when R_f is the fixed parameter and C_{DC} changes can be observed in the appendix (Figure 62 and).

For short lines, it can be observed, how i_{cp} yields results which are not as good as it can be expected. The error reaches its maximum for 10 μF and its stabilizes for higher values of C_{DC} in 40 %. On the other hand, I_k and i_p does have better results, being the best ones for the lowest capacitor value. As happened with i_{cp}, the error stabilizes for the rest of the values of DC capacitor and does not present any further variation.

By changing the ground resistance to other values, the results that are appreciated are practically unchanged for steady state current and total peak current. On the other hand, the capacitor current's peak estimation's performance changes and improves by 10% for an increase to 4 Ω in the ground resistance.

Line length: 30, 50 and 70 km

For medium line lengths, the results of the system's estimations against a change in the C_{DC} are practically the same than for short lines. In this case, the only difference is that not even for values of DC capacitor of 10 μF, the error varies and it remains unchanged regardless of what values does the DC capacitor take. This can be observed in the figures attached in the appendix (Figure 64 and Figure 65).

The ground resistance value has more influence on the error variation than the DC capacitor, but when comparing the changes to the PTP configuration, it can be observed how in multiterminal networks there are many other parameters that affect in the system stability and makes the system more robust against changes. For that reason, a change in the ground resistance does not change as drastically the error as it affected in the point to point configuration. Nevertheless, an increase in the ground resistance improves the estimation accuracy of the total peak current. The steady state current error remains unchanged and the capacitor current's peak error increases slightly.

All these changes can be checked in the figures attached in the appendix (Figure 66 and Figure 67), which represent a 50 km line length multiterminal configuration with the DC capacitor set to 10 μF.

Line length: 100 km

The estimations for long line lengths present the same error variation that intermediate line lengths.

To finish with the sensibility analysis for the different parameters that affect the current behavior in the transient period when a fault occurs, the last parameter to change is the distance to the fault location. The results for these changes can be seen in the appendix (Figure 68 and Figure 69).

This last analysis is very interesting in order to check how good will be results be depending on the line length. By first glance it can be seen how there is one characteristic point which is very sensible to changes in the line length. This value is the capacitor current's peak, which also presents high sensibility to changes in the ground resistance and the DC capacitor. It can be seen how for short and long lines, the error is almost of 50%, while for intermediate values the error can reach values of 10%.

The steady state current estimation's performance does not present big alterations when the distance to the fault changes, and remains for all the range of distances below 2%, having accurate results.

The total peak current's error also presents itself as robust against changes in the distance and the error varies between 10% and 7% in extreme cases. It cannot be concluded that a relation between distance and error exists.

CHAPTER 4 : COMPARISON

In this step of the thesis, both methods have been satisfactory implemented in Matlab and compared to the expected results according to their original thesis. A sensibility test has also been done to the different configurations (both point to point and multiterminal configurations from both methods).

The next step is the main objective of the thesis and consists of the comparison of the performance of the different results when the configurations changes. The results obtained from the sensibility analysis will be used and the comparison will be done with the following approach:

A distinction between transmission networks will be done. The point to point configuration will be the first one to be studied and afterwards the multiterminal network will follow the same steps of the analysis.

For both point to point and multiterminal networks, groups of line lengths will be done in relation to the previous behavior against changes in the parameters. These groups will be: shorter lines (10 km), medium lines (30, 50 and 70 km) and longer lines (100 km). For each one of this group lines, the steady state current, total peak current and capacitor's contribution peak current will be studied and the results from PSCAD will be compared to the PhD's and the TU Darmstadt's methods.

For each one of the group lines, the DC capacitor, as well as the ground resistance will be changed and the errors will be measured and compared.

POINT TO POINT CONFIGURATION

Line length: 10 km

The first case of study are short lines. The results for the steady state current are very satisfactory for both methods.

In the first place, when the ground resistance is fixed, a change in the DC capacitor does not vary the steady state current, so the error is the same. This happens for

every configuration, so from now on, the steady state current will only be studied for changes in the ground resistance, as a change in the DC capacitor does not make any sense in this case.

As discussed before, three different values of ground resistance were studied (0, 2 and 4 Ω). Having a look to all the results obtained for the different resistance values, the TU Darmstadt method presents itself as a better method, obtaining errors of only 0.23 % for the lowest value of ground resistance. The main advantage of this method is that the error changes in a linear way, knowing that for higher values of resistance the error will always increase. It can be said that the method is more predictable in its estimations.

The PhD method also presents good results having in some cases only 0.42% of variation, but, on the other hand, it is more sensible to changes and a variation in the resistance does not always affect in the same way, increasing the error up to 8.71 % for a value of 2 Ω and being reduced again to 2.28% when the resistance acquires a value of 4 Ω.

The next values to be studied are the peak current. When studying these values, both approaches present accurate results for ground resistances of 0 Ω, being all the errors below 6 % for different DC capacitors. For that case, the PhD approach presents outstanding results being below 3% in all cases and having a slightly better performance. On the other hand, when the ground resistance increases its value, none of the methods can be as reliable as they are for zero ground resistance. In an extreme case of 4 Ω, the error for the total peak current is lower for the PhD method, while the capacitor contribution peak's estimation is better for the TUD Dissertation.

As a conclusion for short lines it can be said the TU Darmstadt Dissertation's method presents better results for steady state current and capacitor's current peak, while the total peak current's estimation is better for PhD method. It is noteworthy to keep in mind that in any case the results of one of the methods were significantly worse than the other and in the most extreme case the error difference from one

estimation to the other was around 5%. Figure 30 shows an example of the comparison of both methods in short lines.

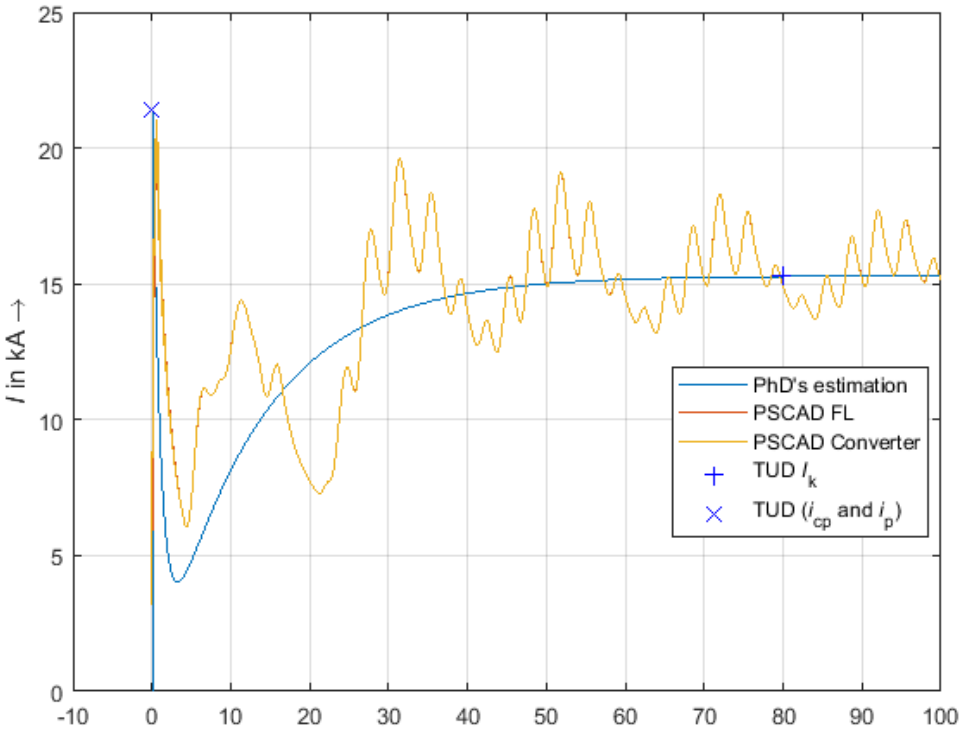

Figure 30. Superposition of PhD-TUD methods and PSCAD simulation (PTP configuration, x=10 km, C_{DC} = 70 μF, R_f = 0Ω)

Line length: 30, 50 and 70 km

For medium lines, the same procedure will be followed than for short lines. First the steady state current will be compared and afterwards the peak values.

As happened for short lines, the results for the steady state current when there is no ground resistance are very accurate, having an error lower than 1.5% for both approaches. It is very difficult for medium lines to analyze the performance to decide which one is better, as both have a very similar behavior when the ground resistance increases its value. The PhD method presents a mean error for all the studied cases of 2.22%, while the TUD dissertation's approach 1.82%. That 0.4% difference represents a value lower than 0.06 kA.

When the peak values are to be studied, a clear difference can be observed between the estimations for the capacitor contribution's peak and the total peak current, being the capacitor contribution peak's estimation significantly worse than the total peak current's estimation.

For the capacitor contribution's peak the first situation to be studied is a variation of the DC capacitor and a fixed value of ground resistance to 0 Ω. The mean error, under these circumstances, for the PhD's method is around 13-14%, while the TU Darmstadt's one is in the range of 10-11%. Knowing this data, it can be said that the PhD's methods performs slightly worse for these estimations. When the ground resistance changes its value, it can be observed that the Darmstadt's method works better for low values of resistance, and when big values are studied, the PhD's approach is the one which works better.

On the other hand, the total peak current presents for both methods, errors below 7%, being in some situations below 0.5% for the TU Darmstadt's approach. In this case the results observed are constant and does not vary with DC capacitor's nor ground resistance's changes. In every situation observed, the TU Darmstadt's method has a better performance.

To gather up all the information obtained for medium lines, it can be concluded that TU Darmstadt's method outperforms the PhD method for the steady state current (by only a difference of 0.4% in the mean error), and the total peak current (in this case by higher difference). When analyzing the capacitor contribution peak's current, the situation must be distinguished. In cases where the ground resistance has high values, the PhD's approach performs better, while the TU Darmstadt's method is better for lower resistances configurations. The following figure (Figure 31) will show an example of the superposition of both methods for medium line lengths.

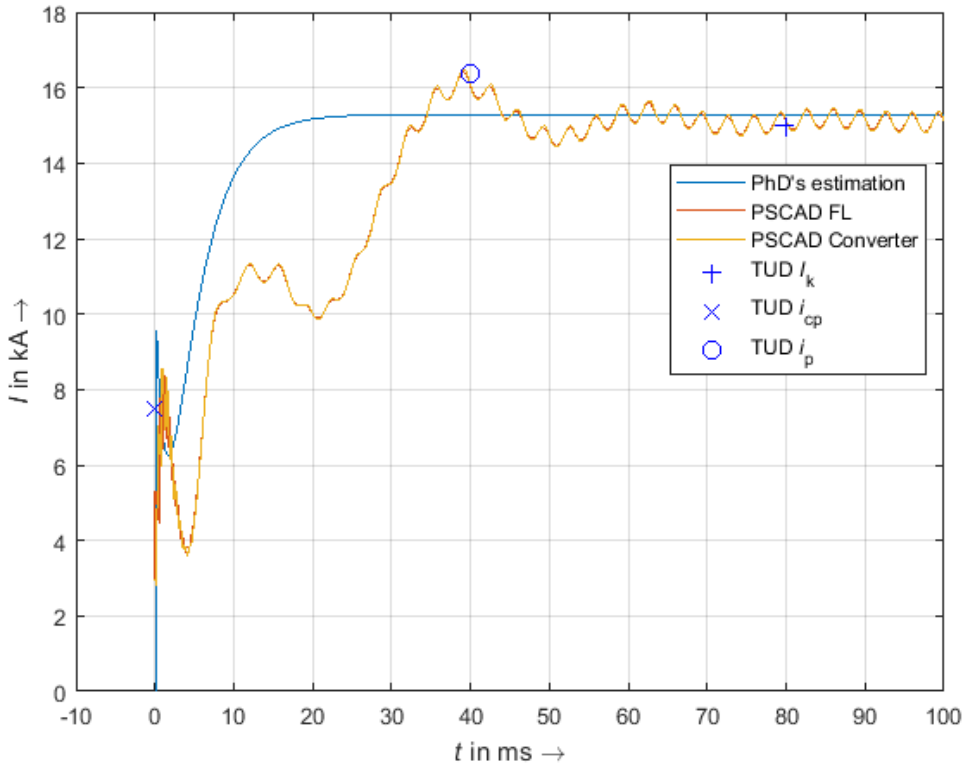

Figure 31. Superposition of PhD-TUD methods and PSCAD simulation (PTP configuration, x=50 km, C_{DC} = 50 μF, R_f = 0Ω)

Line length: 100 km

The last case to be analyzed in the point to point configurations are the long lines. For long lines, it is curious to observe how the TU Darmstadt's method worsens its performance. While the steady state current's estimation has been proved to be better for short and medium lines when the Darmstadt dissertation's equations were applied, in this case the PhD's equations lead to better results. The difference between the methods is more noticeable for low values of ground resistance, while that difference shortens as the ground resistance increases. The reduction in that error's difference is not enough to change which approach is better and the PhD outperforms the TUD's method in every situation by 3% in the most extreme case and 0.3% for higher values of ground resistance.

The capacitor contribution peak current's estimation presents the highest difference in long lines estimations. While the TU Darmstadt's dissertation achieves error below 10% in all cases, the PhD reaches error of almost 17%. This difference is present for every parameter configuration (both for low and high DC capacitor and ground resistance values).

On the other hand, when the total peak current is the value studied, almost no difference can be observed in the estimations. Both methods have very good estimations being the results in most cases below 3%. The only differences that can be observed is that the PhD's approach performs better in situations where the ground resistance is at its maximum level (4 Ω) and the DC capacitor is also at its maximum values (100 μF).

To sum up the analysis of long lines, it can be concluded that the PhD has better estimations for the steady state current in every situation. On the other hand, the dissertation's results for both capacitor contribution's peak and total peak current are better (except the capacitor contribution's peak for configurations with 4 Ω and 100 μF). The following figure (Figure 32) will show an example of the superposition of both methods for long line lengths.

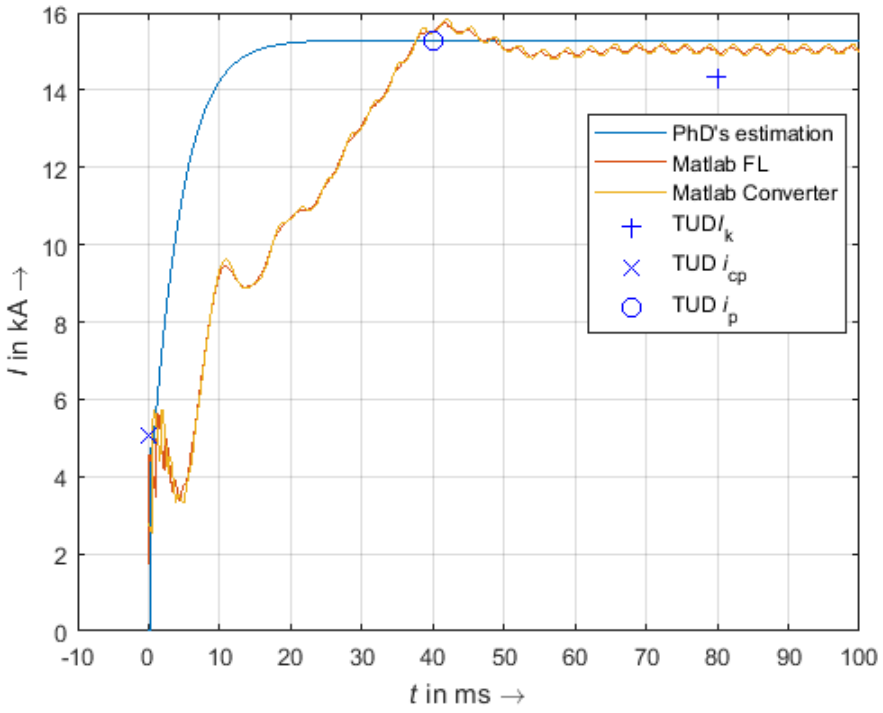

Figure 32. Superposition of PhD-TUD methods and PSCAD simulation (PTP configuration, x=*100 km,* C_{DC} = *50 μF,* R_f = *0Ω)*

MULTITERMINAL NETWORK

Once the PTP configurations have been studied, the approaches will be tested now in multiterminal networks. These networks are characterized by the fact that the transmission interaction occurs between three of more converters. In this case, the topology which is used is the one already mentioned (

). This topology consists of four different converters in which the fault occurs in the line that connects the node 1 and node 2. The distance at which this fault occurs measured from node 1 will be changed. As it was done for PTP configuration, the values of DC capacitor and ground resistance will also change in order to gather as much data as possible and extract the best possible conclusions.

Three different groups will be done: short lines, medium lines and long lines. For each of those groups a wide range of DC capacitor and ground resistance values

will be varied and the steady state current, capacitor contribution peak and total peak current values will be measured and compared to the PSCAD values.

Line length: 10 km

In this first case, the fault occurs at 10 km from the converter in node 1. In this situation, the errors which are measured for the steady state current are under 3% for every parameter combination and for both methods. This means that the estimations done have great accuracy. By the sensibility analysis done in "Comparison with PSCAD simulations" and "Comparison with PSCAD simulations", it can also be seen that changes in the DC capacitor and ground resistance do not yield to big changes in the error. An explanation to this can be that when a multiterminal network is studied, there are much more parameters that affect the transient response of the system and changes in just one parameter are less critical that those same changes for point to point configurations.

Even though both approaches obtain very good results, the PhD's equations are slightly better for steady state current's estimations, having an error of only 0.24 % for this configuration.

When the peak currents (both the capacitor's contribution and the total peak) are analyzed, it can be seen how PhD's approach is very consistent, presenting very little error difference against changes in DC capacitor and ground resistance. On the other hand, the results from the TU Darmstadt's dissertation present a higher variability in the error for changes in the parameters.

Further, the estimations done by the PhD's equations lead to better results, with very low errors in such networks (always below 5%). This low error, added to the fact that it is a very consistent method against changes in the input parameters, makes it as a better choice for the peak current's estimations in short lines. Gathering all the information for short lines, it can be said that the steady state current's estimations can be done with a high level of accuracy with both methods (being slightly better the PhD equations), while the peak currents are significantly better estimated with the PhD approach. The following Figure 33 will show an example of the superposition of both methods for short line lengths.

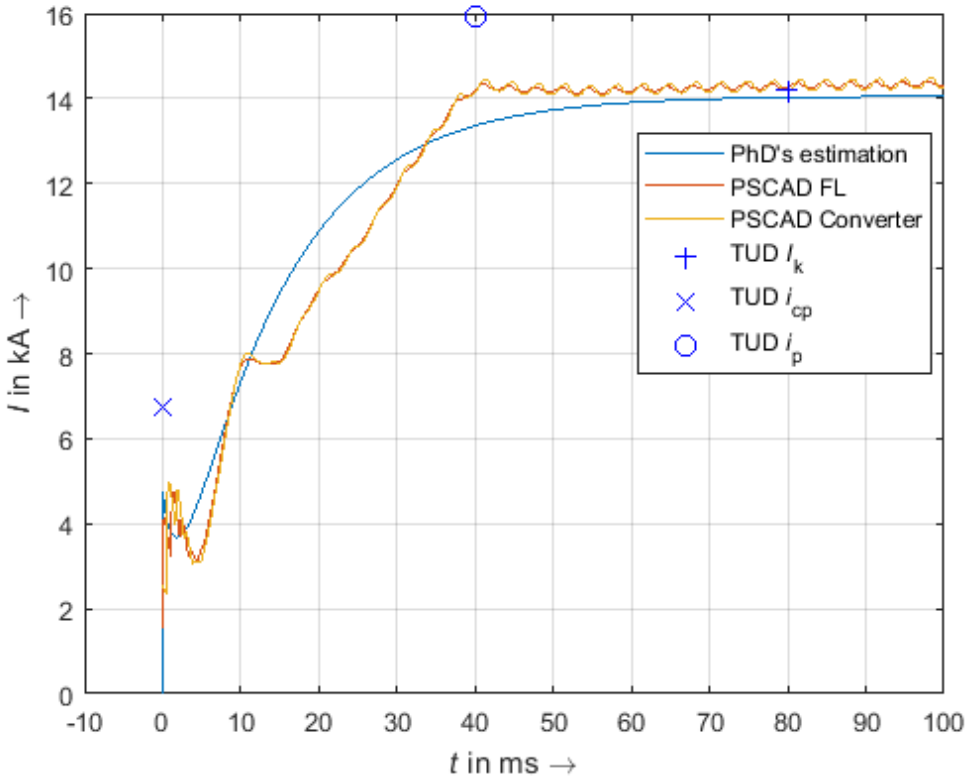

Figure 33. Superposition of PhD-TUD methods and PSCAD simulation (MT configuration, x=10 km, C_{DC} = 50 µF, R_f = 4 Ω)

Line lengths: 30, 50 and 70 km

In these cases, the fault occurs at a medium distance from the converter. Three different cases are studied, which happen to behave the same way, so it makes the sense the aggrupation of these three cases.

As happened for short lines, the accuracy of both methods for the steady state current, regardless of the value of the DC capacitor and ground resistance is very high. In both methods, the maximum error is not above 3.5 % and the differences are very low. Nevertheless, the TU Darmstadt dissertation's equations yield results with errors below 0.25%.

On the other hand, TU Darmstadt's method struggles with the peak values' estimation. Specially with the capacitor current's peak, where errors up to 25% can be observed. In these cases, the PhD approach is more consistent and the errors do not exceed 5%.

If the estimated value is the total peak's current, the error for the TU Darmstadt's dissertation improves significantly to errors below 10%, but the PhD remains as a better choice due to the fact that for the most unfavorable case, the error is 5%.

As a conclusion, it can be said that for medium distances the steady state current is estimated with very low error by both methods, being slightly better with the TU Darmstadt's equations. When the peak values are the studied values, the PhD approach is clearly better for that purpose, presenting itself as a very consistent method, whose error is not altered by changes in the parameter's configuration. The following Figure 34 will show an example of the superposition of both methods for medium line lengths.

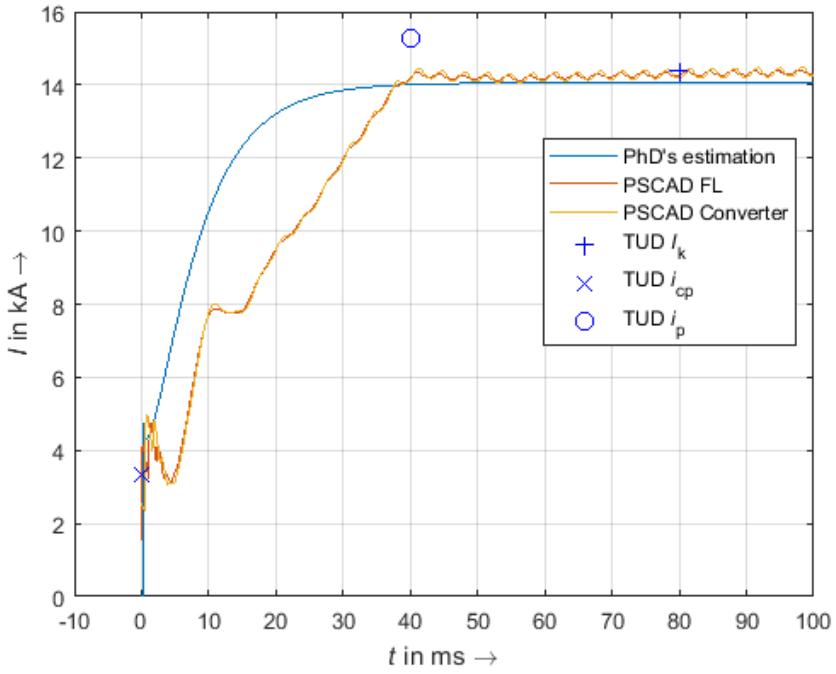

Figure 34. Superposition of PhD-TUD methods and PSCAD simulation (MT configuration, x=50 km, C_{DC} = 50 μF, R_f = 4 Ω)

Line lengths: 100 km

For multiterminal configurations, when the fault occurs at a distance of 100 km the conclusions obtained are the same ones that for medium lines.

SUMMARY

Once the comparison of both methods have been done with the result obtained from PSCAD, it is important to decide which of the approaches lead to better results. To do so, not only the relative error needs to be taken into account, but also the consistency against changes in the parameters. Analyzing the data already obtained and also using the sensibility analysis the following verdict is reached.

The topology situations studied are PTP configuration and MT networks. As the results obtained have big differences between them, one conclusion will be extracted for PTP systems and another one for MT networks.

The results obtained for PTP situations are very accurate with the two different approaches. Checking the results obtained for the steady state current, it can be affirmed that for short and medium lines, Darmstadt's equations have better results, while for long lines, the equations proposed in the PhD are minimally more accurate. In every case, the errors that were obtained are below 5%. This error comes from neglecting the influence that the harmonics have on the steady state current. The equations developed only take into account the sixth harmonic and the rest of them, which do have influence on the steady state value.

For the peak values, also good results were obtained from the simulations. In this case, the PhD equations reach more precise estimations for short lines, while for medium and long lines the Darmstadt method presents itself as more consistent.

With the correct analysis of this information and knowing that some metrics are more beneficial to one or the other method it can be concluded that when the whole range of analysis is studied, the TUD Dissertation presents itself as a more reliable approach for PTP networks. In the total comparison, there are more situations in which this method has better results.

One clarification that must be done is related to the capacitor contribution's peak. As it was already discussed in 0, the PhD method applies a correction factor to this peak value. Even though, in the majority of the situations studied, this factor improves the performance when it is set to 0.88, there might be situations (different parameters, converters, etc.) in which the results do not perform the same manner.

The second configuration tested was the multiterminal network. These kind of networks are characterized by the presence of more than two converters. In the studied case, a four node system was chosen.

In this case, changes in the distance to the fault does not affect so much the final results and for the three lines studied (short, medium and long lines), the same conclusion can be extracted. For MT networks, the results lead to bigger differences in the current estimations. The results of the PhD method are better for every analyzed situation. Also, the changes that the estimations suffer against variations in the parameters are smaller than in the TUD Dissertation's method. These

differences are more noticeable in the peak current's estimations, while for the steady state current, the difference is significantly smaller.

For all the exposed reasons and results, it can be said that for PTP configurations, the TU Darmstadt approach is more accurate, while when MT networks are studied, the PhD method is the best choice for the current estimations.

CHAPTER 5 : CONCLUSIONS

Once all the simulations and comparisons have been done, interesting conclusions can be extracted from the work done. Two main configurations have been studied, which are point-to-point configurations and multiterminal network. In both of these configurations, changes in the parameter's definition have been applied in order to have a wider range of data to analyse. The parameters which have been varied are the value of the DC capacitor, the ground resistance and the distance from the converter to the fault.

The main objective of the thesis is to compare the accuracy that the two proposed methods have under different situations. To do so, first a sensibility analysis was done to determine which are the optimal conditions for the different methods. The outcome of that analysis was the following one:

For point to point configurations the first method (PhD) presents differences in the results for short, medium and long lines. Nevertheless, in general, the steady state current's estimation is better when low values of ground resistances are defined, while it does not present any changes against variations of the DC capacitor. Moreover, the peak values of the current have better results under low DC capacitors.

The second method (TUD) also presents differences between parameters changes for short, medium and long lines. General results conclude that the DC capacitor does not affect the results of the steady state current. This current is only affected by changes in the ground resistance, and presents better estimations for low values. On the other hand, the peak currents do not present a clear tendency against changes in the DC capacitor, whereas an increase in the ground resistance increases the error in the peak estimations.

The conclusions obtained for the point to point configurations can be extrapolated to the multiterminal networks with some differences. One of the most important differences is that changes in the DC capacitor and ground resistance, as well as the

fault distance have less influence in multiterminal networks, as there are more parameters which affect the transient behaviour of the system.

This analysis is very important to see which situations or parameters affect more to the proposed methods and is very helpful in order to decide which approach presents better and more reliable results.

With the objective to reach a verdict on determining which approach is better for the purpose, all the information must be gathered up. Not only one result can be used in order to determine a final decision. The sensibility analysis and the comparison chapters were key analysis to reach a conclusion. As it was said before, the results obtained are different for PTP configurations and MT networks, so different conclusions will be exposed for each case.

By using the whole range of parameters combinations and analysing the different configurations, it can be said that two main aspects determine which method is more suitable. The first condition is the relative error that the estimations have for the three characteristic points of the transient current (steady state, total peak, capacitor contribution's peak). The second aspect that must be taken into account is the robustness that the results have for different situations. It is desired a method that do not experiment big changes in the error when the parameters change.

Taking these features into account, it can be said that PTP configurations are more suitable for TU Darmstadt's dissertation method, while MT networks are better for the performance of the PhD's approach.

CHAPTER 6 : OUTLOOK

Once the analysis in order to determine how much difference exists between the two proposed methods in the exposed situations is done, there are some areas which seem to be unsolved. These areas can be applicable both for point to point configurations and multiterminal networks or it can be specific only to one of them.

One of the aspects that can be changed are the characteristics of the converter. Even though, the PhD method is only applicable to two-level converters, the characteristics that define these converters can be changed and studied.

These changes in the converter can be done both for PTP and MT networks. It is interesting to check if the obtained results are equivalent for different voltage levels or armature inductances.

Another feature to have in mind is the type of line and the internal resistance of them. In the original publications, it is exposed that the proposed equations are valid also for overhead lines, but in none of the publications an extent analysis have been done.

Being more specific into MT networks, in the actual thesis only one topology has been studied. This decision was taken due to the fact the proposed equations for equivalent resistances and inductances were only valid for the given configuration. An interesting improvement in this topic would be to propose formulas for these equivalent resistances and inductances regardless the number of nodes and the connections between them.

Another aspect, related also with the equivalent resistances for MT networks is the location of the fault. In the studied cases, the fault always occurs at the same place. By changing the location of the fault (in other nodes), the transient current may be more or less affected.

REFERENCES

[1] M. Eghlimi and S. G. Hamed, "Economic analysis of Iran-Turkey power network interconnection: HVDC vs. HVAC," *PECon 2008 - 2008 IEEE 2nd Int. Power Energy Conf.*, no. PECon 08, pp. 164–168, 2008.

[2] M. P. Bahrman and B. K. Johnson, "The ABCs of HVDC transmission technologies," *IEEE Power Energy Mag.*, 2007.

[3] A. Wasserrab and G. Balzer, "Determination of DC Short-Circuit Currents of MMC-HVDC Converters for DC Circuit Breaker Dimensioning."

[4] X. Feng, L. Qi, and Z. Wang, "Estimation of short circuit currents in mesh DC networks," in *IEEE Power and Energy Society General Meeting*, 2014.

[5] A. Wasserrab and G. Balzer, "Calculation of Short Circuit Currents in HVDC Systems."

[6] A. Wasserrab, B. Just, and G. Balzer, "Contribution of HVDC converters to the DC short circuit current," in *Proceedings of the Universities Power Engineering Conference*, 2013.

[7] J. Brown, J. Allan, and M. B. Mellitt, "Six-pulse three-phase rectifier bridge models for calculating closeup and remote short circuit transients on DC supplied railways."

[8] V. Akhmatov *et al.*, "Technical guidelines and prestandardization work for first HVDC Grids," *IEEE Trans. Power Deliv.*, 2014.

[9] P. Pozzobon, "Transient and steady-state short-circuit currents in rectifiers for DC traction supply," *IEEE Trans. Veh. Technol.*, 1998.

[10] S. Skok, A. Marusic, and S. Tesnjak, "Transient short - Circuit currents in auxiliary DC installations in power plants and substations," in *2003 IEEE Bologna PowerTech - Conference Proceedings*, 2003.

[11] M. K. Bucher, "Transient Fault Currents in HVDC VSC Networks During Pole-to- Ground Faults ETH Library," 2014.

[12] M. K. Bucher and C. M. Franck, "Analytic Approximation of Fault Current Contribution from AC Networks to MTDC Networks during Pole-to-Ground Faults," *IEEE Trans. Power Deliv.*, 2016.

[13] M. K. Bucher and C. M. Franck, "Analytic approximation of fault current contributions from capacitive components in HVDC cable networks," *IEEE Trans. Power Deliv.*, 2015.

[14] Dipl-Ing Andreas Wasserrab, D.-I. Gerd Balzer Korreferent, rer M. nat Christian Franck Korreferent, and D.-I. Jutta Hanson, "Kurzschlussstromberechnung in Gleichstromnetzen der elektrischen Leistungsübertragung," 2016.

[15] W. Wang et al., "Cascaded H7 Current Source Converter Based Power Transmission System and Fault Analysis," pp. 0–6, 2006.

[16] M. Alhasheem, T. Dragicevic, M. Rivera, and F. Blaabjerg, "Losses Evaluation for a Two-Level Three-Phase Stand-Alone Voltage Source Converter Using Model Predictive Control."

APPENDIX

PHD IMPLEMENTATION SIMULATIONS

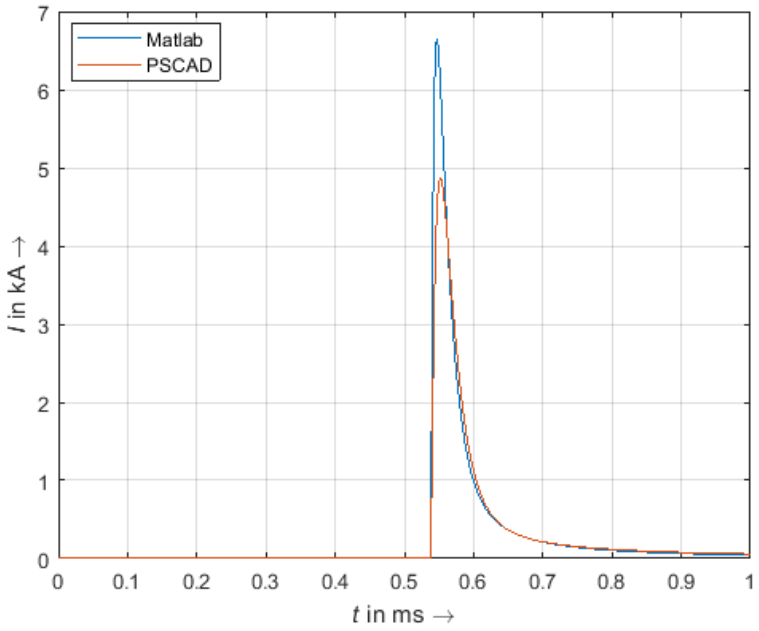

Figure 35.Current capacitor contribution for Layout 3 and CF 1

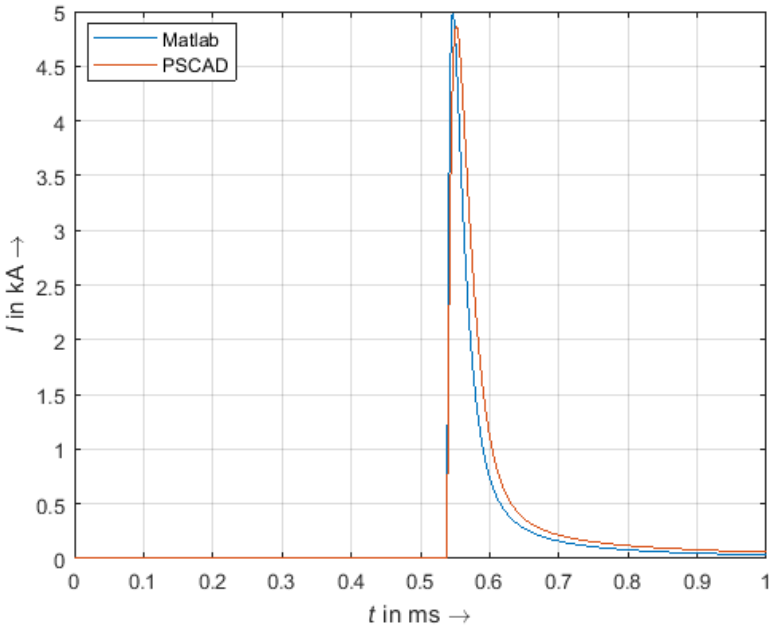

Figure 36. Current capacitor contribution for Layout 3 and CF 0.75

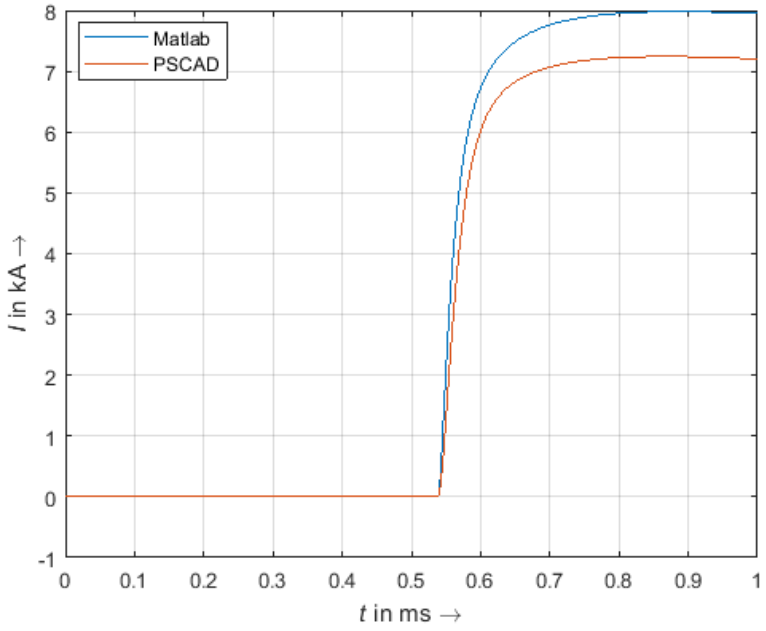

Figure 37. Current adjacent feeder contribution for Layout 3 and CF 1

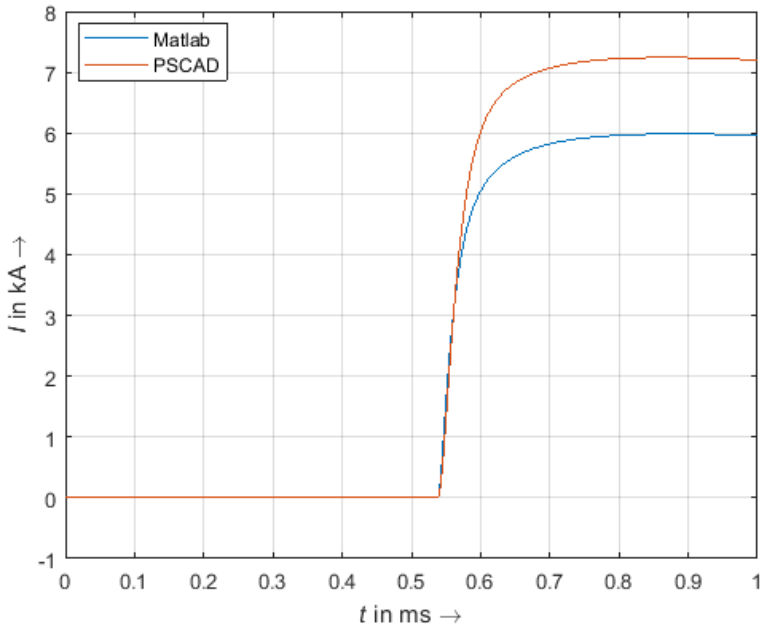

Figure 38. Current adjacent feeder contribution for Layout 3 and CF 0.75

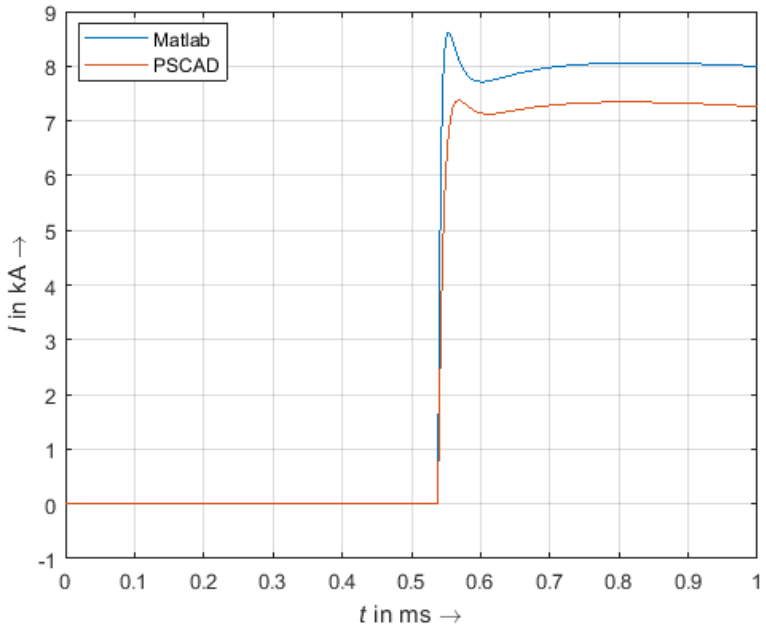

Figure 39. CB Current for Layout 3 and CF 1

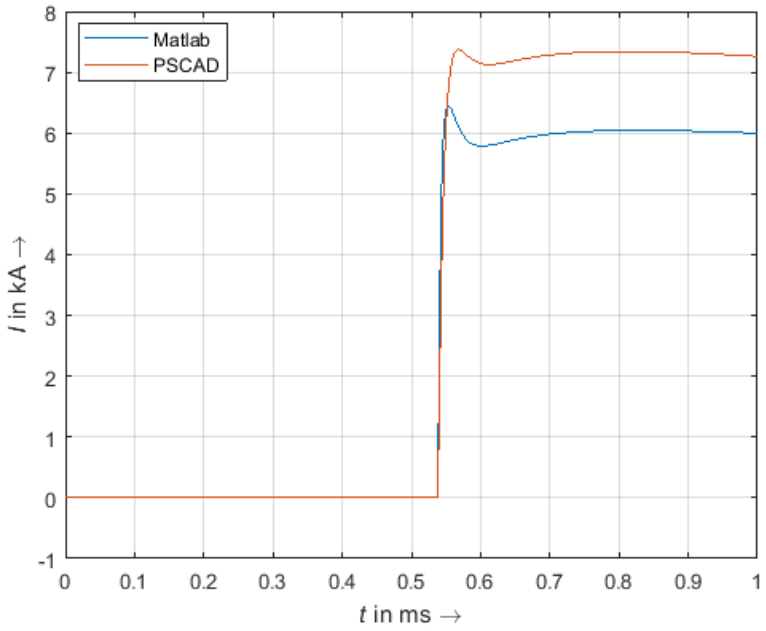

Figure 40. CB Current for Layout 3 and CF 0.75

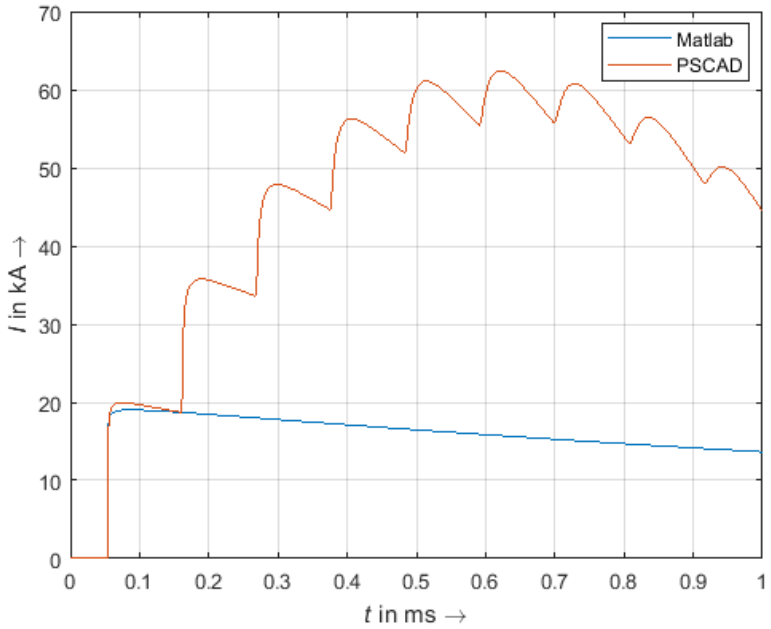

Figure 41. CB Current for Layout 1and CF 0.88

PHD – PSCAD COMPARISONS

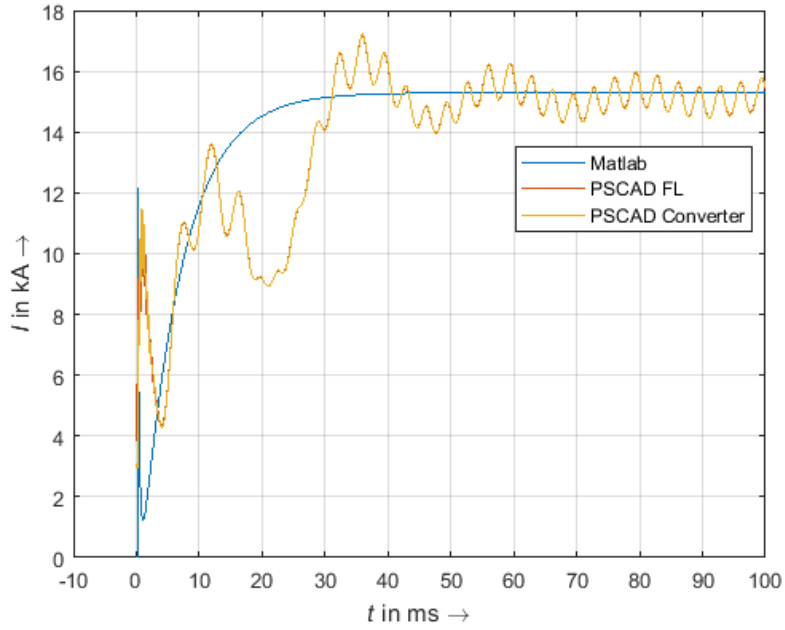

Figure 42. PSCAD- Phd method Current behavior comparison

(PTP, x=30 km, 10 μF, 0 Ω)

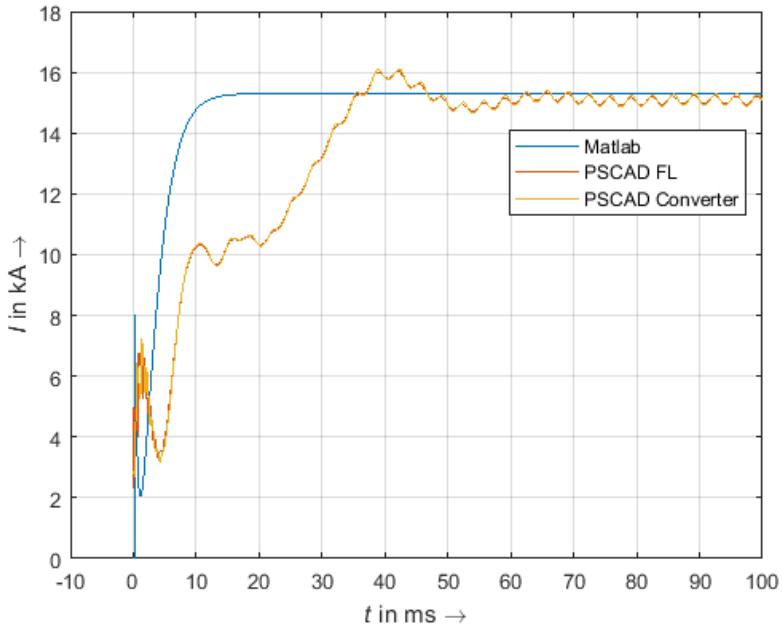

Figure 43. PSCAD- Phd method Current behavior comparison

(PTP, x=70 km, 10 µF, 0 Ω)

PHD METHOD'S SENSIBILITY ANALYSIS

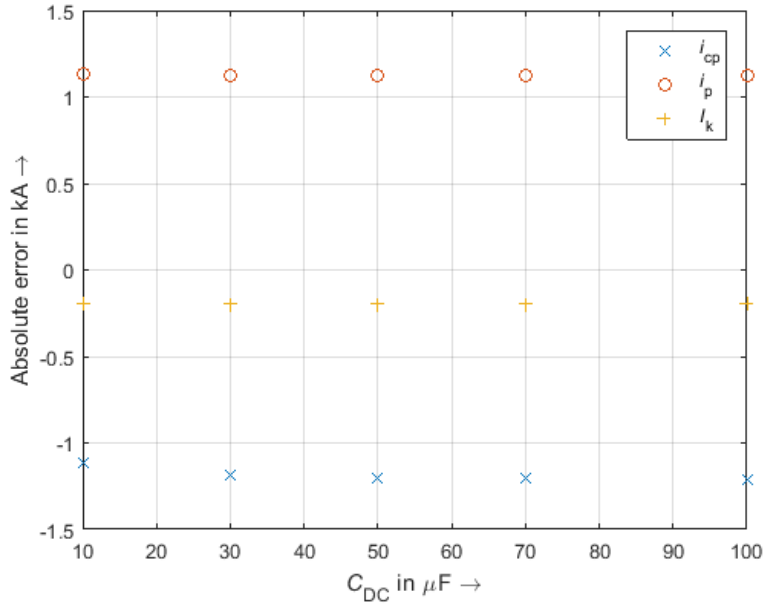

Figure 44. Absolute error for PTP x=*50 km,* R_f *= 0* Ω *and variation in* C_{DC}

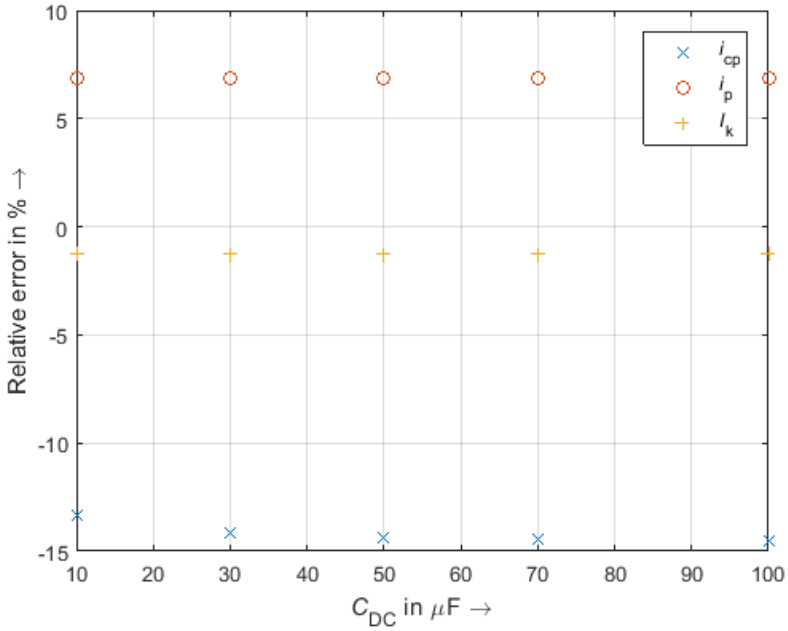

Figure 45. Relative error for PTP x= *50 km,* R_f*=0*Ω *and variation in* C_{DC}

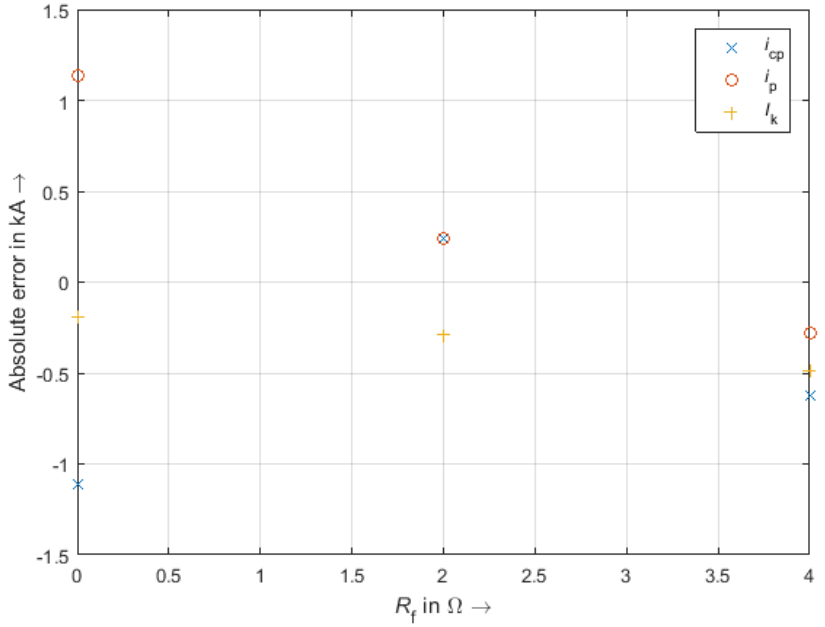

Figure 46. Absolute error for PTP x= *50 km,* C_{DC}*=10 µF and variation in* R_f

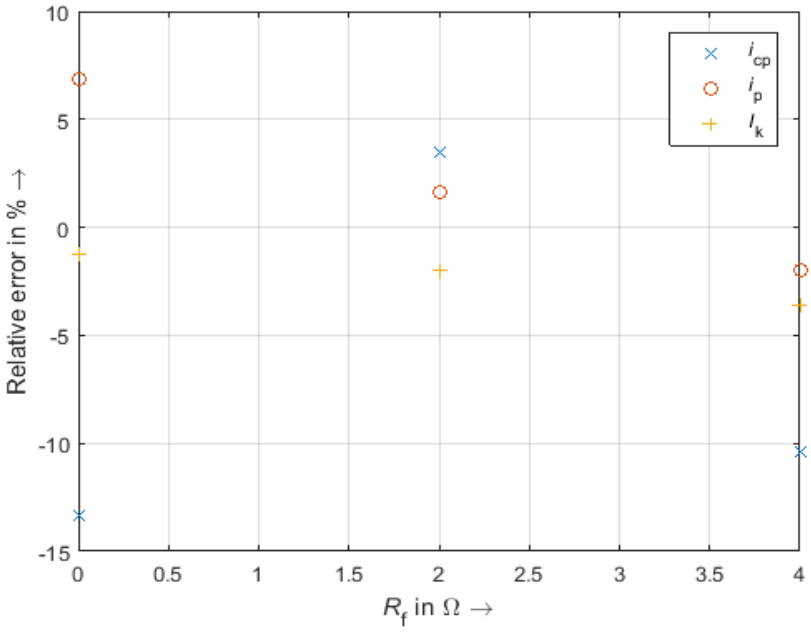

Figure 47. Relative error for PTP x= *50 km,* C_{DC}*=10 µF and variation in* R_f

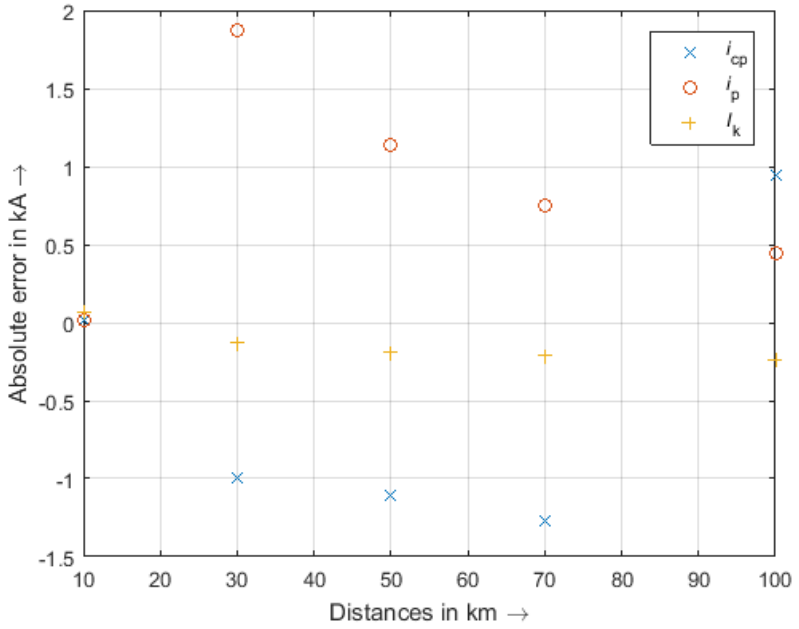

Figure 48. Absolute error for PTP configuration and different distances

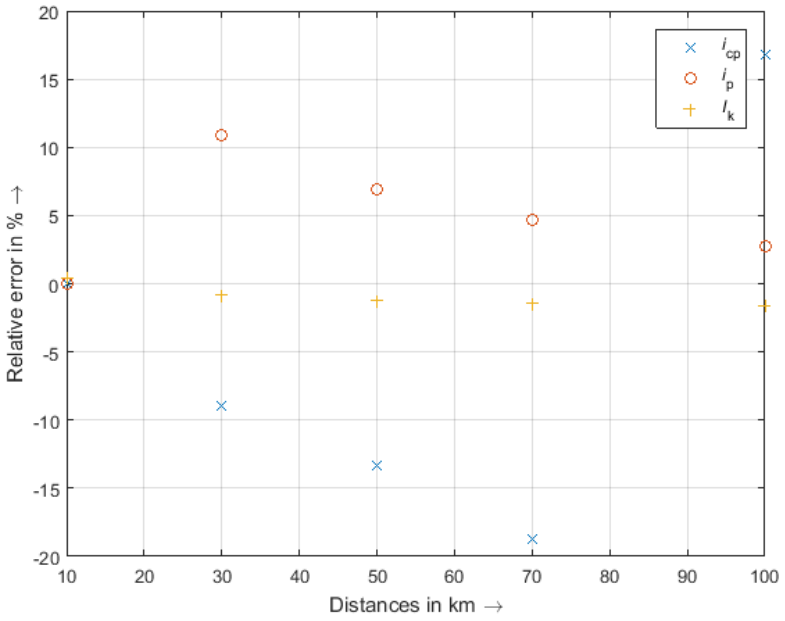

Figure 49. Relative error for PTP configuration and different distances

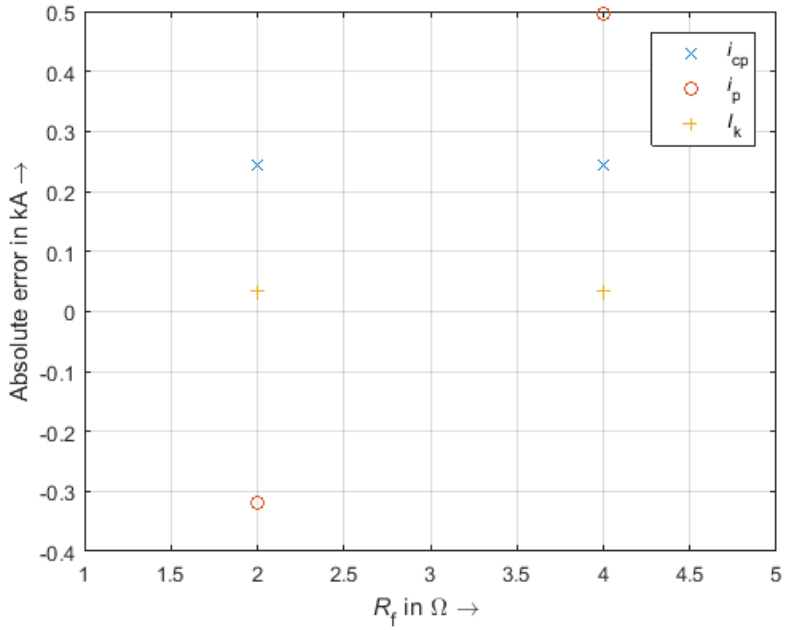

Figure 50. Absolute error for MT x *= 10 km,* C_{DC} *= 10 µF and variation in* R_f

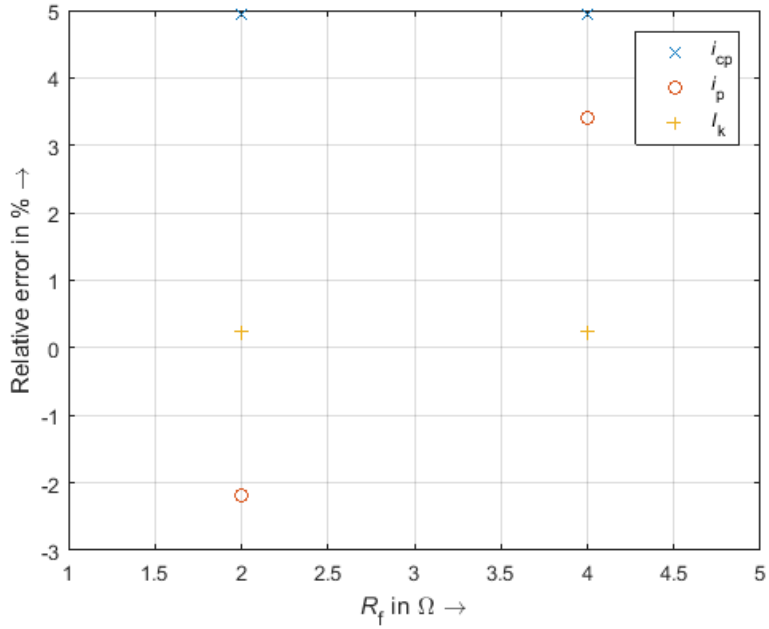

Figure 51. Relative error for MT x *= 10 km,* C_{DC} *= 10 µF and variation in* R_f

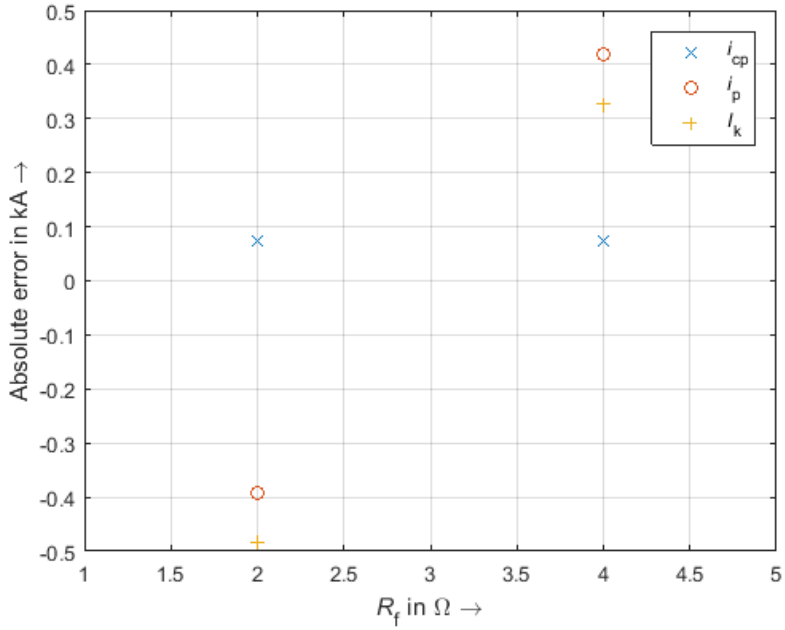

Figure 52. Absolute error for MT x *= 50 km,* C_{DC} *= 10 µF and variation in* R_f

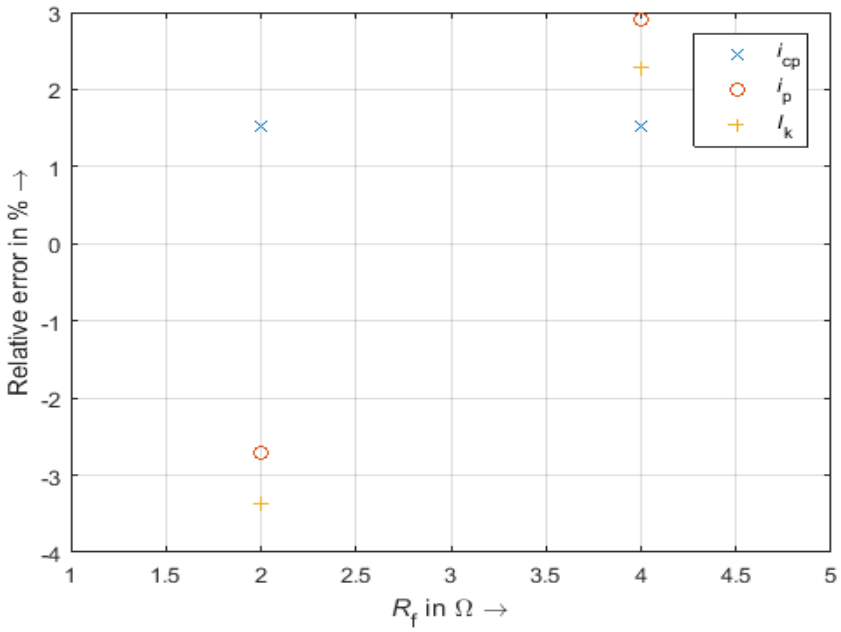

Figure 53. Relative error for MT x *= 50 km,* C_{DC} *= 10 µF and variation in* R_f

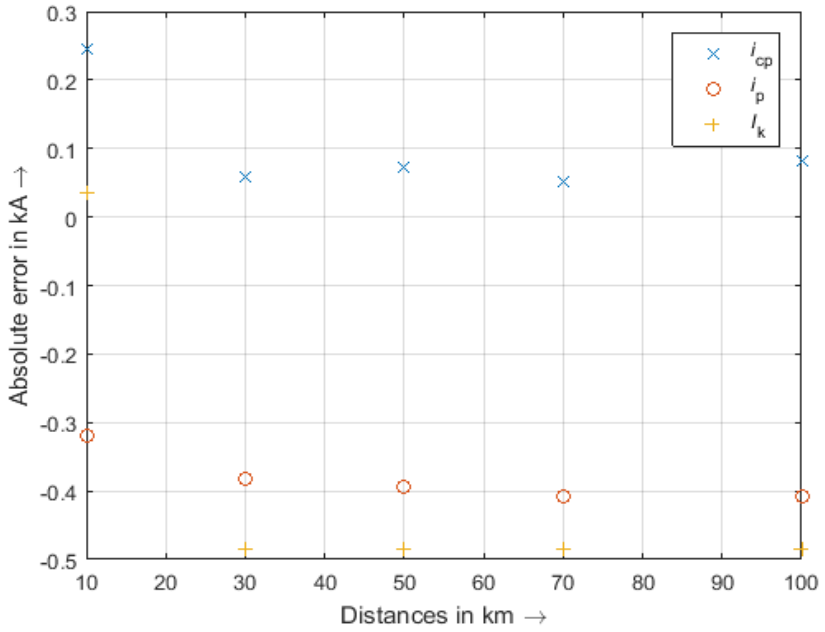

Figure 54. Absolute error for MT configuration and different distances

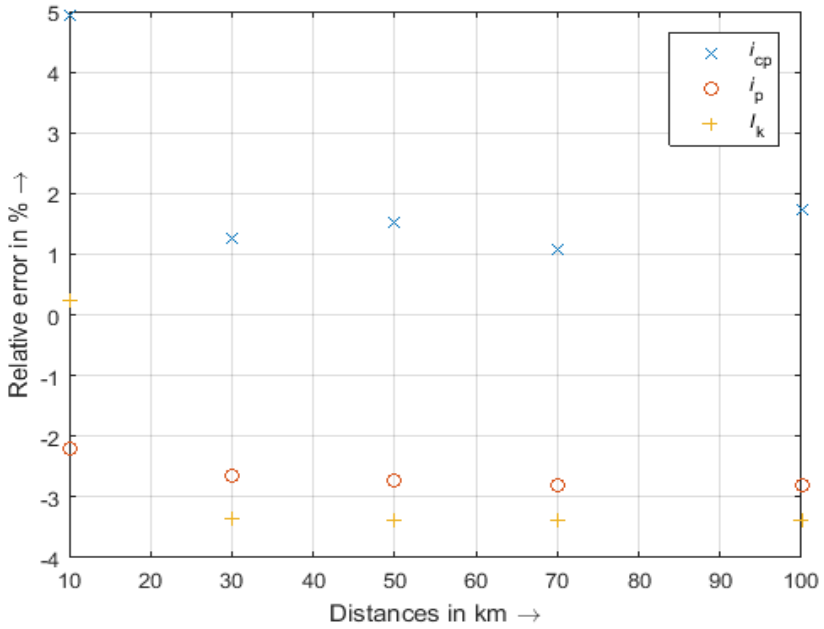

Figure 55. Relative error for MT configuration and different distances

TUD METHOD'S SENSIBILITY ANALYSIS

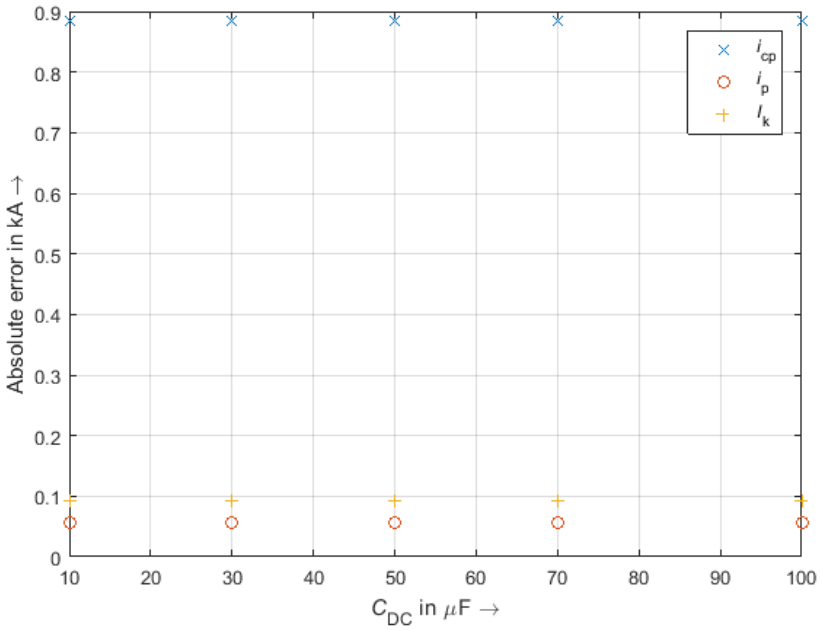

Figure 56. Absolute error for PTP x = *50 km,* R_f = *0* Ω*and variation in* C_{DC}

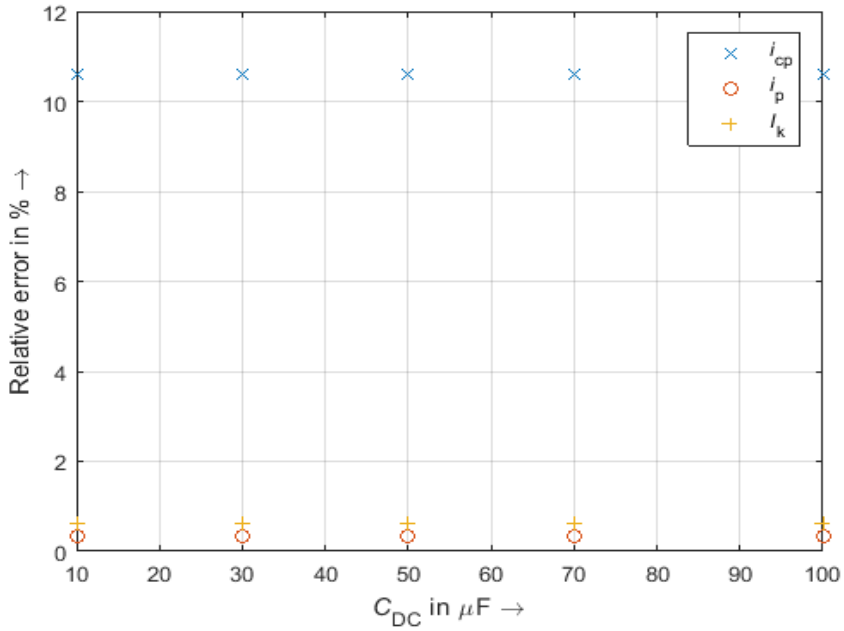

Figure 57. Relative error for PTP x = *50 km,* R_f = *0* Ω*and variation in* C_{DC}

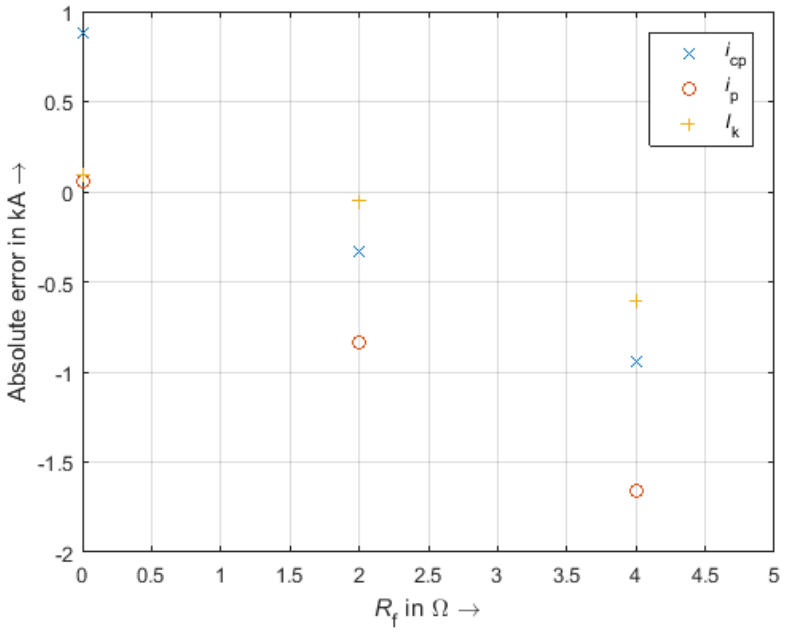

Figure 58. Absolute error for PTP x = *50 km,* C_{DC} = *10 µF and variation in* R_f

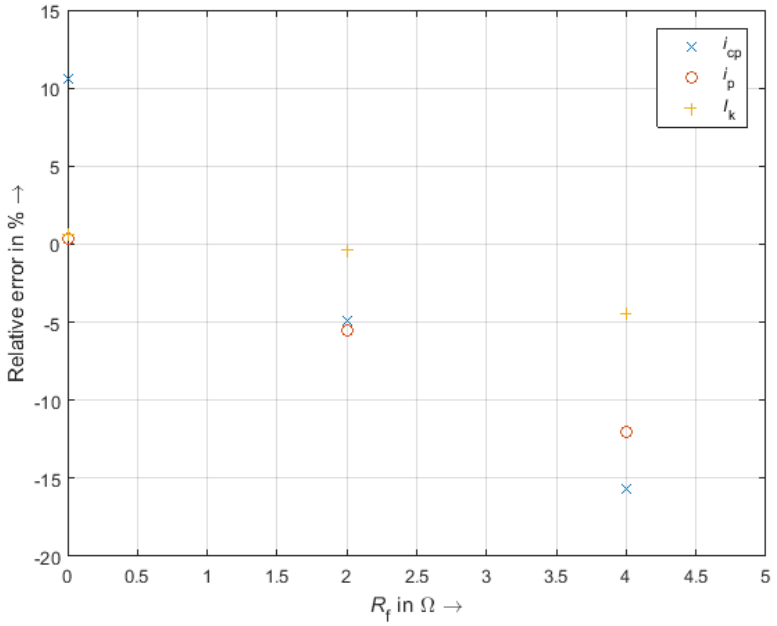

Figure 59. Relative error for PTP x = *50 km,* C_{DC} = *10 µF and variation in* R_f

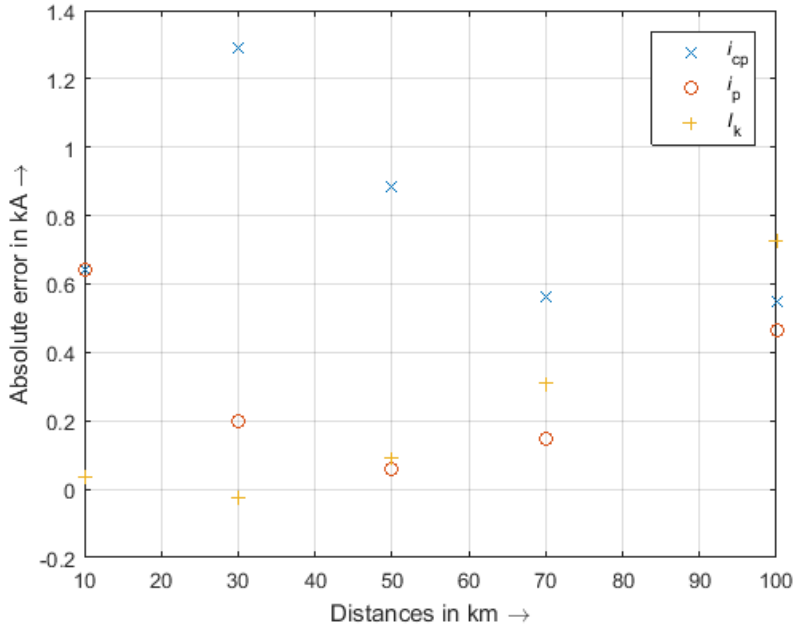

Figure 60. Absolute error for PTP configuration and different distances

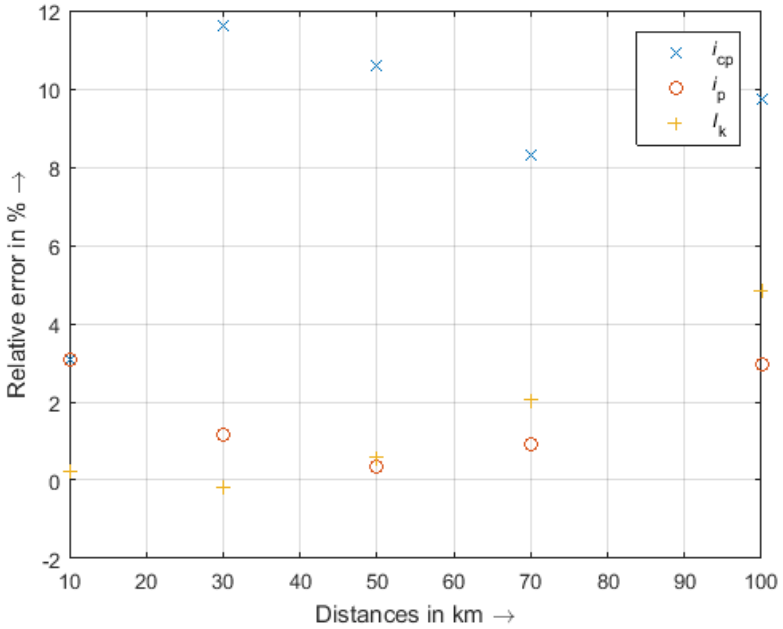

Figure 61. Relative error for PTP configuration and different distances

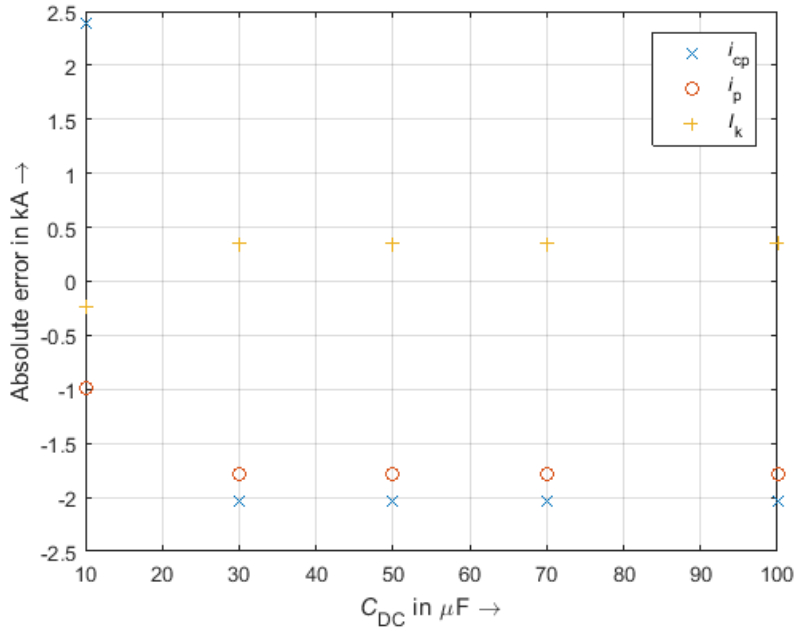

Figure 62. Absolute error for MT x = *10 km,* R_f = *2* Ω*and variation in* C_{DC}

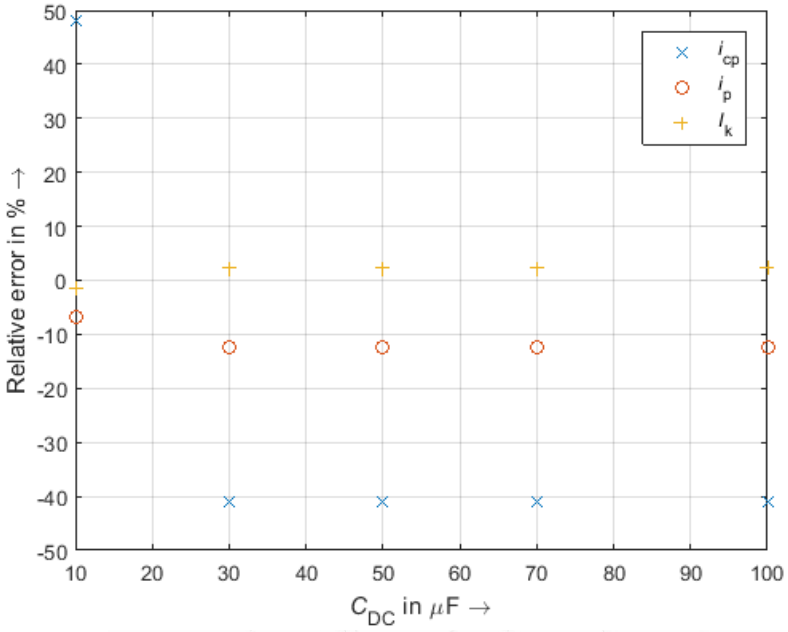

Figure 63. Relative error for MT x = 10 km, Rf = 2 Ω *and variation in CDC*

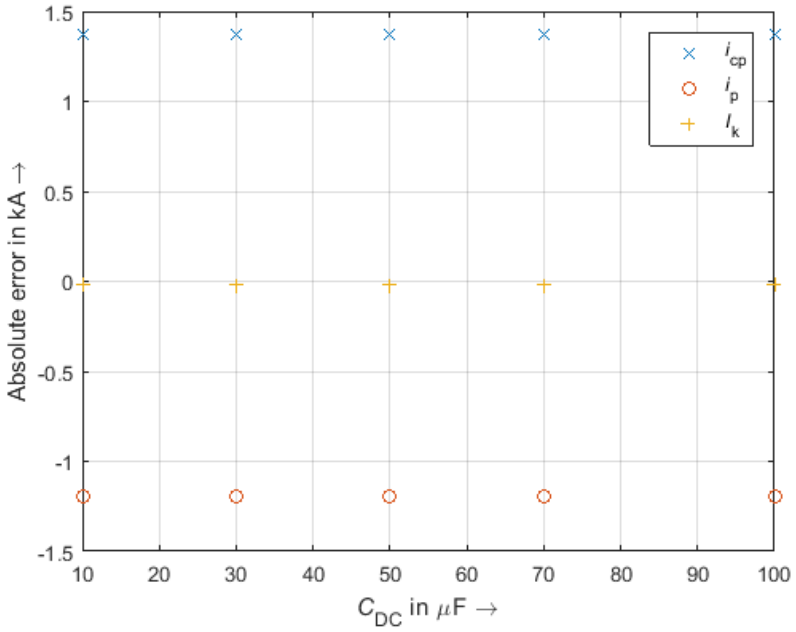

Figure 64. Absolute error for MT x = *50 km,* R_f = *2* Ω *and variation in* C_{DC}

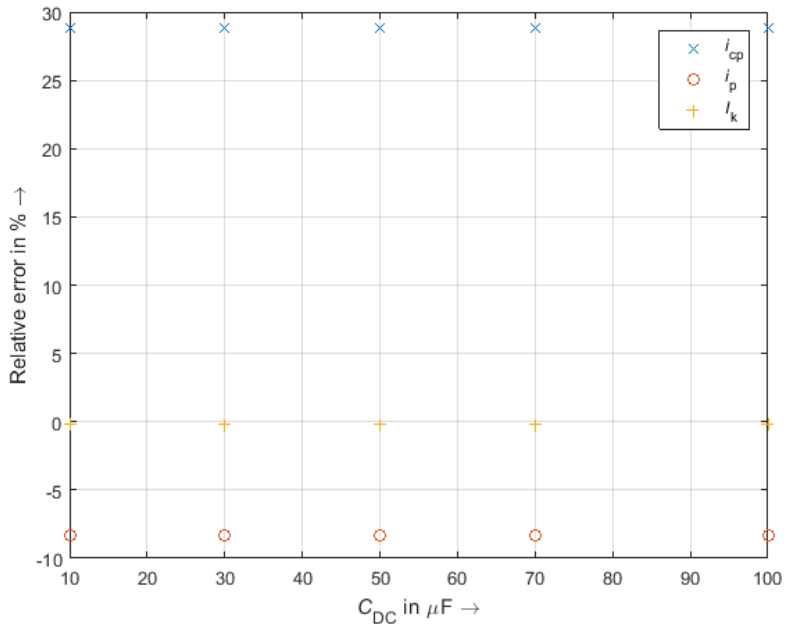

Figure 65. Relative error for MT x = *50 km,* R_f = *2* Ω*and variation in* C_{DC}

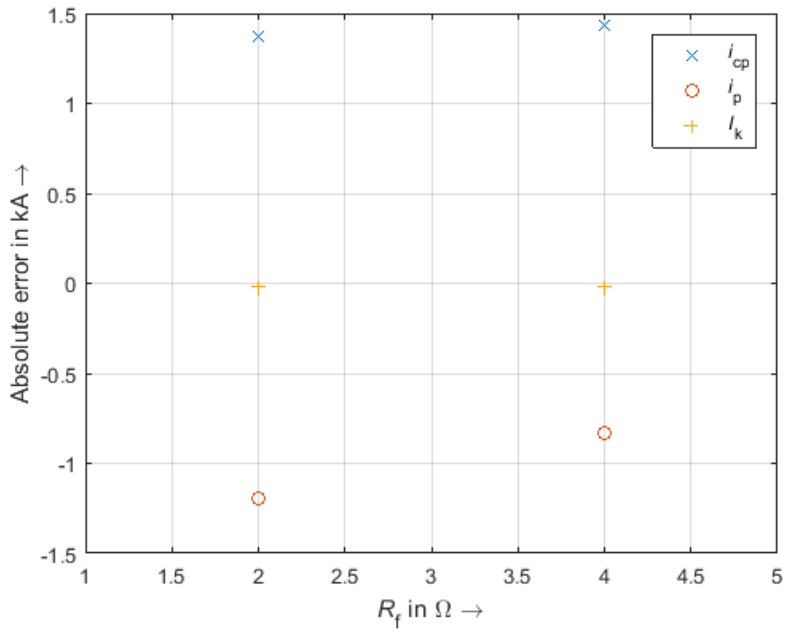

Figure 66. Absolute error for MT x = *50 km,* C_{DC} = *10 µF and variation in* R_f

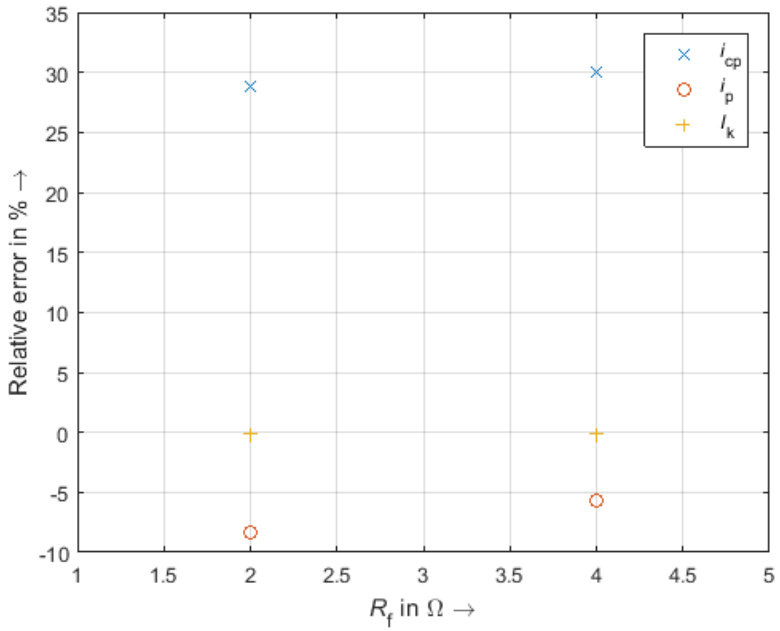

Figure 67. Relative error for MT x = *50 km,* C_{DC} = *10 µF and variation in* R_f

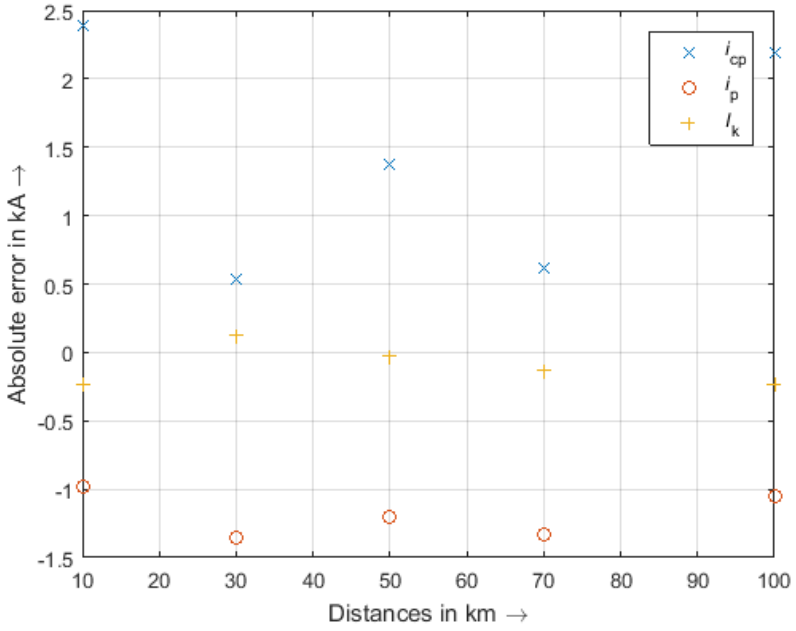

Figure 68. Absolute error for MT configuration and different distances

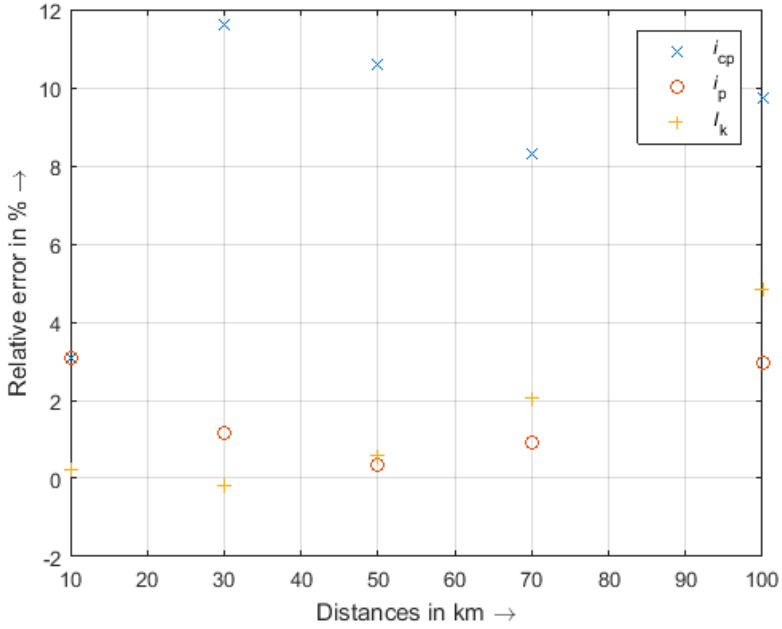

Figure 69. Relative error for MT configuration and different distances